

WUFR-27

Leads: Jesse Koeppel

Members: Lumi Lee

Suspension

Steering Final Design Review

21st October 2026

OVERVIEW

I have no brain and I must think

WUFR-27 steering FDR will be more focused on low end validation, with no ground up steering geometry redesign. The nominal WUFR-26 rack, tie rod, steer arm, and rack placement geometry is retained as the development baseline because we have not reviewed physical evidence showing that this geometry is the dominant steering weakness. The clearest known weaknesses are instead mechanical free play, shaft/column coupling reliability, serviceability, manufacturing repeatability, and the lack of a traceable path from tire behavior and vehicle state to steering targets.

The main R&D result at FDR is a reproducible steering analysis architecture. It includes a deterministic rigid mechanism evaluator, bounded geometry search, suspension pose and vehicle state interfaces, tire informed force demand inversion, motion aware target composition, standardized/reproducible figures, and a 3D viewer. That architecture is now complete for the current steering only software scope. The remaining high value questions depend on upstream suspension and vehicle state data, plus later physical correlation on the actual car. In other words: the math is there, the data ain't.

Here's that Geometry Table from last year in case someone needs a reference.

Rack Offset (in)	3.12
Rack Ratio / C-factor (in/rev)	3.5
Rack Displacement (in)	1
Tie Rod Length (in)	13
Steer Arm Length (in)	2.75
Outside Wheel Heading (deg)	22.22
Inside Wheel heading (deg)	32.81
Steer Input (deg)	102
Effort Decrease compared to 2025	14%
Tie Rod Inner (mm)	[-79.298, 220.980, 162.865]
Tie Rod Outer (mm)	[-61.933, 549.102, 192.223]

This figure came in handy last year so we're leaving it here.

DESIGN EVOLUTION

WUFR-26 Design Recap

The WUFR-26 aimed to address shortcomings identified in the previous year's design with the primary goal of lowering steering effort. The design targeted a 20% reduction in steering effort, and to achieve this, the location of the tie rod pickup points and steer arm size was modified via solidworks motion studies. A NARRco steering rack with a rack ratio of 3.5in/rev was chosen over that with a rack ratio of 4 in/rev to allow for more flexibility in optimizing steering geometry. The steering rack location was optimized within packaging constraints while also minimizing bump steer. The 47mm bevel box was retained, but upgraded with stiffer internal components and precision shims to improve meshing. The housing was corrected from the previous year to fit the size limit. The final geometry targeted approximately 75% Ackermann although the achieved value from the spec sheet is 67.7%.

As a result of the design changes, steering effort was reduced to 17.2Nm from 20Nm. This is a 14% reduction in steering effort, indicating some success in the design changes in achieving its primary goal although short of the 20% mark. Reduced steering effort improved consistency in dynamic event performance by decreasing driver fatigue, although a tradeoff was that the maximum steering angle was increased to -102°/+102°.

WUFR-26 steering geometry was developed with SolidWorks motion studies, OptimumK derived geometry, and historical design study response fits. For WUFR-27, those sources were recovered and reconciled into one canonical body frame (+x forward, +y vehicle left, +z upward) and one nominal steering configuration. The recovered design source is internally consistent enough to serve as a regression and development baseline, but it is not treated as an as-built vehicle measurement.

The nominal rack provides 3.5 in/rev travel and the retained design study domain is ±25.4 mm of rack displacement. The recovered steering axis, rack joint, tie rod, static toe, and static camber definitions are source preserved. WUFR-27 therefore carries the WUFR-26 geometry forward while changing the analysis process around it.

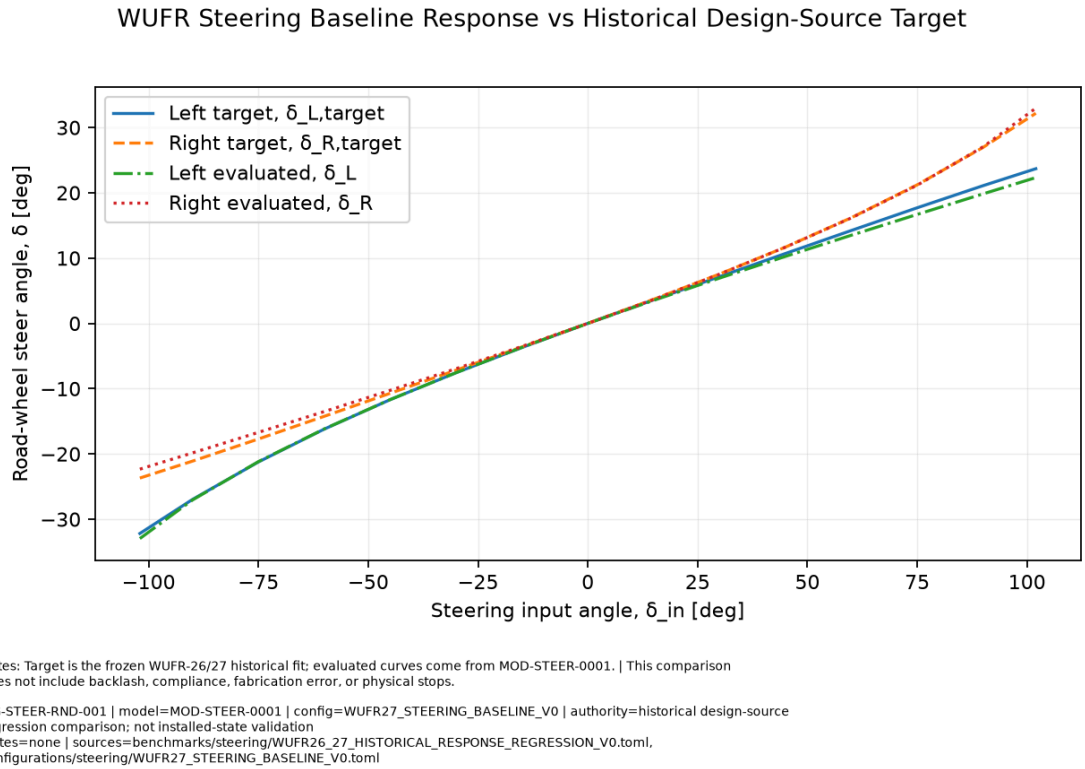

Figure 1. WUFR-27 nominal rigid steering response compared with the frozen WUFR-26/27 historical design-source target. This is design-source regression evidence, not installed-state validation.

WUFR-26 Failures/Lessons Learned

The steering column to shaft connection experienced rotational slip, excessive free play of around 5 degrees was measured, and the set screw at the connection sheared. These problems were identified both after dynamic testing by drivers (e.g. reported steering “getting very loose due to set screw slipping”)and also by members during servicing ahead of testing. This was a recurring issue over multiple separate occasions. Interim containment was to replace the sheared screw with a new setscrew, careful not to overtorque the screw. The problem *is* rotational slip, setscrew threads shearing, and free play, but *is not* axial separation or complete steering disassembly. Why did free play reach ~5 degrees? ➔ the set screws lost clamping force and slipped/sheared across the smooth shaft surface under load. Why did the setscrews slip or shear under load? ➔ the joint relied purely on localized friction and point shear on set screw threads rather than a positive mechanical lock, and failed under operational loads and service conditions. Why did the joint fail under operational loads and service conditions? ➔ The peak operational

steering torque was greater than the static friction limit of the set screw, and set screws can be overtorqued. Root Cause: The root cause was selecting a friction dependent, single point loading geometry for transferring high rotational torque to the shaft from the collar, rather than a positive mechanical engagement.

Therefore, the WUFR-27 design will aim to resolve this root cause by replacing the smooth shaft and collar+setscrew arrangement with a positive mechanical engagement geometry. (double d profile). With this change, torsional loads can be transferred across mating faces/surfaces as opposed to a single point, eliminating the rotational slip as possible failure.

The main R&D lesson was not that the nominal geometry was obviously wrong; it was that the previous workflow made it difficult to separate geometry, tire, suspension, and vehicle state effects. Several gaps were addressed:

- Steering definitions and sign conventions were distributed across spreadsheets, CAD studies, and fits rather than enforced by one evaluator;
- Ackermann percentage was easy to over interpret as a universal performance target even though tire slip demand and vehicle motion change the desired left/right wheel headings;
- Tire work was largely used for tire selection rather than tied directly to steering force demand;
- Steering calculations previously had no standard way to receive kinematic position, vehicle motion state (u, v, r), or tire data. Results for OptK, Solidworks, or Spreadsheets each had to be interpreted differently making calculations prone to errors;
- Missing or out-of-domain data could be hidden by manual plotting or informal assumptions;
- Installed backlash, compliance, stops, and as-built left/right correlation were not part of the rigid design-source model.

The WUFR-27 R&D response was to build explicit contracts around these boundaries rather than patching one more steering study.

DESIGN GOALS & TARGETS

Points and Car Goals

The R&D contribution to the car is primarily repeatability, traceability, and better design decisions. A steering geometry recommendation should be explainable from the same underlying mechanism, tire, suspension, and vehicle state definitions every time it is regenerated. This supports the team goal of a stable and predictable platform and directly strengthens design event evidence by distinguishing verified model behavior from assumptions, development proxies, and physical measurements.

The physical work does not claim a lap time gain since we're pretty much splitting hairs here regardless of content. A wise man once said: Ackermann optimization beyond purely geometric Ackermann is the last of your worries in terms of overall vehicle performance. Or something of that nature. Think he said his name was Tim. Anyway, steering doesn't weigh much and it is for the most part, reliable. Instead, we're here to reduce the risk of optimizing a subsystem around an inconsistent target and create a validation chain that can later connect design intent to measured steering wheel, rack, and wheel response. We're saving time. And time is money 🤑

Design Goals

The steering goals for WUFR-27 are:

- Create one deterministic rigid steering evaluator and canonical wheel heading definition;
    - Preserve hard mechanism infeasibility separately from objective error;
    - Allow bounded multi-objective geometry optimization;
    - Support multiple suspension poses and vehicle operating states without hardcoding an upstream suspension or load transfer model;
    - Convert reviewed tire force demand into bounded required slip angle without extrapolation;
    - Make the final steering target aware of the supplied vehicle velocity field when u, v, and r are available (come data or a more complex lap sim);
    - Preserve source-tire (R25B) and intended-tire (R20) data identity;
    - Generate reproducible figures and an interactive viewer directly from machine readable results;
    - Fail visibly when source data are missing rather than silently filling gaps.
- Maintain approximately the same torsional stiffness and mass while only changing the material and coupling methods.

- Fix the coupling problem.

The intended dry tire remains the Hoosier 43104 18 x 7.5-10 R20. The available TTC source used for steering development is the Hoosier 43105 18 x 7.5-10 R25B, treated as an approved proxy while retaining the two identities separately.

Historical target is a polynomial fit of the left and right wheel angle from the 2026 steering geometry using the new software as a comparison for future analysis. “Ideal” Ackermann is the pure low speed geometric ackermann required to make a set minimum radius turn. The peak slip-informed target is the slip angle at which maximum F_y can be generated through the wheel heading. The correction is the slip angle deviation from the historical target required to meet the peak slip informed one. As you can see, that correction ain’t huge.

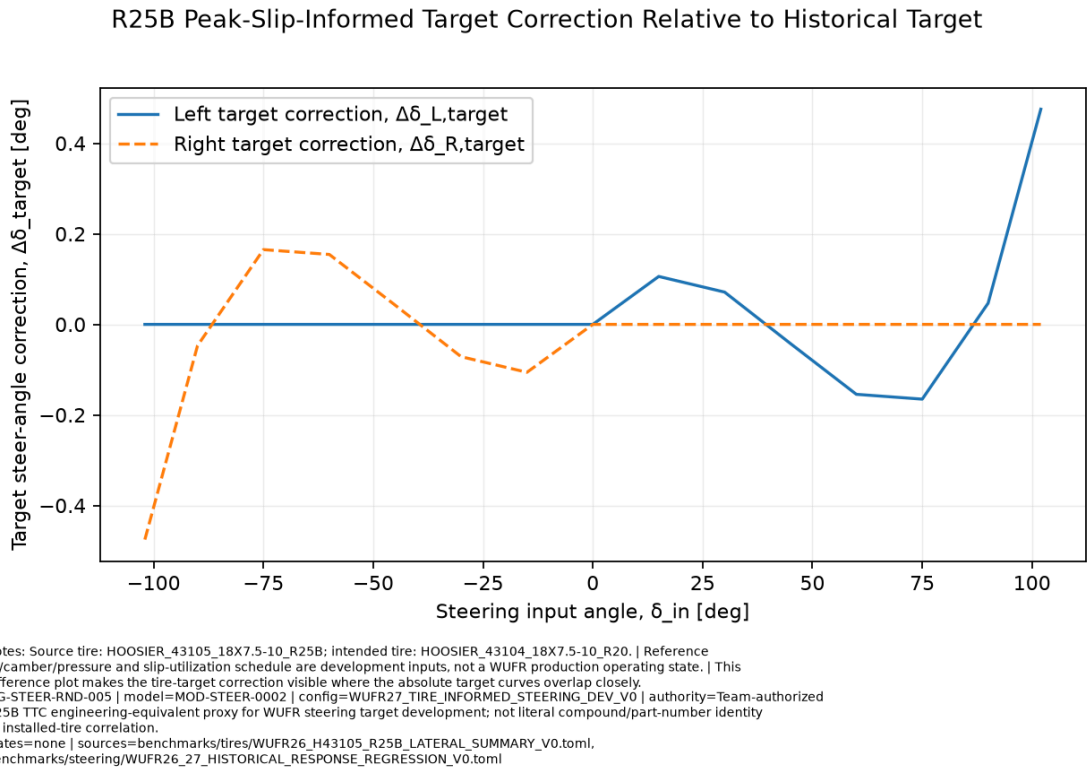

Figure 2. R25B peak-slip-informed steering-target correction relative to the historical target. The correction is development evidence from the approved R25B proxy; it is not a production tire-optimal steering target

The R25B source has been processed into an exact source specific runtime with preserved slip angle, load, inclination, and pressure states. A strict monotonic pre peak branch policy was

selected for force demand inversion because it gives a unique bounded inverse without smoothing or modifying source values .

What this source can support:

- Exact or bounded force-demand inversion inside the reviewed R25B domain.
- Development comparisons between steering targets and tire slip demand.
- Verification that one universal Ackermann target is not physically sufficient.

What it cannot currently support:

- A “perfect” WUFR-27 tire-optimal steering geometry ranking.
- A claim that the inside tire “wants” 4–5° and the outside tire “wants” 5–7° in EVERY corner.
- A claim that the existing dynamic toe curve keeps either tire in its optimal range.

Those stronger claims require synchronized per wheel normal load, inclination, pressure, lateral force demand, suspension pose, and vehicle motion. The current vehicle state evidence does not supply that entirely since the car ain’t built yet and we ain’t run the tests.

Exact R25B Steering Force-Demand Branch Handoff

Source branch identity is selected before projection to |Fy| and |α|. The graphic reports exact coverage without inventing a curve shape.

Reference state	Exact operating point	Samples	Slip-angle domain	Force domain	Source branch
Inside reference	Fz = 222 N γ = 0° p = 82.7 kPa gauge	64	0.07547° to 9.58491°	50.97 N to 694.04 N	negative_slip_pre_peak
Outside reference	Fz = 1112 N γ = 2° p = 82.7 kPa gauge	86	0.06349° to 10.85714°	275.84 N to 2737.89 N	negative_slip_pre_peak

Preserved boundaries

No zero-force anchor • no smoothing or refit • no sample deletion • no state interpolation • no force extrapolation • no track-surface scaling

Use boundary: these branches support bounded exact-state inversion and regression, not a WUFR steering target until synchronized vehicle demand is supplied.

Supplemental Figure 1. Exact source-backed R25B pre-peak branch coverage for the two authorized steering reference states. The figure reports exact states, sample counts, and domains without inventing a curve shape or promoting these branches to a WUFR force schedule.

DESIGN CONSTRAINTS

Rules

V.3.2 Steering

V.3.2.1 The Steering Wheel must be mechanically connected to the front wheels

V.3.2.2 Electrically operated steering of the front wheels is prohibited

V.3.2.3 Steering systems must use a rigid mechanical linkage capable of tension and compression loads for operation

V.3.2.4 The steering system must have positive steering stops that prevent the steering linkages from locking up (the inversion of a four bar linkage at one of the pivots). The stops:

> *a. Must prevent the wheels and tires from contacting suspension, bodywork, or Chassis during the track events*
>
> *b. May be put on the uprights or on the rack*

V.3.2.5 Allowable steering system free play is limited to seven degrees (7°) total measured at the steering wheel.

V.3.2.6 The steering rack must be mechanically attached to the Chassis F.5.14

V.3.2.7 Joints between all components attaching the Steering Wheel to the steering rack must be mechanical and be visible at Technical Inspection. Bonded joints without a mechanical backup are not permitted.

V.3.2.8 Fasteners in the steering system are Critical Fasteners, see T.8.2 V.3.2.9 Spherical rod ends and spherical bearings in the steering must meet V.3.1.5 above V.3.2.10 Rear wheel steering may be used.

> *a. Rear wheel steering must incorporate mechanical stops to limit the range of angular movement of the rear wheels to a maximum of six degrees (6°)*

b. The team must provide the ability for the steering angle range to be verified at Technical Inspection with a driver in the vehicle

c. Rear wheel steering may be electrically operated

T.1.2 Internal Cross Section

T.1.2.1 Requirement:

a. The cockpit must have a free internal cross section

b. The template shown below must pass through the cockpit

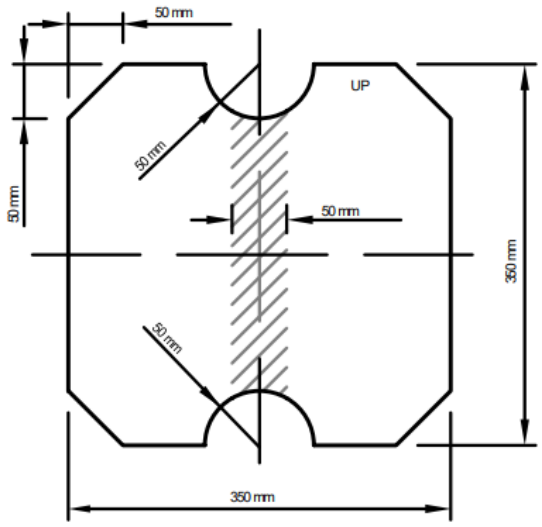

Template maximum thickness: 7 mm

T.1.2.2 Conduct of the test. The template:

a. Will be held vertically and inserted into the cockpit opening rearward of the rearmost portion of the steering column.

b. Will then be passed horizontally through the cockpit to a point 100 mm rearwards of the face of the rearmost pedal when in the inoperative position

c. May be moved vertically inside the cockpit



System Integration

Ergonomics

For the FDR, an alternative aluminum quick release from MPI was considered, and as a result a steering column material change from steel to aluminum was proposed as welding a steel quick release to an aluminum quick release is metallurgically unfeasible without bimetal transition inserts. However, the quick release stock required for the proposed change has an estimated lead time of 3~4 months due which is incompatible with our design timeline. Therefore the final design will retain steel for the steering columns which will also spare us from looking for thick column stock. In the end the aluminum column material change had yielded marginal standalone weight reduction of the new quick release hub and was driven mostly due to compatibility with quick release, but as it may be implemented next year the Solidworks part files and relevant information can still be found in Box and a copy of the FDR respectively.

EDA

We are keeping the linear steering potentiometer we had but also implementing a second rotary potentiometer for the primary shaft. The second sensor would be secured with a quick 3d printed mount and some light machining for a flat or a pin hole depending on what the potentiometer we choose relies on. Choosing a 3d printed mount keeps the alteration to integrity of the column minimal.

Chassis

Steering cannot be optimized independently of the rest of the vehicle. The implemented R&D interfaces make the required dependencies explicit.

Vehicle Dynamics

The native OptK suspension model supplies a named zero steer upright reference pose for each bounded suspension state. This reference retains the reviewed static wheel alignment but excludes front tie rod induced steering rotation. MOD-STEER-0001 then solves the additional upright rotation required by rack position and rigid tie rod closure, preventing bump steer from being applied twice. The historical OptimumK result is not consumed directly because its front upright poses already contain tie rod constrained steering. Instead, the implemented source adapter reconstructs and removes that rotation in three dimensions, allowing the workbook to serve as validation evidence for the native zero steer suspension transport. The remaining

integration gap is synchronization of these poses with reviewed per wheel tire loads, camber, pressure, force demand, vehicle motion, and state weighting—not generation of the suspension poses themselves.

The shared vehicle operating state contract carries per wheel normal load F_z, inclination/camber γ, tire pressure, lateral-force demand F_y, longitudinal force demand F_x, state weighting, and source authority. It deliberately does not solve load transfer or equilibrium.

The motion aware target provider accepts an externally supplied planar body state (u, v, r). It does not infer body sideslip or yaw rate from lateral acceleration alone. These quantities must eventually come from a reviewed vehicle model, QSS/trim solver, telemetry, or equivalent higher authority source. The majority of this has been completed by the time of the FDR, outside telemetry data, since this car ain't built yet.

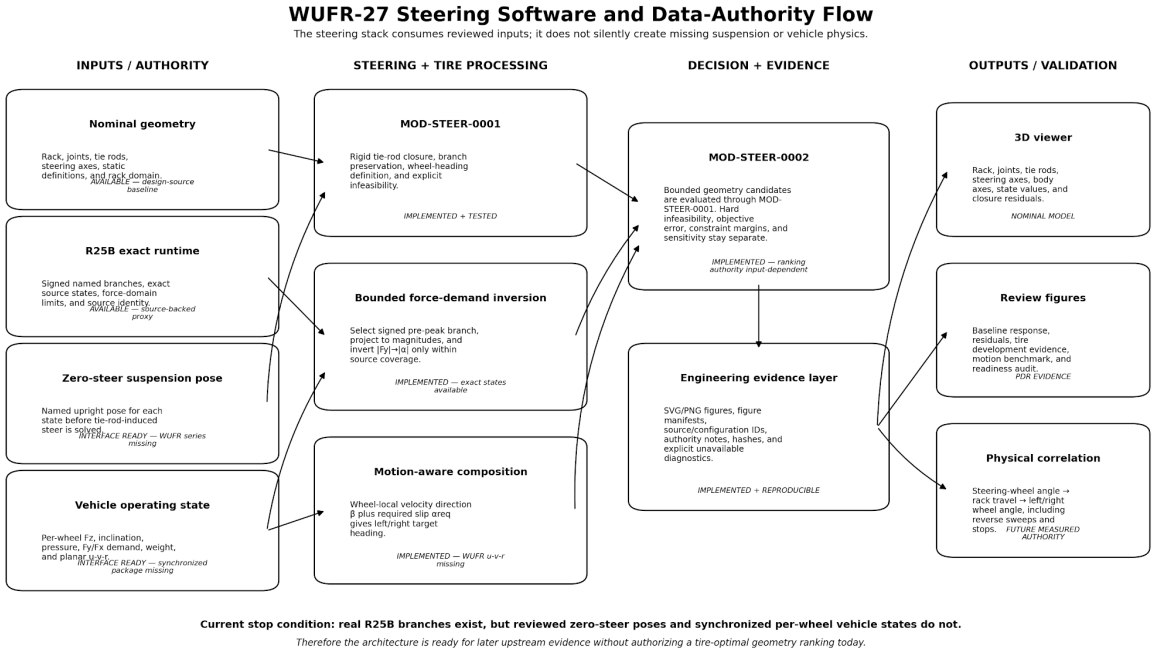

Supplemental Figure 2. Steering software and data-authority architecture. The implemented mechanism, tire, optimization, visualization, and exchange layers are separated from the missing zero-steer suspension poses and synchronized vehicle-state authority.

Limiting Factors



Limitations

- Manufacturing a double-d profile requires high precision and tight tolerances are necessary to prevent rotational slop which may require precise indexing.
- The internal double d bore may be especially tricky to manufacture.

Risks

- Aluminum has a smaller shear modulus; under high steering loads it will experience greater torsional twist, degrading steering feedback.
- Aluminum is prone to galling and rapid mechanical wear under cyclic loading, which may create slop. Aluminum and steel in contact can also leave aluminum prone to galvanic corrosion. We could mitigate these risks through anodizing.
- Aluminum does not have a true fatigue limit
- The change in cross section of the shaft from circular to double d can cause stress concentrations, though this can be mitigated through generous fillets.

The current steering development stop is explicit and intentional. The remaining missing inputs are:

- Reviewed zero steer suspension poses;
- Synchronized per wheel F_z, inclination, pressure, and F_y demand;
- Reviewed body motion states u, v, and r;
- Installed rack stops, interference limits, backlash, compliance, hysteresis, repeatability, and left/right as built geometry.

The R25B processing and branch classification are complete. The current readiness audit reviewed two available 1.2 g vehicle states and found zero states ready for exact R25B steering handoff, zero ready for bounded complete cell tire queries, and zero ready for motion-aware target construction. One or both front wheel loads were outside the source load domain, and the states also lacked camber, pressure, F_y demand, suspension pose, motion, and nonzero target weighting.

R25B Steering-Target Input Readiness Audit

Two existing 1.2 g development states were reviewed. A complete synchronized state is required; one usable field does not make a state ready.

State	Front inside Fz	Front outside Fz	Inclination	Pressure	Fy demand	Zero-steer pose	u-v-r	Weight	Ready?
1.2 g right turn	186.214 N BELOW 222 N min	1719.575 N ABOVE 1112 N max	Missing	Missing	Missing	Missing	Missing	0	NO
1.2 g left turn	516.848 N inside load interval; not exact knot	1388.941 N ABOVE 1112 N max	Missing	Missing	Missing	Missing	Missing	0	NO

Readiness counts: exact two-branch handoff = 0 • bounded complete-cell query = 0 • motion-aware target = 0

Blocked substitutions: no clipping, nearest-state selection, nominal camber/pressure insertion, inferred force allocation, Ackermann-derived motion, or hidden target weighting.

Program result: steering/tire target work pauses here until reviewed suspension pose and synchronized vehicle-state authority exist.

Supplemental Figure 3. R25B steering-target input readiness audit. Neither available 1.2 g state supplies a complete in-domain, synchronized tire/suspension/motion package, so geometry ranking remains unauthorized rather than being filled with convenient guesses.

Therefore, further steering only or tire only development is paused. The next useful step is not “more equations until morale improves.” It is better upstream evidence.

DESIGN RISK ASSESSMENT (FMEA)

FMEA Summary

WUFR-27 Steering FMEA Steering FMEA diagrams

The steering FMEA evaluates 26 potential failure modes across the driver interface, quick release, steering columns, double-d coupling, clevis pin, welds, support bearings and trusses, bevel box, steering rack, rack stops, tie rods, rod ends, critical fasteners, environmental exposure, assembly setup, and cockpit integration. Because steering is a safety critical mechanical system, most failures involving disconnection, fracture, binding, or uncontrolled free play were assigned severity ratings of 9 or 10.



The highest initial RPNs are associated with corrosion, galling, fretting, and contamination of steering surfaces; incorrect bevel gear shim stack or bearing preload; double-d fit and wear; column-collar weld integrity; and fatigue or wear of the shafts and bevel gears. The RPN values are used to prioritize design and validation effort, but low RPN alone is not considered sufficient justification to accept a failure mode with a severity of 9 or 10.

The principal risk reduction action is replacement of the previous friction dependent setscrew joint with a positive double-d torque interface and separate a clevis pin for axial retention. Remaining actions include defining the double-d fit tolerance and engagement length, qualifying the selected steel weld procedure, verifying pin shear and edge distance, establishing bevel gear backlash and bearing preload limits, specifying corrosion protection and lubrication, validating positive rack stops, completing steering load and fatigue checks, and creating a documented steering fastener and inspection map.

Before CoG, representative assemblies should be proof torque tested and subjected to repeated reversing cycles. Testing should measure backlash growth, fretting, galling, weld condition, pin retention, gear contact, running torque, and repeatable angular indexing after service. The complete installed system should then be correlated through steer in-wheel angle, rack displacement, and left/right wheel angle. The final FMEA ratings will be reassessed after these actions are completed and physical evidence is available.

WUFR-27 DESIGN

Design Decisions

The selected WUFR-27 upper steering column (UPSC) and lower steering column revert to the prior steel construction. RIP MPI. The aluminum column/quick-release concept discussed later in is a rejected alternative kept for documentation, not the current design or an active load/weight/cost assumption. All legacy 6061-T6/0.900-in tube, aluminum filler/HAZ, and aluminum fatigue numbers elsewhere in this FDR are historical comparisons only and must not be cited as final WUFR-27 capacities. Their full original calculations and associated figures will be preserved and transferred into design materials.

Current geometry (upper / lower): steel tubes OD 0.750 / 0.750 in, ID 0.625 / 0.625 in; free column lengths 4.878 / 6.600 in; free shaft lengths 0.787 / 2.753 in. Male/female double-D profiles share nominal 0.590-in major diameter (0.295-in radius) and 0.472-in across-flats dimension, giving 0.059-in flats depth per side and approximately 0.354-in chord width. Intended minimum functional engagement at each joint is 0.375 in. Retention at the double-D is axial only via McMaster 90378A114 18-8 stainless clevis pin (0.125-in nominal, 0.121–0.123-in actual diameter) in DOUBLE shear, with a cotter retainer. Torque flows primarily through the D flats; the NaRRco rack's separate heavy-duty spring-pin interfaces require their own torsional checks and are not equivalent to these axial-retaining pins.

Manufacturing: independent in-house +/-0.005-in across-flats machining tolerance is NOT the specified acceptable mating fit. Two nominally identical components at +/-0.005 in could have -0.010 to +0.010 in size difference (interference to excessive clearance). Recommend wire EDM for the internal female adapter D, with final size/tolerance selected from measured male parts and a specified small positive sliding clearance. Validate engagement, circumferential weld access, fit and backlash before drawing release. Revised CAD has an approximate 0.298-in weld-intrusion clearance, 0.200-in weld joint overlap and 0.130-in shoulder (dimensions to be verified on the issued section drawing). ER70S-2 filler, standard steel welding and no postweld heat treatment are currently planned.

Geometry Carryover

The overall steering geometry from WUFR-26 will be carried over into WUFR-27 because it successfully met the team’s performance objectives and contributed to the team’s strongest competitive season to date. WUFR-26 introduced significant changes to WUFR-25, including revised steering geometry, a reduced rack ratio, optimized tie rod pickup locations, resulting in a



measurable reduction in steering effort and improved driver consistency. Since these changes have not yet revealed major performance deficiencies, especially under an overall team goal of a modest design season with “new design iterations only as necessary,” it would be unwise to introduce unnecessary risk through a complete redesign.

Based on the vehicle mass properties, the static front tire load is approximately 687N per front tire with a 68kg driver. During a 1g corner, the load transfer analysis from 26 predicts approximately 471N of front axle load transfer, resulting in an estimated outside front load of 923N and inside front load of 452N. These loads correspond closely to the TTC test conditions of 445N, 667N, 112N, which were used as representative operating points of tire analysis.

Examining the F_y vs slip angle curves, the heavily loaded outside tire reaches near-max lateral force at around 5-7 degree slip angle, while the lightly loaded inside tires saturate at a slightly lower slip angle of approximately 4-5. In other words a useful steering geometry would help produce the useful slip angle range of somewhere around 4-7 degrees over the expected front wheel loads.

The available tire data demonstrate that useful slip angle demand changes with normal load, inclination, pressure, lateral force demand, and vehicle motion. The current geometry produces increasing left/right wheel angle divergence with steer, but we do not yet have a synchronized operating state package sufficient to determine whether that divergence is tire optimal for most operating states. Geometry carryover is therefore justified by risk management and the absence of a demonstrated deficiency, rather than by a claim of perfect tire optimality.

Because the inner tire saturates at a lower slip angle than the outer, too much wheel angle at the inner tire would cause it to exceed its peak lateral force capacity. The dynamic toe plot steering 27 plots confirms that the current geometry progressively adds toe out as steer angles increase, keeping the inside tire close to within an “optimal” 4~5 degree slip angle during sharp cornering.

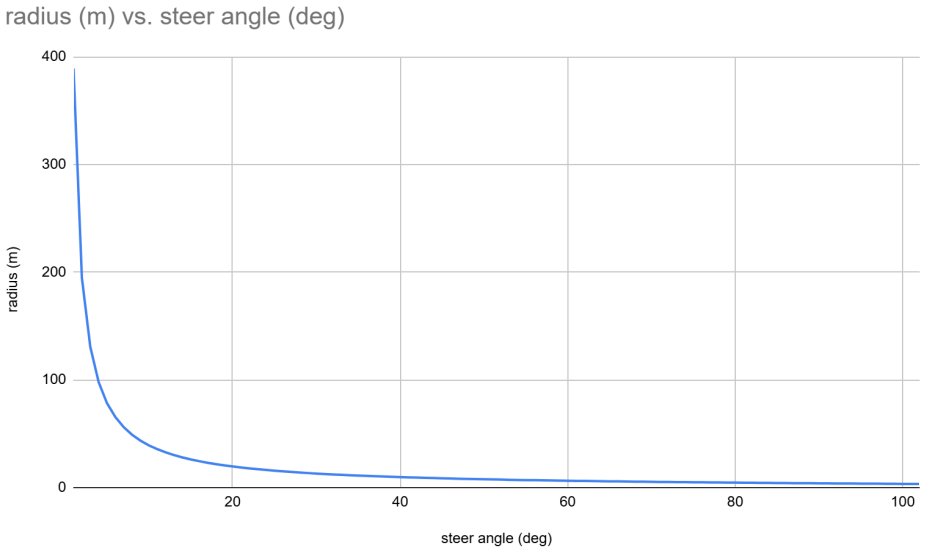

The wheel angle and turn radius plots show the current geometry reaches a maximum inner wheel lock of 32.81 degrees and outer wheel lock of 22.22 degrees at full rack travel. This ~9.5 degree divergence ensures the inside tire rolls smoothly along its tighter turn path, preserving grip and protecting tire life for endurance.

Furthermore, FSAE rules D.11.1.1.d and D.11.1.1.g state a minimum outside diameter of 9m (a 4.5m radius turn) and a 3.5m minimum track width. The turn radius plot for our current geometry shows a 3.20 m minimum turning radius at max steer, showing the driver can comfortably navigate the tightest turns without hitting rack stops. Installed rack stops, tire clearances, compliance, and as-built wheel angles must be measured as is before this is treated as vehicle level turning capability.

Design efforts for WUFR-27 will therefore focus on targeted improvements that address known issues without altering the steering geometry. These improvements include the steering column - shaft connection, bevel box serviceability, and potential weight reduction opportunities while maintaining stiffness and safety. This approach would preserve a proven steering system while addressing reliability, manufacturability, and serviceability concerns.

Physical Changes

Coupling method change

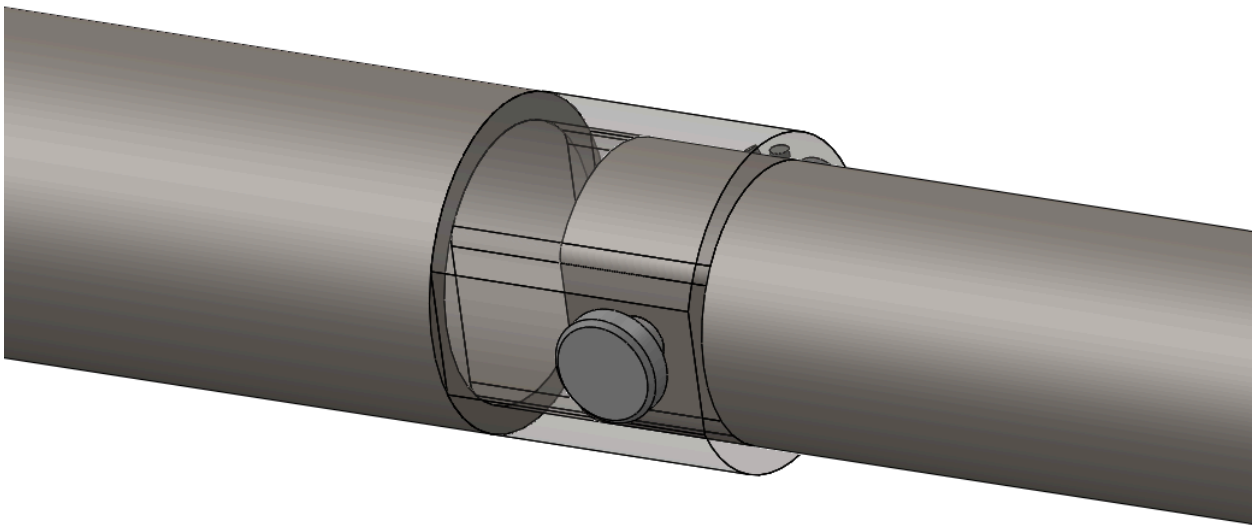

A double-d profile shaft was chosen to replace the set screw method. As opposed to the friction dependent point contact of a set screw, the double-d profile provides a positive mechanical lock across mating surfaces, eliminating sudden slipping which was an issue reported in the past season. Furthermore, while a set screw failure typically results in a sudden loss of steering control due to sudden shearing or slippage, a double d method will allow more predictable/remediable failure due to detectable gradual wear. Also, the two flats allow for easy repeatable alignment as there are only two obvious self aligning orientations.

The length of the double-D profiled section was increased by 0.275 in on both steering columns to provide additional clearance for the welded joint. The extended profiled section will allow actual engagement length to remain shorter than the actual profiled length of the column, preventing surface irregularity on the inside due to weld bead potentially interfering with fitment during assembly and causing free play.



To transmit torque reliably through the flat-to-flat shaft interface without inducing localized plastic deformation, the contact surface $W \times L$ must be sized against compressive bearing stress. Under high steering torque, insufficient contact area risks localized crushing, leading to slop and faster wear.

The effective contact flat width W is governed by shaft geometry and flat depth; W=2w where w is the perpendicular distance from the shaft center to the flat. Assuming a symmetrical interface, the torque T is resolved to a compressive force F acting at r_{eff} .

The material's yield strength must be higher than bearing stress; thus the minimum required column/shaft engagement length is:

$$L_{min} = \frac{T \cdot FoS}{2 \cdot r_{eff} \cdot W \cdot S_y}.$$

Evaluating for the most conservative boundary condition (shallowest flat depth h = 0.8mm) to find an upper bound in required engagement length. Using an FoS of 2, required engagement length was calculated as L_{min}=2.97 mm.

While this mechanical minimum is very small, practical design limits would be governed by manufacturing tolerances rather than bearing stress. A longer engagement helps minimize slop by decreasing allowable angular tilt. Furthermore, it helps reduce progressive wear by keeping peak contact stresses well distributed.

Therefore, the final engagement length was selected to be .375". In summary the profiled section of the the columns are .65" and the profiled section of the shafts are .375".

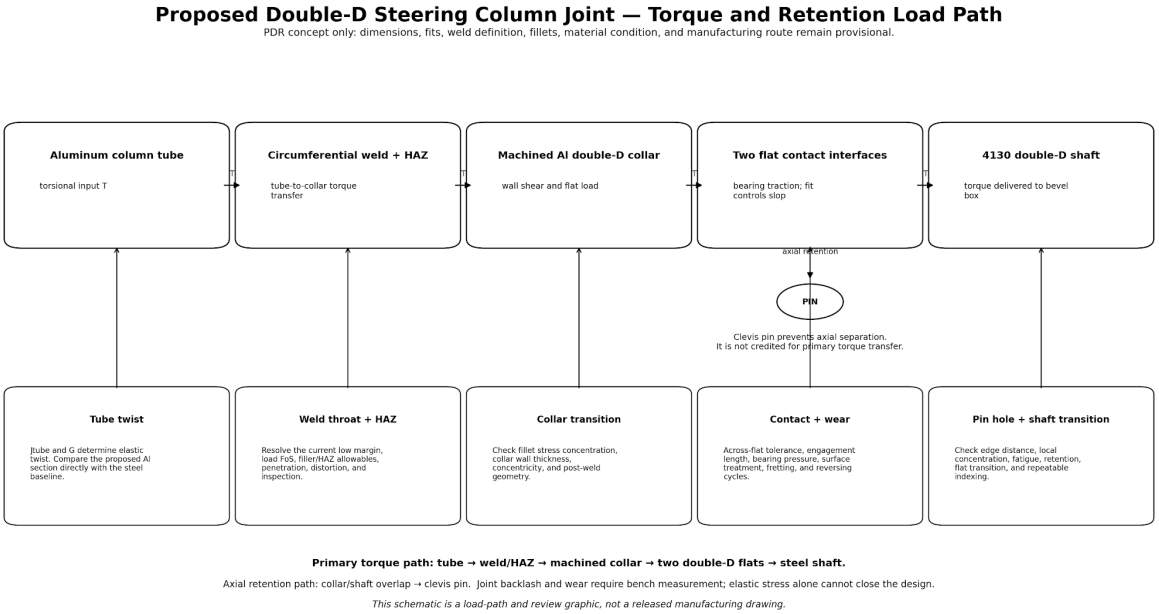

Supplemental Figure 4. Proposed double-d column-joint torque and axial-retention load path. identifies the weld/HAZ, collar transition, flat contact, pin-hole, tolerance, wear, fatigue, and inspection questions that still govern design closure.

While a keyed shaft was initially considered, the current thin walls of the steering columns cannot accommodate a keyway without gaining additional material and weight. The keyed shaft also has many sharp internal corners that cause stress concentrations, and result in asymmetric loading. Under reversing cyclic torsional loads, the key can deform the side walls of the keyway as it hammers repeatedly, causing deformation and backlash. Furthermore, with the material (next section), a keyway would be even more prone to wear. Backlash is better resisted with a double-d profile since it has a much larger contact area (flats) compared to a narrow face of the key, reducing bearing stress.

In WUFR-26, the setscrew connection carried steering torque and also held the shaft in the column. The double-D profile now carries torque through its flats, but a separate retainer is still needed to prevent axial withdrawal. The pin capacity will therefore be checked independently of the torsional strength of the connection.

A 1/8-in clevis pin secured with a cotter pin was selected because it can be removed without tools, preserving the serviceability improvement gained by removing the setscrew. The smaller



hole also removes less material from the connection, although the pin and surrounding steel must still be checked for axial loading.

Using Roark's non circular torsion formula:

$$\tau = \frac{35{,}547\,B}{9.525^3} = 41.13\,B \quad .$$

Calculating for several different flat depth choices,:

Distance from center to flat **w** ($= r - h$)	Flat depth **h**	Flat width **W** ($=2\sqrt{r^2 - w^2}$)	**h/r**	**B** factor	Shear stress **τ**
8.57 mm	0.95 mm	8.30 mm	0.10	0.79	32.5 MPa
7.62 mm	1.90 mm	11.43 mm	0.20	0.91	37.4 MPa
6.67 mm	2.86 mm	13.60 mm	0.30	0.98	40.3 MPa
5.71 mm	3.81 mm	15.24 mm	0.40	1.04	42.8 MPa

While torsional stress analysis using Roark's noncircular torsion formula shows that all evaluated configurations in the table operate below the shear yield strength of steel, the ultimate selection of the flat dimension would balance torsional capacity, bearing stress, and backlash sensitivity. Tradeoff comparison below:

	Shallow flat (low h/r)	Deep flat (high h/r)
Torsional strength, torsional stiffness		Too deep of a flat removes shaft material, raising stress without meaningful contact area gain
Contact area	If too shallow, contact area decreases and bearing stress	



	increases	
backlash	higher risk of slop with wear, more sensitive to minor tolerance issues	
Stress concentration at transition		Worse since larger step ratio increases stress concentration factor

The table above summarizes the earlier flat-depth trade study. A depth of 0.125 in was considered under that profile's assumptions, but the current WUFR-27 shaft uses a 0.590 in major diameter and 0.472 in across flats, giving a selected depth of 0.059 in. The corresponding torsional analysis, fit tolerance and axial-retention checks are presented in the Steel Shaft and Column Analysis section below.

Stress concentration at shaft profile transition

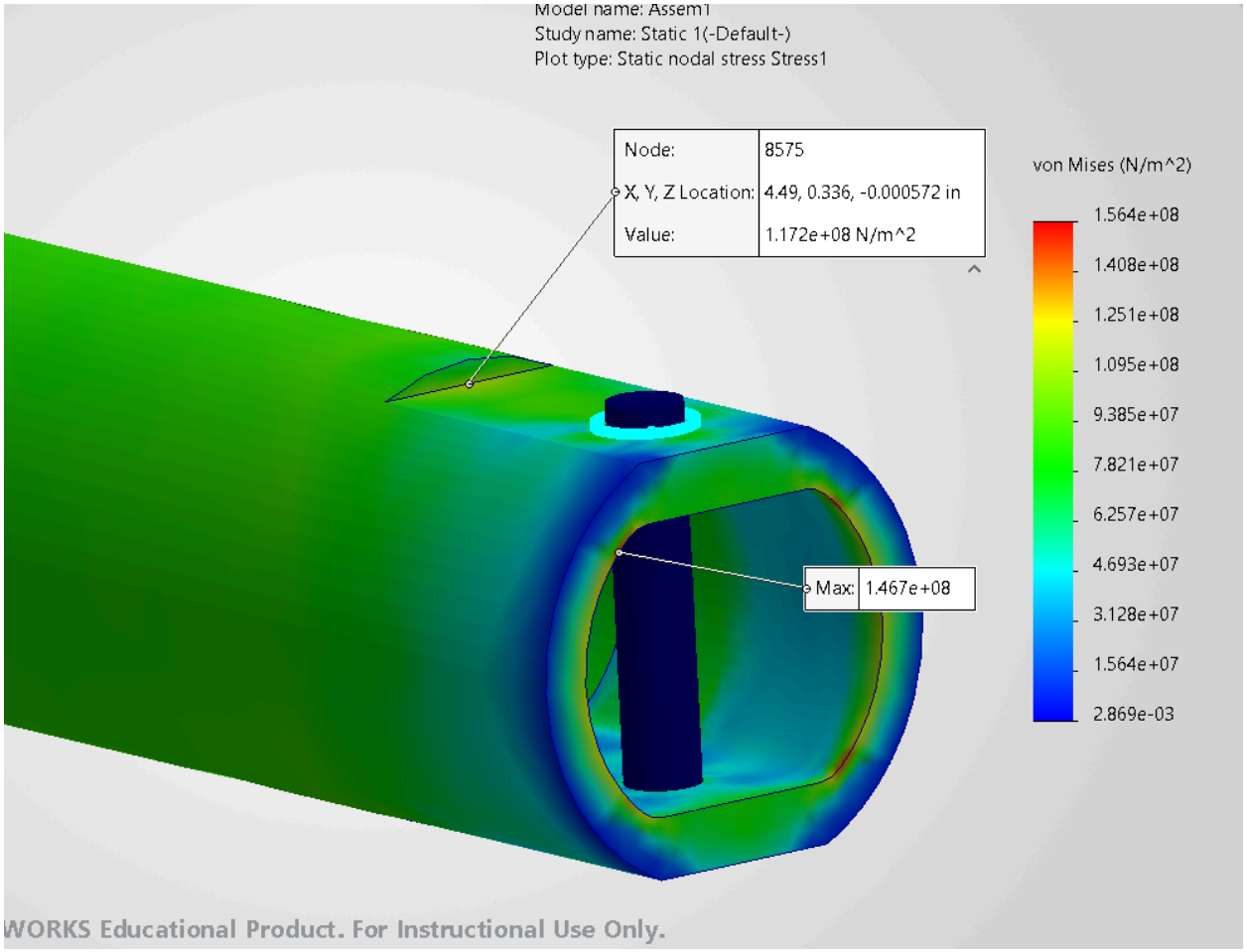
Model name: Assem1
Study name: Static 1(-Default-)
Plot type: Static nodal stress Stress1
Node: 8575
X, Y, Z Location: 4.49, 0.336, -0.000572 in
Value: 1.172e+08 N/m^2
Max: 1.467e+08
von Mises (N/m^2)
1.564e+08
1.408e+08
1.251e+08
1.095e+08
9.385e+07
7.821e+07
6.257e+07
4.693e+07
3.128e+07
1.564e+07
2.869e-03
WORKS Educational Product. For Instructional Use Only.

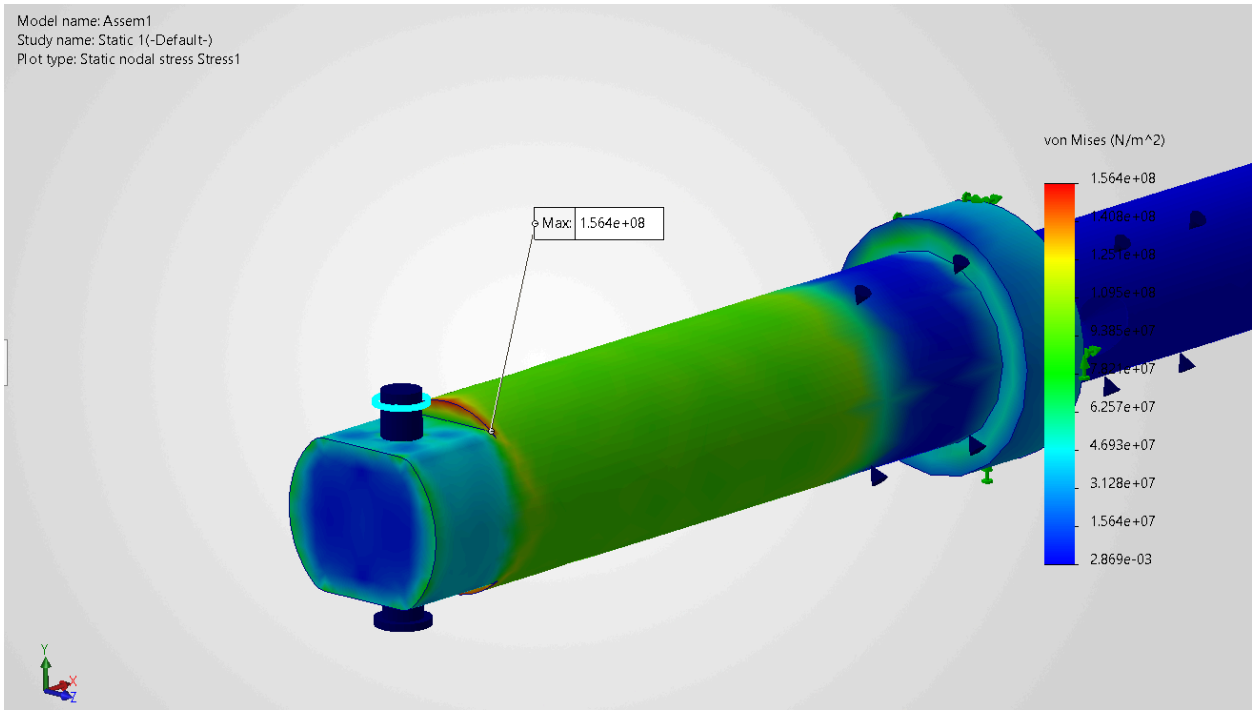

The change from a circular to a double-D profile introduces a stress concentration, particularly at the internal profile corners and at the shaft transition. The earlier FEA study reported a peak von Mises stress of 146.7 MPa and identified those regions as potentially critical. Since this is von Mises stress, the appropriate first comparison is the tensile yield strength of the relevant steel in its actual condition, rather than a shear-yield value. The earlier 251 MPa property and the resulting stated factor of safety should not be treated as verified. It was also noted that the peak stress decreased while displacement increased by approximately seven times between FEA revisions.

Weld

Approximating the weld joint as a thin-walled ring, the weld-as-line method (table 5 in section 7.4-7) gives $J_{weld} \approx 2\pi R_{avg}^{3} t_{weld}$. Using the already-factored parked steering torque of 35.547 N·m, the peak torsional shear stress is calculated as such, $\tau_{max} = TR/J \approx 46.75\ MPa$ for the weld line. This was originally compared with an aluminum concept value of 105.1 MPa, although the joint geometry and material conditions differ. ER70S was the reference filler for the earlier calculation. The quoted 145 MPa shear allowable was derived from filler-metal UTS alone, so the resulting 3.1 ratio is a preliminary filler-only screen rather than a verified weld-joint factor of safety.

The selected steel weld is analyzed below using the effective-throat-dependent shear calculation.

Welding feasibility was reviewed by our team's welders (Cristian & Gabe).

Bearing serviceability

To improve serviceability time for WUFR-27, different options were assessed with an aim of required tool reduction. In 26, we needed 4 tools to open the bevel box. 3/16" hex key, 7/16" wrench, 3mm hex key, 5/16" wrench. First off, we will eliminate the setscrews connecting column and shaft so the 3mm hex key is eliminated. To further eliminate either the 5/16" or 7/16" wrench and standardize on two tools, three design modifications were considered

option	Proposed change	impact
A. Upsize flange nuts	Replace 5/16" width flange nuts with 7/16" width	Requires enlarging the housing clearance and flange geometry, adding unwanted structural mass
B. Downsize locknuts	Replace 7/16" locknuts with 5/16"	¼-28 nuts with 5/16" width are unavailable through McMaster-Carr, requiring additional specialty hardware
C. Change bolts and locknuts	Replace bolts to #10 and replace locknuts with 5/16"	10-32 nuts with 5/16" also unavailable through McMaster-Carr

Final design preserves the existing bevel box housing and maintains a 3 tool setup, as:

- Avoids increase in mass due to upsized flange
- Avoids introducing specialty hardware by using fasteners already in stock



While 2 tools was the initial target lighter housing and more reliable fastener supply has higher benefit than forcing a redesign.

Steel Shaft and Column Analysis

With the aluminum column proposal no longer being pursued, the final design uses steel columns with the double-D shaft connection described above. The full aluminum sizing and fatigue calculations remain in Design Materials as a record of the original material comparison. The following calculations use the current steel geometry, but material certification and the final welded-joint dimensions are still required before the component can be released.

Torsional Strength and Stiffness

The upper and lower columns have an outer diameter of 0.750 in and an inner diameter of 0.625 in. Their free lengths are 4.878 in and 6.600 in, respectively. The circular shaft sections are 0.590 in diameter, with free lengths of 0.787 in (upper) and 2.753 in (lower). Taking a representative steel shear modulus of 80 GPa, the polar moments and shaft twist can be estimated using the circular-section equations below.

$$J_{\text{tube}} = \frac{\pi}{32}(D_o^4 - D_i^4), \quad \tau_{\max} = \frac{TD_o}{2J}, \quad \theta = \frac{TL}{GJ}$$

The hollow column has J = 6.694 × 10^{-9} m^4, while the equivalent full circular shaft has J = 4.952 × 10^{-9} m^4. At the calculated cornering load of 14.444 N·m, the tube and round shaft reach nominal shear stresses of 20.55 and 21.86 MPa. At the unfactored parked load of 23.698 N·m, these increase to 33.72 and 35.86 MPa; at the factored parked load of 35.547 N·m, the corresponding values are 50.58 and 53.79 MPa. The four free circular sections contribute approximately 0.638°, 1.047°, and 1.571° of elastic twist under these three load cases. This is an estimate for the free spans only; it does not include torsion through the double-D engagement, welds, gearbox or rack. The 35.547 N·m calculation already includes the original 1.5 structural load factor.

For the actual solid double-D shape, a preliminary prismatic torsion calculation gives $J \approx 3.805 \times 10^{-9}$ m^4, or roughly 77% of the full circular shaft value. Its estimated local peak surface shear at the



factored load is approximately 81 MPa. This comparison shows why a circular shaft calculation alone is not sufficient to assess the profiled section. The results do not yet account for the pin holes, profile transition, mating adapter or weld.

Double-D Fit and Contact

The selected profile has a nominal major radius of 0.295 in and an across-flats dimension of 0.472 in. The flat lies 0.236 in from the center, giving a flat depth of 0.059 in and a flat chord width of 0.354 in. Both components use the same nominal profile before the mating clearance is specified, with at least 0.375 in of functional engagement.

$$b = \sqrt{R^2 - a^2}, \quad h = R - a, \quad w = 2b$$

The existing in-house across-flats machining capability is approximately ±0.005 in per component. This is not a sufficiently controlled finished fit for the intended low-backlash sliding joint. If the male and female profiles are machined independently at the same nominal dimension, the relative across-flats difference could be anywhere from −0.010 in to +0.010 in. One limit interferes with assembly, while the other permits substantial rotational take-up.

For a nominal clearance C_0 with independent male and female size tolerances t_m and t_f, the dimensional limits are:

$$C_{\min} = C_0 - t_m - t_f, \qquad C_{\max} = C_0 + t_m + t_f$$

To examine the sensitivity of the fit, we modeled the male as a rigid, centered double-D profile rotating inside a geometrically matching female profile. The circular boundaries are assumed concentric, and contact first occurs at the flat chord endpoints. This model gives the one-direction take-up angle and the total bidirectional angular lost motion:

$$\theta_{\text{one}} = \sin^{-1}\left(\frac{a + C/2}{R}\right) - \sin^{-1}\left(\frac{a}{R}\right), \quad \Delta\theta_{\text{bi}} = 2\theta_{\text{one}}$$

For example, across-flats clearance of 0.0005, 0.0010, 0.0015 and 0.0020 in gives about 0.162°, 0.324°, 0.487° and 0.650° of bidirectional rotational lost motion per connection. At 0.010 in

clearance, this grows to approximately 3.30° per connection. Two such joints could consume much of the steering-system free-play allowance even before play in the quick release, gearbox and rack is considered. The result is a centered ideal-profile sensitivity, not a verified worst case: eccentricity, roundness, chord corner radii, angular alignment and wear must be included when releasing tolerances.

If we provisionally allocate no more than 0.5° of total bidirectional lost motion to each double-D connection, the centered geometric model requires Cmax ≤ 0.00154 in. A more restrictive 0.25° budget would require Cmax ≤ 0.00077 in. These are candidate allocation examples, not approved drawing limits. Importantly, wire EDM on the female part alone does not correct a male across-flats dimension varying independently by ±0.005 in. The male should also be machined to a controlled limit or measured individually so that the EDM bore can be matched to it. The final clearance must remain positive after dimensional and form tolerances.

The double-D transmits torque through the two opposing flats rather than the transverse clevis pin. If the contact reaction on each loaded flank acts at the maximum possible lever arm b, the minimum normal reaction per flank at the factored parked torque is about 3.95 kN:

$$N_{\min} = \frac{T}{2b}, \qquad p_{\text{est}} = \frac{N}{L_e w_c}$$

This is a lower bound on the ideal flank reaction, not a contact-pressure result. The actual area is concentrated near the contact edges when clearance is present, so dividing the load by the entire flat area would underestimate local pressure. Will need either a contact analysis of the mating steel parts or a clearly justified effective contact width and acceptable local bearing/wear criterion before the interface is considered structurally verified.

Column and Adapter Weld

We are retaining the steel collar and circumferential weld arrangement, with ER70S-2 filler planned for fabrication. The selected tube wall is 0.0625 in (1.5875 mm). Approximating the weld as a circular line at the tube mean radius of 8.731 mm, the torque produces a shear flow that can be compared with an assumed effective weld throat:

$$q = \frac{T}{2\pi r_m^2}, \qquad \tau_w = \frac{q}{a_{\text{eff}}}$$

At 14.444, 23.698 and 35.547 N·m, the idealized shear flows are 30.16, 49.47 and 74.21 N/mm. If the weld developed the full 1.588 mm nominal wall as an effective throat, the corresponding average shear stresses would be 19.0, 31.2 and 46.8 MPa. At the factored load, an allowable stress of 50 MPa would require an effective throat of at least 1.484 mm, while 40 MPa would require 1.855 mm, greater than the nominal tube wall. This does not imply that the actual weld is inadequate; it establishes the importance of the weld type, throat and as-welded material properties. The earlier quoted weld factor of safety cannot be retained as a final steel-joint result without reviewing these details.

Axial Retention and Lug Analysis

The selected McMaster 90378A114 clevis pin retains the double-D connection axially; the flats carry the steering torque. The 18-8 stainless pin has an actual diameter of 0.121–0.123 in, giving 0.002–0.004 in of diametral clearance in a nominal 0.125 in hole before allowing for hole tolerance. For an assumed yield strength of 205 MPa and a factor of safety of 3, the nominal double-shear capacity is approximately 585 N. One 0.094 in loaded wall gives an estimated 501 N in bearing, while a 0.300 in wide lug provides approximately 725 N in net-section tension. These are separate component checks, rather than the allowable load of the complete joint.

The corresponding shear, bearing and net-section capacities are calculated using the assumed minimum pin diameter, local wall thickness and lug width:

$$F_{\text{pin, shear}} = \frac{2(\pi d^2/4)S_y}{\sqrt{3}\, n_y} \simeq 585 \text{ N}$$

$$F_{\text{wall, bearing}} = \frac{tdS_y}{n_y} \simeq 501 \text{ N}$$

$$F_{\text{net}} = \frac{(w - d_h)tS_y}{n_y} \simeq 725 \text{ N}$$

Pin bending may be more restrictive, depending on the spacing between the two outer support reactions. Treating the pin as simply supported across span L with a central transverse force yields:

$$F_{\text{bend}} = \frac{\pi d^3 S_y}{8 L_s n_y}$$

For illustration, support spans of 0.10, 0.25 and 0.50 in give allowable bending screens of about 307, 123 and 61 N at the same assumed material strength and safety factor. These are not the dimensions of a verified assembled pin support; distributed bearing between the male and female components could change the result.

Likewise, shear-out depends on the actual distance e from the pin center to the free edge in the direction of axial withdrawal:

$$F_{\text{tear}} = \frac{2t(e - d_h/2)S_y}{\sqrt{3}\, n_y}$$

With an assumed 0.094 in loaded wall, 0.125 in hole and the same conservative material properties, e = 0.200, 0.367 and 0.687 in would give approximately 658, 1,457 and 2,988 N per wall. The previously reported 0.367 and 0.687 in dimensions still need their physical datums and loaded directions confirmed. The unreinforced column wall is only 0.0625 in, so the stated 0.094 in local thickness must be checked against the adapter section. As the axial service force is not yet established, these calculations do not establish an in-service retention factor of safety. The separate rack-interface spring pins transmit torque and require an independent assessment. Regardless, these force values at failure are extraordinarily high for a steering column, so even without a load case, can be assumed to be adequate.

Fatigue and Stress Concentrations

The steering shaft is subjected to repeated torque reversals, making the transition into the double-D profile and the welded collar important fatigue details. Without a verified loading history or final notch radii, a life prediction would be premature. We can instead determine the corrected material endurance strength that would be needed under different assumed reversing-torque amplitudes:

$$S_{e,\tau,\mathrm{req}} = n_f K_f \tau_{a,\mathrm{nom}}$$

For an illustrative fatigue factor of safety of 2, a hypothetical fully reversed torque of ±14.444 N·m produces about 33.1 MPa of nominal peak double-D shear. Required corrected torsional endurance strength would then be about 99 MPa for K_f = 1.5, or 132 MPa for K_f = 2.0. If the hypothetical amplitude were ±23.698 N·m, these requirements increase to approximately 163 and 217 MPa. The factored parked torque is a structural test case, not a measured cyclic load amplitude.

The transition stress can be bounded separately by considering a range of additional geometric stress-concentration factors:

$$\tau_{\mathrm{local}} \approx K_t \tau_D, \qquad S_{y,\mathrm{req}} \approx \sqrt{3}\,\tau_{\mathrm{local}}$$

Using the preliminary 81.4 MPa double-D shear at the factored parked torque, assumed transition factors of 1.0, 1.5 and 2.0 correspond to nominal local shear sensitivities of 81.4, 122.1 and 162.8 MPa. A finished fillet and profile should be analyzed in 3D before a material-yield or fatigue conclusion is made; the shaft, weld toe and heat-affected zone should not share a single fatigue-strength assumption.

The archived column drawings identify annealed 4130 steel, while the archived secondary shaft drawing identifies normalized 4130. However, these drawings belong to the previous vehicle and do not certify the selected WUFR-27 material stock. We still need to resolve the 4140 designation in the cost table, confirm the current adapter and shaft material, inspect the section controlling pin span and weld throat, and revisit the previous FEA results in which displacement changed much more than peak stress. Those are the remaining structural closeout tasks before final release.*

Steering Performance and Vehicle Dynamics

The current WUFR-27 steering geometry remains based on the WUFR-26 rack, tie-rod and steering-arm hardpoints. The main improvements in this design are directed at mechanical reliability, serviceability and reducing steering-system play rather than making an unvalidated

change to the steering geometry. The steering model has since been extended to compare the nominal rigid mechanism with the additional steering-wheel rotation lost to elastic deflection under an applied torque.

The 1:1 nominal bevel transmission and the recovered 3.5 in/rev input-to-rack relationship are used to convert steering-wheel input into rack travel. The software then solves the left and right tie-rod mechanisms and calculates the projected wheel heading, retaining the nominal toe and camber geometry. For each case, the elastic twist of the four modeled shaft and tube spans is subtracted from the driver's commanded steering input before recalculating rack displacement and both wheel headings.

$$\delta_{j,\,\mathrm{loaded}} = f_j\left(k_r\left[\delta_{\mathrm{in}} - \theta_{\mathrm{elastic}}\right]\right), \quad \Delta\delta_j = \delta_{j,\,\mathrm{loaded}} - \delta_{j,\,\mathrm{rigid}}$$

Figure 5 shows the resulting rigid and elastically loaded wheel-angle curves across the nominal steering input range. The 14.444 N·m cornering, 23.698 N·m parked and 35.547 N·m factored parked values originate from the steering force calculations. Their signs are applied as prescribed resisting torques to illustrate the mechanism's sensitivity; the curves do not include a tire-generated self-aligning moment prediction or a measured steering-wheel effort.

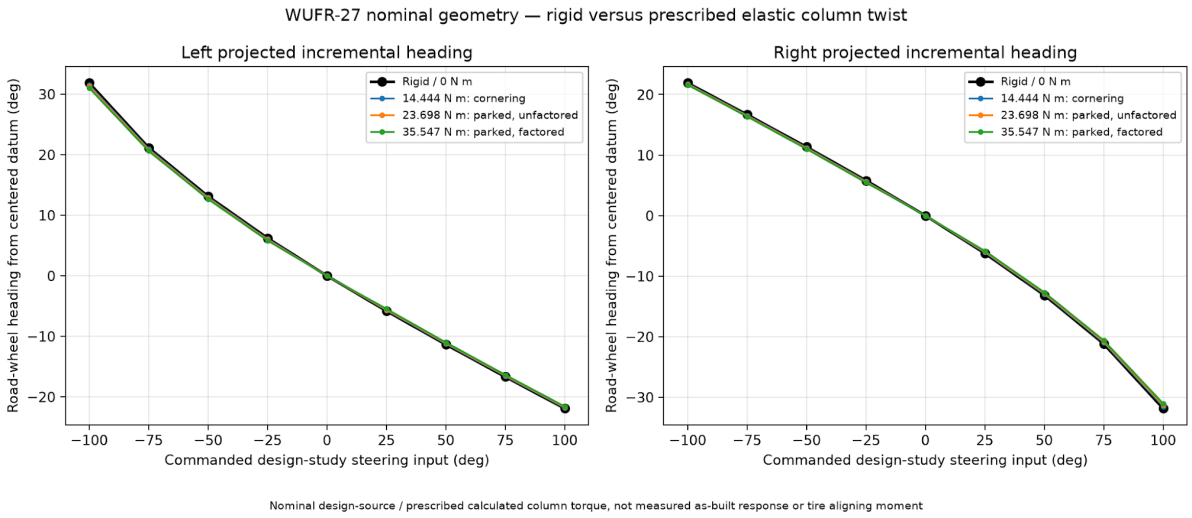

Figure 5. WUFR-27 nominal left and right wheel heading versus steering input, comparing the rigid mechanism with the four-span elastic model at the stated calculated torques. The results use design-source geometry and the nominal rack ratio.

Figure 6 isolates the difference between the rigid and elastic wheel angles. At +75° of commanded input, the predicted differences for the calculated cornering case are approximately +0.135° on the left and +0.227° on the right. Under the unfactored parked case, the changes increase to +0.221° and +0.372°. The already-factored parked case gives approximately +0.332° and +0.557°, respectively. These values describe sensitivity to torsional compliance, not actual tire slip-angle errors in a driven maneuver.

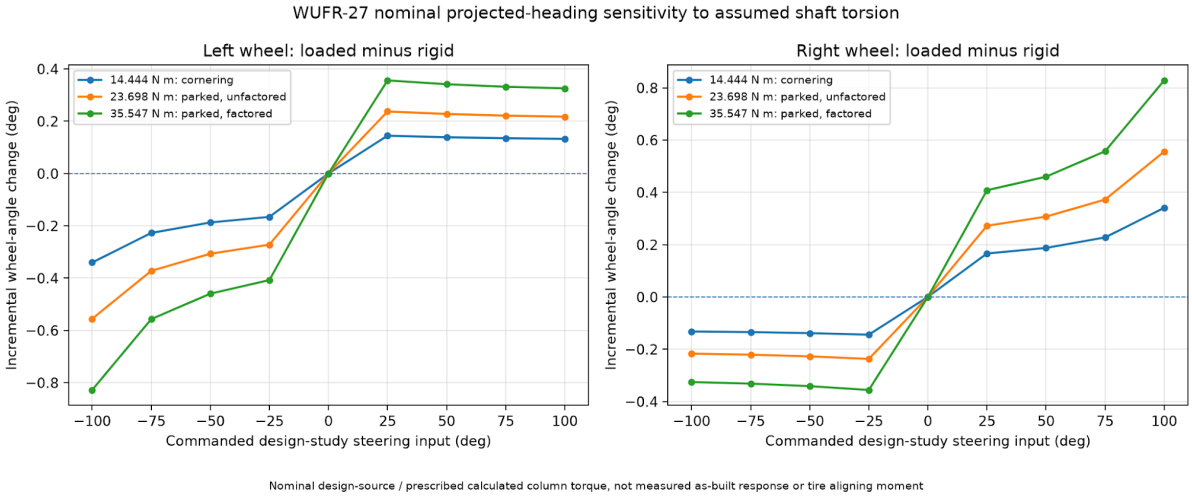

Figure 6. Incremental projected wheel-angle difference between the prescribed elastic and rigid cases. Positive or negative plotted values depend on the defined steering and resisting-torque signs.

The column torsional response is nearly linear in the assumed load range, since the model uses constant steel shear modulus and idealized elastic free spans. Figure 7 shows the resulting input-side twist. The factored structural load case produces approximately 1.571° of predicted column and shaft rotation, while the unfactored parked and cornering cases produce approximately 1.047° and 0.638°. This deflection is separate from free play: a structure can elastically twist under load without exhibiting lost motion when torque is reversed.

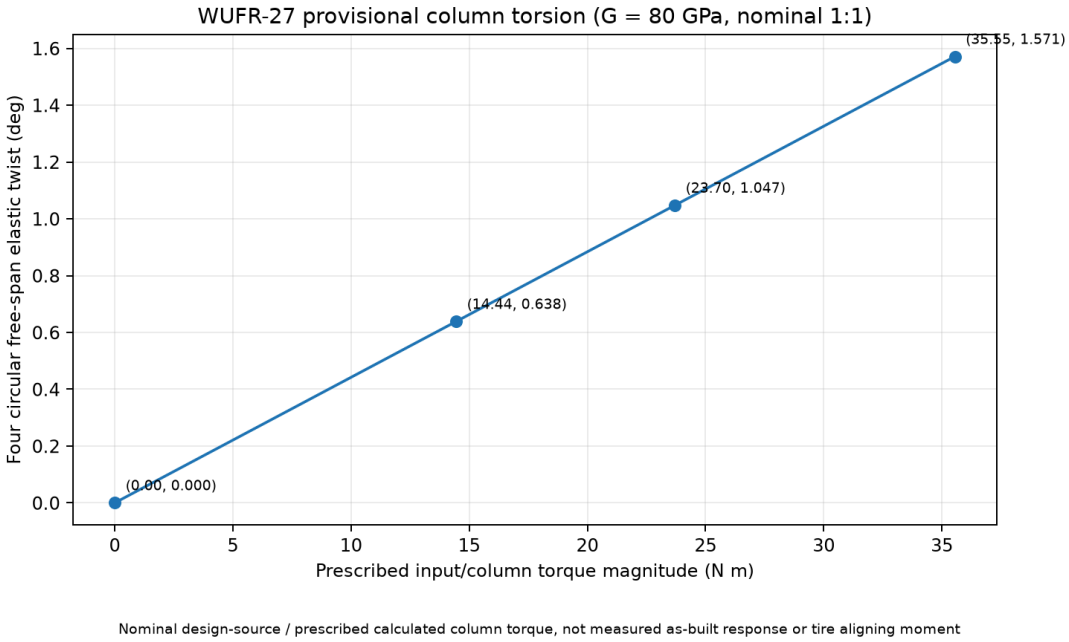

Figure 7. Calculated elastic twist of the four modeled free steel shaft/column sections under the prescribed structural load cases; additional compliance of the double-D joint, gearbox, quick release and rack is not included.

Figure 8 shows how the same modeled twist reduces the effective rack travel for the prescribed resisting-torque scenarios. With the nominal 3.5 in/rev mapping, the 1.571° factored-torque twist corresponds to approximately 0.388 mm of rack displacement difference relative to the rigid prediction. The rack position changes the inside and outside wheel angles by different amounts because the mechanical steering linkage is not perfectly symmetric in its angular response through a turn.

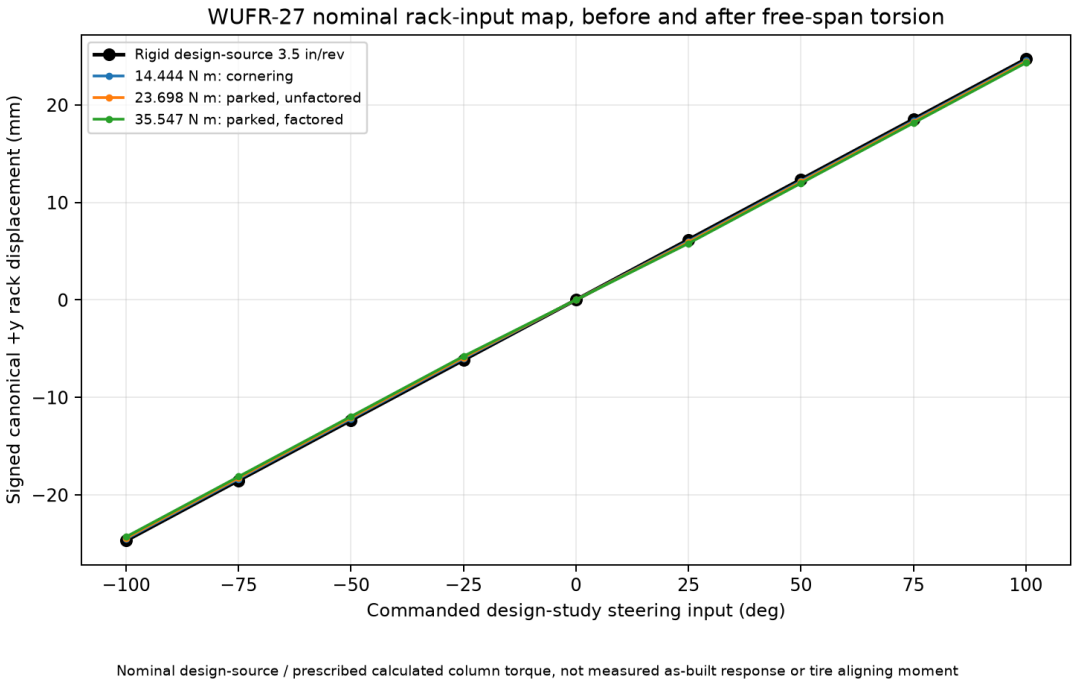

Figure 8. Nominal +y rack displacement as a function of steering-wheel input, showing the rigid mapping and the change associated with the prescribed elastic twist.

The vehicle-dynamics interpretation is important. A change in road-wheel heading affects the tire slip angle only after vehicle velocity direction, yaw rate, wheel location and tire state are accounted for. The tire slip angle that produces a useful lateral force is not a single fixed target over every corner, and therefore these plots are not evidence that one Ackermann percentage is optimal across the vehicle operating envelope. They instead quantify a mechanical steering-compliance effect while holding the nominal geometry fixed. The results support the decision to address known shaft coupling and free-play problems first. A fully coupled prediction would additionally require tire-aligning moments and a verified installed steering system; these comparisons are therefore presented as nominal design predictions for the FDR, not measured vehicle performance.

R&D

1. Retain nominal geometry as the development baseline.



No reviewed physical evidence currently identifies the WUFR-26 nominal rack/tie rod/steer arm geometry as the dominant steering weakness. Carryover avoids introducing a geometry change before the team can evaluate the existing design under synchronized tire, suspension, and vehicle states.

2. Make one rigid mechanism evaluator authoritative.

MOD-STEER-0001 solves each side from rigid tie rod closure over the reviewed rack domain:

$$\|\mathbf{p}_{\text{out}}(\theta_u) - \mathbf{p}_{\text{in}}(x_r)\|^2 - L_{\text{tr}}^2 = 0$$

where x_r is rack displacement, θ_u is upright rotation, and L_{tr} is tie rod length. The solver preserves the intended assembly branch and returns explicit failure for out of domain input, branch loss, singularity, or failed closure. Road wheel steer angle δ is derived from the oriented wheel plane intersected with the road plane, retaining the effects of steering axis inclination and camber.

3. Put optimization downstream of the mechanism.

MOD-STEER-0002 generates bounded symmetric geometry candidates and evaluates every candidate through MOD-STEER-0001. Rack position, inner joint spacing, and steer arm pickup offsets can be varied within declared bounds. Hard infeasibility never receives a compensating objective score. Feasible candidates retain objective decomposition, constraint margins, and local sensitivity instead of being reduced to an unexplained “optimal” point.

4. Use force demand rather than peak slip only logic when source data support it.

The tire interface can invert a monotonic pre peak branch as

$$(F_z,\ \gamma,\ p,\ |F_{y,\text{req}}|) \mapsto |\alpha_{\text{req}}|$$

only inside the supplied source domain. Extrapolation is prohibited. The source specific R25B exporter preserves the WUFR processing route and sign conventions without applying the historical 2/3 track scaling factor.



5. Make steering targets motion aware when vehicle motion is known.

For wheel j at body frame position (x_j, y_j),

$$V_{x,j} = u - ry_j$$

$$V_{y,j} = v + rx_j$$

$$\hat{\beta}_j = \operatorname{atan2}\left(V_{y,j},\, V_{x,j}\right)$$

with the project slip convention

$$\alpha_j = \delta_j - \hat{\beta}_j$$

so the required wheel heading is

$$\delta_{\text{target},j} = \hat{\beta}_j + \alpha_{\text{req},j}$$

Exact low speed Ackermann remains a limiting/reference case when the velocity center lies on the rear axle and required tire slip is zero. The motion aware formulation does not discard Ackermann; it avoids assuming the low speed no slip velocity field after a different vehicle state is known.

Key R&D Result — Ackermann Regime Is State-Dependent

A frozen synthetic benchmark holds the tire operating points and required slips constant while changing only the supplied velocity center position. The same required slips—2.5° for the inside front tire and 9.7143° for the outside front tire—produce a pro-Ackermann wheel pair in one motion state and an anti-Ackermann wheel pair in another.

This is software/kinematic evidence, not a WUFR handling prediction. Its importance is architectural: the tire does not globally “want” one Ackermann percentage. The final left/right wheel heading target depends on both tire slip requirement and the vehicle velocity field.

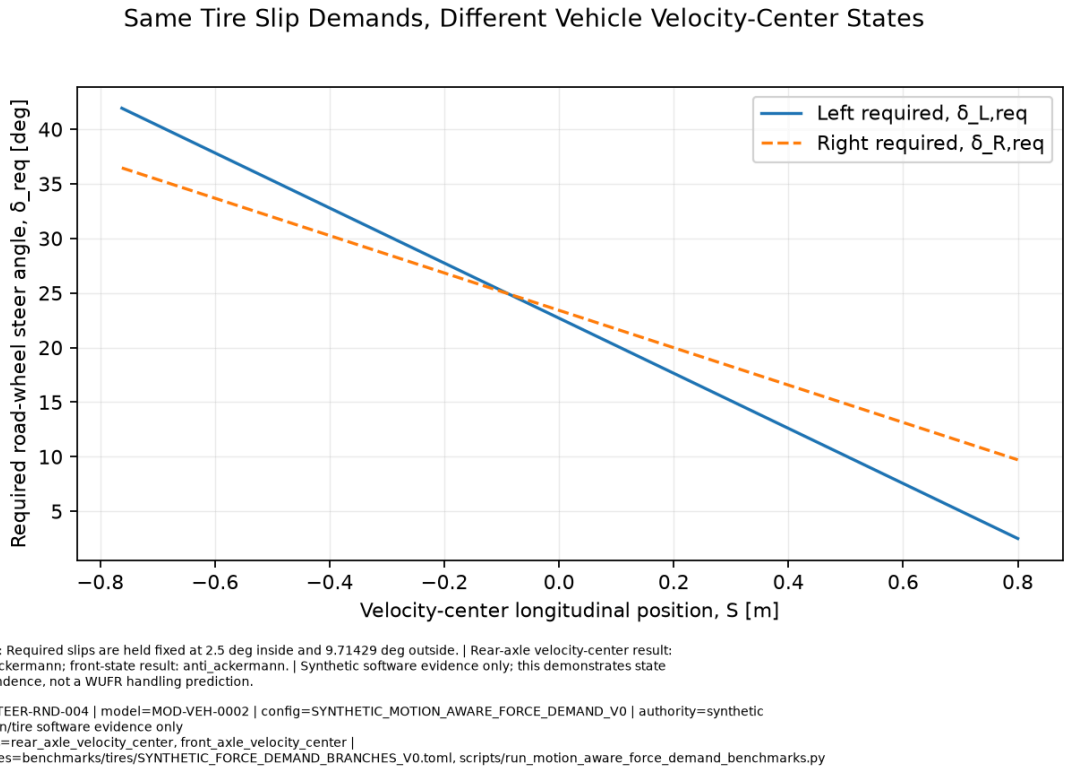

Figure 3. Motion-aware steering benchmark with identical tire slip demands and two velocity-center states. The change from pro- to anti-Ackermann is synthetic verification of state dependence, not a whole-vehicle performance prediction.

Visualization

The R&D visualization layer is downstream of the physics. Static report figures are generated from machine readable results with standard terminology, symbols, units, source/configuration IDs, and explicit authority notes. Missing source data render a visible “FIGURE UNAVAILABLE” diagnostic rather than a blank or inferred plot.

The 3D viewer uses the same principle. MOD-STEER-0001 supplies solved rack and tie rod states to a provider neutral scene; the browser only renders those states. The current steering scene includes the rack, inboard joints, tie rods, outboard joints, steering axes, canonical body axes, rack displacement x_r, upright rotations θ_u,L/R, and tie rod closure residuals ΔL_{tr},L/R. Wheel centers, wheel planes, suspension links, and tire envelopes.

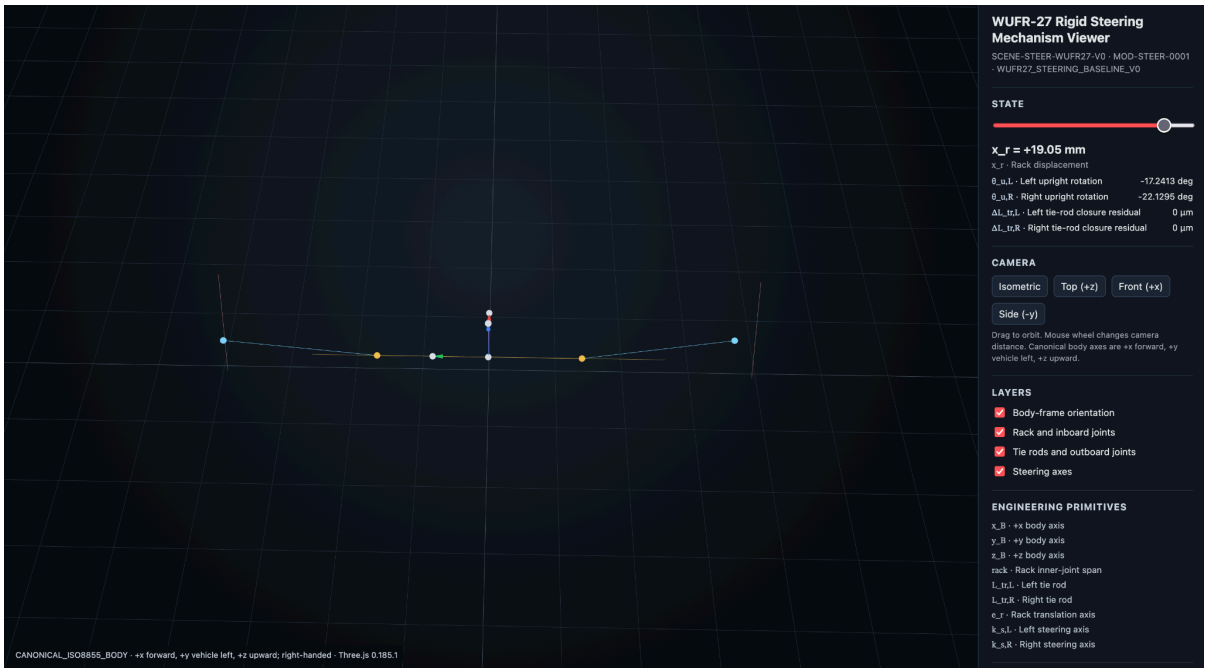

Figure 4. Working WUFR-27 rigid steering mechanism viewer at x_r = +19.05 mm. The displayed geometry is the nominal design-source model and is not an as-built vehicle scan.



WUFR-26 vs WUFR-27 Design Comparison

WUFR-26 vs. WUFR-27 Steering Spec Sheet		
	WUFR-26	WUFR-27
Quick release		
Assembly Weight	171.78 [g]	171.78 [g]
Stiffness	Untested	Not Quantified
Compliance	Untested	Not Quantified
Steering Rack & Mounting		
Assembly Weight	688.98 [g]	510.26 [g]
Stiffness	Untested	Not Quantified
Compliance	Untested	Not Quantified
Tie rods		
Assembly Weight	210.19 [g]	205.55 [g]
Stiffness	Untested	Not Quantified
Compliance	Untested	Not Quantified
Steering Column & Bevel Box		
Assembly Weight	3,284.7 [g]	1,868.62 [g]
Stiffness	Untested	22.63 [N•m/°]



Compliance	0.2223 [°/N•m] Predicted	0.04420 [°/N•m] Predicted
FSA		
System Weight (SolidWorks)	**7.8 [lbs]**	**6.076 [lbs]**
Full System Compliance	**~5° Measured @ Max**	**~1.895° Predicted**

We should test stiffness, compliance, and overall twist for the untested / not quantified ones for future notice.



Steering Column & Bevel Box Backlash Breakdown			
Steering Column			
	Stiffness [N•m/°]	Compliance [°/N•m]	Predicted Twist [°]
Upper Steel Tube	75.44	0.01326	0.471
Lower Steel Tube	55.76	0.01794	0.638
Upper Shaft Span	345.86	0.00289	0.103
Lower Shaft Span	98.87	0.01011	0.360
Ideal double-D joint at 0.0005” clearance	-	-	0.124
Steering Column			
Miter Gear	-	-	0.1146



WUFR-26 vs. WUFR-27 Steering Cost Comparison			
	WUFR-26	**WUFR-27**	**Change Δ**
Part Name			
KHK Gears	$254.62	$254.62	$0
Bevel Box Housing	Didn't Buy	$300	+$300
NaRRco Rack	$600	$600	$1200
Column 4140 Steel	$20	$20	$20
Shafts 4140 Steel	$30	$30	$30
Clevis Pin	$10	$10	$10
Collars / Adapter	$120	Need Quote	Might be less
Welding	Potter	Gabe Labor	Less
Full Subsystem			
Subsystem Total Cost	$914.62	$1,214.62	**+300**

MANUFACTURING

Manufacturing Process

Manufacturing considerations for the column+shaft

Manufacturing the solid shaft to the desired profile is highly straightforward; we would just mill the sides off.

Manufacturing the hollow column to the desired profile might be more complicated; these are some manufacturing approaches involving welding that were considered:

- ☐ Welding d shaped inserts inside a small diameter column is not much feasible due to tool access restrictions and possible blind operation. Also if there are welding beads on the inside wall of the column, they would interfere with the shaft fitting.
- ☐ Holes or slots could be cut on either side of the column and the inserts plug-welded from the outside. This still requires high manufacturing complexity. Accurately positioning the loose inserts would be very difficult. Furthermore, the heat from welding can warp the column or inserts, messing tolerance necessary for the shaft to slide in.
- ☑ What I think would be best is a two piece assembly where one piece is a hollow column and the other a piece with a double d profile (entirely through) machined from a short collar blank. Once the hub is machined from the latter piece the two can be joined via an external full circumference butt weld. A full circumference weld will also distribute torsion well.

Maintaining concentricity would be important, maybe a simple jig if necessary.



Part Timeline/Expectations: Outsourced Parts					
Component	**Supplier & Location**	**Quantity**	**Lead Time**	**Order Date**	**Expected Ready Date**
Gears	KHK	2	2 Weeks	ASAP	Before CoG
Bevel Box Housing	Rapid Direct	2	2 Weeks	ASAP	Before CoG
Rack	NaRRco	2	2-5 weeks	ASAP	Before CoG
Clevis Pin	McMaster	2	1-2 Weeks	ASAP	Before CoG

Part Approval Process (PAP)

The solid shaft double-d can be milled conventionally. The internal column profile is the difficult feature. The preferred provisional process is a machined collar plus tube, fixtured for concentricity and joined externally.

Manufacturing capability and wire-EDM decision

The mating male and female double-D profiles have a common nominal major diameter of 0.590 in, across-flats dimension of 0.472 in, and minimum intended engagement of 0.375 in. The steering torque is carried by the double-D flats; the transverse 1/8-in clevis pin provides axial retention, not primary torsional drive.

The team's feasible in-house across-flats machining capability is approximately +/-0.005 in (five thousandths) per feature. This is a PROCESS CAPABILITY, NOT an acceptable released FIT TOLERANCE. If both mating components are independently produced to +/-0.005 in around the same nominal size, their relative across-flats difference can span -0.010 to +0.010 in: one extreme may prevent assembly, while the other may produce excessive looseness. For scale only, a simplified flat-contact clearance sensitivity of about 0.162 degrees per 0.001 in yields about 1.62



degrees at 0.010 in clearance PER CONNECTION; this is not a validated worst-case backlash calculation. Accumulated play from two joints, bevel box, rack, and quick release must be assessed separately.

MANUFACTURING RECOMMENDATION: Do not machine the precision internal female double-D adapter bore in-house to the existing +/-0.005 in capability when a low-backlash sliding fit is required. Outsource the female profile to wire EDM (or a demonstrably equivalent precision process), with actual male profile measurements used to establish matched-fit dimensions. The nominal profile should remain identical before tolerancing; the final male/female dimensional limits, achievable EDM tolerance, minimum positive running clearance, and maximum acceptable rotational backlash must be specified and verified before drawing release. Avoid an unqualified zero-clearance or interference specification for a hand-assembled service joint.

Part approval requires independent inspection of both mating profiles, hand-assembly without forcing, verification of >=0.375 in functional engagement after welding, and measured bidirectional angular lost motion at the completed D interface. These controls are intended to justify an outsourced precision machining operation rather than imply that wire EDM automatically guarantees a fit.

Part approval must include:

- Shaft flat depth and symmetry;
- Across flat size and fit class;
- Engagement length;
- Angular backlash before assembly;
- Pin-hole diameter, position, edge distance, and retention;
- Column straightness and runout;
- Weld size, penetration, visible defects, and post-weld distortion
- Fit through the upper steering support and cockpit template envelope;
- Assembly inspection with the actual quick release and bevel-box shafts.

Calipers alone probably aren’t sufficient for the internal double-d. Go/no-go gauges, gauge pins, optical measurement, CMM inspection, or a dedicated mating master should be considered. PROBABLY NOT CMM if machined in house but we’ll throw it on there for good measure.

TESTING VERIFICATION AND VALIDATION

Component Testing

The steering R&D stack is verified through deterministic unit tests, source contract tests, exact limiting cases, branch preservation tests, bounded interpolation and inversion, tie-rod closure residuals, and explicit failure on invalid or out of domain requests. Figures and viewer scenes are generated from machine readable results with recorded source/configuration identity.

Before installation, the shaft/column joint should be tested for:

- measurable backlash at low torque;
- torque capacity above the validated design load;
- repeated reversing cycles;
- wear or fretting after cycling;
- pin retention and service removal;
- repeatable angular indexing after disassembly;
- weld or joint inspection before and after testing.

The pass/fail values still need to be finalized. At minimum, total steering backlash must remain comfortably below 7°, and Vehicle Dynamics down the road should set a stricter internal target so compliance is not consumed by one joint.

Part Testing

The next model level validation steps are not additional steering equations. They are source correlations:

- Regenerate and archive engineering figures from the authorized source backed R25B branches; retain the exact operating state and source authority metadata in each artifact manifest.
- Build the suspension kinematics evaluator and reproduce reviewed OptimumK channels before promoting its zero steer upright poses;
- Feed synchronized suspension, tire, and vehicle operating states through the existing steering interfaces;
- Compare future candidate behavior against the retained WUFR-27 baseline using the same evaluator and reporting path.



Full Car Testing

The installed validation chain should measure:

- Steering wheel angle → rack displacement → left/right road wheel angle.

Bidirectional sweeps should quantify backlash, hysteresis, compliance, repeatability, and left/right asymmetry. Rack stops, tire clearances, chassis clearances, and linkage inversion margins must be measured physically rather than inherited from nominal CAD.

The added rotary steering sensor on the primary shaft, combined with the existing linear rack sensor, can help separate upper column free play from rack and linkage motion. Wheel angle measurement can be added using alignment equipment, optical targets, or temporary angle fixtures.

FDR resume path for tire informed steering

The tire informed steering path resumes only when a reviewed synchronized target state package supplies, for every steering sample used in a target:

- front inside/outside F_z;
- Inclination;
- gauge pressure;
- F_y demand;
- Suspension pose;
- Planar u, v, and r;
- Explicit nonzero state weighting;
- Source identity and units.

A reviewed QSS or vehicle simulation could satisfy this requirement. Until then, geometry ranking from the R25B proxy remains unauthorized.

Maintenance and Repairs

The steering system is considered endurance critical. A failure that disconnects a steering joint, allows the rack or bevel box to move, produces binding, or creates excessive free play can prevent the vehicle from safely operating. Any crack, missing retention feature, loose critical fastener, abnormal steering effort, sudden increase in play, damaged rod end, or incomplete



quick release engagement should remove the vehicle from service until the cause is identified and corrected.

Before every run, the quick release should be visually and tactilely checked for complete engagement and verified with an axial pull test. The steering should be swept slowly from stop to stop with the front wheels unloaded and on jacks to check for binding, roughness, interference, or asymmetric effort. Critical fastener witness marks, rack mounts, rack stops, bevel box mounts, tie rod fasteners, rod ends, jam nuts, clevis pin retention, and steering column supports should be inspected. Tie rod thread engagement and static toe should also be checked whenever an adjustment has been made.

Total steering free play should be measured and recorded at initial assembly, before each competition, and whenever the driver reports a change in steering feel. The final internal freeplay limit has not yet been selected, but it should remain comfortably below the 7° rules limit. Bidirectional measurements using the rotary primary shaft sensor and linear rack sensor can help separate quick release and column joint play from bevel box, rack, tie rod, or wheel end motion. A sudden change from the recorded baseline should trigger a detailed inspection rather than being treated as normal wear.

After each testing day, the steering system should be inspected for loose fasteners, shifted witness marks, rod end play, tie rod damage, rack mount movement, corrosion, fretting debris, lubricant leakage, and damage to cable routing. A separate inspection is required after any wheel impact, curb strike, crash, steering lock up, unexpected overload, or wet event. Post impact inspection should include the tie rods, rack mounts, rack stops, rod ends, chassis tabs, bevel box truss, shafts, column supports, and wheel angle alignment.

The bevel box and double-d coupling should be periodically disassembled for inspection. The exact service interval should be finalized after cyclic and vehicle testing establishes a wear rate. Until then, teardown should occur before each competition, after substantial wet exposure, after a major impact, or whenever backlash or steering effort changes. Inspection should include geartooth condition, contact pattern, backlash, shim stack condition, bearing play and running torque, lubrication, shaft corrosion, double-d contact face wear, galling, fretting, clevis pin and pin hole condition, weld cracking, and post weld runout.

Service procedures should preserve the recorded shim stack, shaft indexing, spacer arrangement, tie rod length, and fastener orientation. Reassembly should be followed by a quick release pull test, full travel sweep, freeplay measurement, rack center confirmation, toe check,

and verification that the positive stops prevent interference or linkage inversion throughout bump and droop.

The intended bevel box service tool set remains the 3/16 in hex key, 7/16 in wrench, and 5/16 in wrench, subject to final hardware selection. The clevis pin retention should remain removable without introducing the overtightening risk of the previous setscrew arrangement. Recommended steering spares include clevis pins and keepers, approved locknuts and critical fasteners, bevel gear shims, rod ends and misalignment spacers, lubricant, a matched bevel gear set, and a verified spare steering rack. Replacement parts should not be installed without repeating the applicable fit, backlash, torque, and full travel checks.



TECHNICAL ORGANIZATION

Item	Description	Needs Work	Pass
BOM	Are parts, materials, and fasteners in the Bill of Materials spreadsheet? Do parts have correct Part Numbers? Does it follow the correct Cost Report categories? Are quantities and vendors correct?	☐	☐
CAD	Does it follow good modeling practices (named parts and folders in the tree, proper mates instead of fixed components)? Does it have rebuild errors? Does it have Full Car Model (FCM) configurations? Is it placed in relation to the frame planes correctly? Are all components in the CAD? Does it match its real life counterpart? Are part properties filled out? Intersections?	☐	☐
Drawings	Do all parts have drawings? Have all machined parts been reviewed? Do drawings follow team standards? Do all assemblies have drawings? Have leads signed off on drawings? Are tolerances considered for machining, fitment, and stacking? Are bounding boxes listed?	☐	☐

:

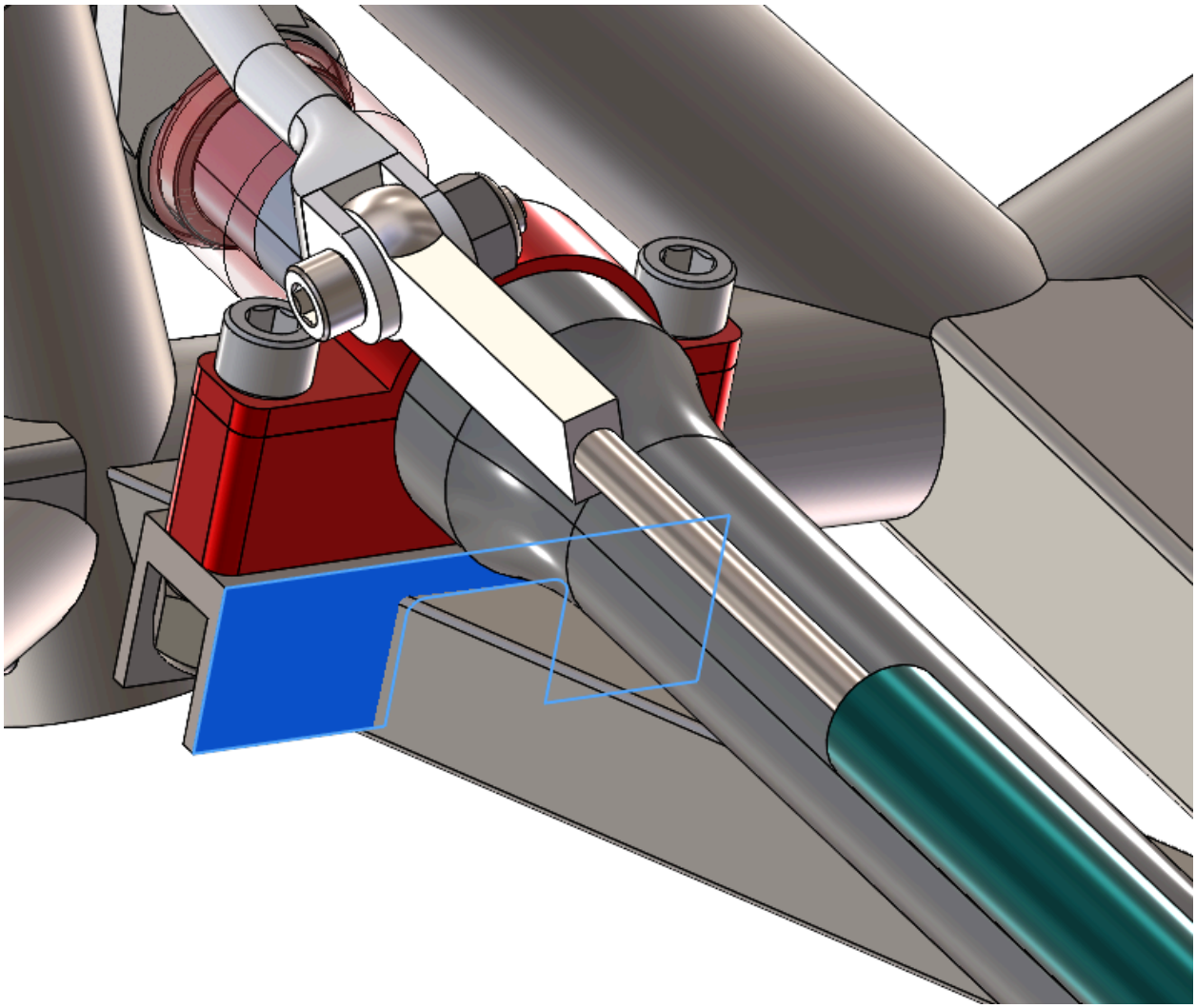



SIGNATURES

Designer(s): Jesse Koeppel, Lumi Lee

System Lead(s): Jesse Koeppel

Exec Member: _____

Exec Member: _____

DESIGN MATERIALS/APPENDIX

Math/Equations

Evaluation of shaft/column profiles

To ensure the structural integrity of the steering column assembly, the max torsional shear stress in each component must remain below the shear yield strength of the respective material:

Shaft: 4130 normalized steel, max shear yield 251 MPa

Column: 6061-T6 Aluminum, max shear yield 159.3 MPa

The assembly features four distinct cross-sectional regions across its length:

1. Solid circular shaft (4130 steel, main span)
2. Double-d shaft profile (4130 steel, joint interface)
3. Double-d hollow sleeve (6061-T6 aluminum, joint interface)
4. Hollow circular column (6061-T6 aluminum, main span)

(Granted, other regions may be weaker and need to be checked also: stress concentrations where the profile changes, or the weld at the column if it's manufactured as described later.)

Because the assembly transitions between two different materials, bounding cases were established for the shaft and column separately:

Profile 4 is the bounding case for the column; geometrically, they share the same outer tube profile but profile 3 has material added inward, increasing torsional rigidity. Evaluating profile 4 will give a conservative lower bound.

Profile 2 represents the bounding case for torsional stress on the shaft. Removing material from the outer diameter reduces its stiffness, concentrating torsional shear stress at the outer flats.

Profile 4 outer diameter selection & max stress calculation:

- New outer diameter selection: To compensate for 6061-T6 aluminum's lower shear modulus, and outer diameter of .9" is selected.
- With new dimensions and T=35547 Nmm, max shear stress is calculated to be 19.94 MPa. This is only 7.99% of allowable yield for aluminum.



Profile 2 flat depth selection & max stress calculation:

Angle of Twist

The overall torsional compliance of the column+shaft assembly is additive:

$$\phi_{total} = \phi_{column} + \phi_{overlap} + \phi_{shaft}$$

Segment by segment analysis:

ϕ_{column}: Increasing the outer column diameter from .75” to .9” increases J_{column}, which compensates for the lower shear modulus of the new material.

$\phi_{overlap}$: Because the stiffness acts in parallel, stiffness here adds up and $\phi_{overlap}$ is very small.

ϕ_{shaft}: The exposed shaft remains a full circular cross section, maintaining max solid circular torsional rigidity.

Because the overlap area is very stiff, compliance in the system will likely be more due to mechanical play that from the fit of the flat to the bore than due to elastic deformation, hence attention should be given to tolerance.

$$\phi_{total} = T \cdot \left[\frac{L_1}{G_{St} J_1} + \frac{L_{overlap}}{G_{St} K_2 + G_{Al} K_3} + \frac{L_4}{G_{Al} J_4}\right]$$

Inputs

- Torque T= 35547 Nmm
- Free column length L_4 = 4.765”
- Overlap length $L_{overlap}$ = 0.375”
- Free shaft length L_1 = 5.71”
- J_1, K_2, K_3, J_4: Since noncircular cross sections experience warping which can overestimate torsional rigidity, a correction factor from Roark’s table was used for K_2, and K_3 estimated using K_2 ($K_3 \approx J_{outer} - K_2$).

$\phi_{column} = 0.46°, \phi_{overlap} = 0.04°, \phi_{shaft} = 1.45°$



$\phi_{total} = 1.95°$

*this is an estimation and I think solidworks FEA like in last years FDR will be valuable for the FDR once there is cad

option	Outer diameter	density	Shear modulus	Column twist	Total twist	tradeoff
6061-t6	0.9”		26 GPa	0.46°	1.95°	Weight reduction and simple manufacturing, matches baseline stiffness
CFRP ($\pm$ 45°)	0.9”	1.60	35 GPa	0.33°	1.83°	Smallest twist and weight, but requires bonded inserts for joining
Steel (baseline)	0.75”		80 GPa	0.47°	1.96°	baseline

While carbon fiber tubes offer the lowest compliance (0.12° reduction) and 29.2g in weight savings compared to aluminum, it has other tradeoffs:

- Aluminum allows direct machining of the internal double-d socket and directly accommodates standard axial retention features such as a clevis pin without structural damage / delamination.
- CFRP requires metal inserts due to stress concentrations which adds back mass.

Weld failure

Approximating the weld as as a thin walled ring, the weld-as-line method (table 5 in section 7.4-7) gives $J_{weld} \approx 2\pi R_{avg}{}^{3} t_{weld}$. Using J calculated as such, $\tau_{max} \approx 105.1\ MPa$ for the weld. Common welding materials for aluminum are ER4043 and ER5356 filler metal. The allowable



shear stress of the the former metal is less than our τ_{max}. For the latter, there is a FoS of 1.11 which isn't very large but I think the T value used to get τ_{max} already had a factor of safety applied to it? An option to increase this FoS could be slight weld crown reinforcement. ER4043 should not be chosen.

torsional fatigue analysis

Shafts:

Steering shafts experience fully reversed cyclic torsion over use, requiring fatigue analysis. To guarantee infinite life, Marin modification factors were applied to estimate the torsional endurance limit from the ultimate tensile strength of steel (670 MPa).

$$S_{se} = k_a \cdot k_b \cdot k_c \cdot k_d \cdot 0.577 S_e'$$

- Surface factor (machined profile) $k_a \approx 0.70$
- Size factor $k_b \approx 0.90$
- Torsional load factor $k_c \approx 0.59$
- Uncorrected endurance limit $S_e' \approx 0.5\, S_{ut}$

We get $S_{se} \approx 124.5\ MPa$ which is 1.79 times greater than the 69.4 MPa we calculated above for max shaft stress.

Columns:

Because the columns are aluminum, with no true endurance limit, they cannot be assessed in the same way as the steel shafts. Thus, evaluating fatigue strength at a finite life of N = 5x10*8 cycles, which would be well over a year/one WUFR season:

$$S_{sf} = k_a \cdot k_b \cdot k_c \cdot S_f'$$

- Fatigue strength or N=5x10*8, $S_f' = 96.5\ MPa$
- Surface factor $k_a \approx 0.83$
- Size factor $k_b \approx 0.90$
- Torsional load factor $k_c \approx 0.577$



Gives 41.6 MPa, which is 2.09 times greater than the 19.94 MPa calculated above for max column stress.

Roark's formula for noncircular shaft

$\tau_{max} = \frac{TB}{r^3}$ where

$B = 0.6366 + 2.5303\frac{h}{r} - 11.157(\frac{h}{r})^2 + 49.568(\frac{h}{r})^3 - 85.886(\frac{h}{r})^4 + 69.849(\frac{h}{r})^5$

Weld Static failure

- Outer radius $R_{out} = 9.525\ mm$
- Average radius $R_{avg} = (R_{out} + R_{in}) / 2 = 8.763\ mm$
- Weld throat thickness $t_{weld} = R_{out} - R_{in} = 0.762\ mm$
- Approximating as a thin walled ring, $J_{weld} \approx 2\pi R_{avg}^3 t_{weld}$ (from table 5 in section 7.4-7)
- $J_{weld} \approx 3222\ mm^4$
- $\tau = \frac{T \cdot R_{out}}{J_{weld}} \approx 105.1\ MPa$

Additional steering software and joint mathematics

Rigid tie-rod closure and road-wheel heading

For side s ∈ {L,R}, the mechanism solves

$$g_s(\theta_{u,s}, x_r) = \|\mathbf{p}_{\text{out},s}(\theta_{u,s}) - \mathbf{p}_{\text{in},s}(x_r)\|^2 - L_{\text{tr},s}^2 = 0$$

Here x_r is rack displacement, $\theta_{u,s}$ is upright rotation about the steering axis, and $L_{tr,s}$ is tie-rod length. The intended assembly branch is preserved; absence of a valid root, branch loss, singularity, or excessive closure residual is a hard failure rather than an objective penalty. If n_w,s is the oriented wheel-plane normal and k = [0,0,1] is the road-plane normal, the wheel-plane/road-plane intersection direction may be written

$$\mathbf{t}_s = \text{normalize}(\mathbf{k} \times \mathbf{n}_{w,s}), \qquad \delta_s = \text{atan2}(t_{y,s}, t_{x,s})$$

with orientation selected consistently with the project wheel heading convention. This retains steering axis inclination and camber rather than treating upright rotation as road wheel steer directly.



Bounded tire force-demand inversion

The reviewed tire interface evaluates

$$|\alpha_{\text{req}}| = B^{-1}\left(F_z,\ \gamma,\ p,\ |F_{y,\text{req}}|\right)$$

where B is a selected strictly monotonic pre peak source branch. The signed source branch is selected before projection to magnitudes. Inversion is permitted only within the authorized normal load, inclination, pressure, slip-angle, and force domains. No force extrapolation, nearest-state substitution, hidden zero anchor, smoothing, or track scaling is introduced.

Motion-aware target heading

For wheel j at body-frame position (x_j, y_j),

$$V_{x,j} = u - r y_j$$

$$V_{y,j} = v + r x_j$$

$$\hat{\beta}_j = \operatorname{atan2}\left(V_{y,j},\ V_{x,j}\right)$$

Using the project convention $\alpha_j = \delta_j - \hat{\beta}_j$ the required road-wheel heading is

$$\delta_{\text{target},j} = \hat{\beta}_j + \alpha_{\text{req},j}$$

Exact low-speed Ackermann is recovered as a limiting reference when the velocity center lies on the rear axle and $\alpha_{req} = 0$; it is not assumed after another vehicle motion state is supplied.

Circular tube torsion and elastic compliance

For a hollow circular tube,

$$J_{\text{tube}} = \frac{\pi}{2}\left(r_o^4 - r_i^4\right)$$

$$\tau_{\max} = \frac{T r_o}{J_{\text{tube}}}$$

$$\phi = \frac{TL}{GJ_{\text{tube}}}$$

For several shaft/column segments in series,

$$\phi_{\text{total}} = \sum_i \frac{T_i L_i}{G_i J_i}$$

This predicts elastic twist only. Mechanical clearance, backlash, fretting, bearing play, gear lash, and hysteresis must be measured separately and cannot be justified by a low elastic-stress result.

Double-D flat geometry and simplified bearing screen

Let r be the original shaft radius, w the center-to-flat distance, h the removed flat depth, W the chord width, and L_e the engaged length:

$$h = r - w$$

$$W = 2\sqrt{r^2 - w^2}$$

For a symmetric two-flat load share, a first-order contact-force screen is

$$F_{\text{flat}} \approx \frac{T}{2w}$$

$$p_b \approx \frac{F_{\text{flat}}}{WL_e} = \frac{T}{2wWL_e}$$

$$L_{e,\min} \approx \frac{T}{2wWp_{\text{allow}}}$$

This is a sizing screen, not a complete contact solution. Edge loading, fit clearance, shaft/collar deformation, surface condition, manufacturing error, and reversing-cycle wear require tolerance analysis and physical testing.



Circumferential weld-group torsion

For a thin circular weld line of mean radius r_m,

$$J_{w,\text{line}} = \oint r^2 \, \mathrm{d}s = 2\pi r_m^3$$

$$q = \frac{T r_m}{J_{w,\text{line}}} = \frac{T}{2\pi r_m^2}$$

$$\tau_w = \frac{q}{t_w} = \frac{T}{2\pi r_m^2 t_w}$$

where q is weld shear flow and t_w is effective throat thickness. The allowable torque must be based on the governing filler/base-material/heat-affected-zone condition, and the applied torque must state clearly whether a load factor is already embedded. For the current geometry screen, the already-factored parked torque corresponds to 74.21 N/mm of ideal weld shear flow. Without an established effective throat, weld/base-metal strength and local stress concentration, no complete weld-joint factor of safety has been verified.

Final Steel Double-D and Retention Calculations (WUFR-27)

The equations below supplement the original shaft and column material study, which remains above without changes. They apply to the selected steel joint with a nominal 0.590 in shaft major diameter, 0.472 in across flats and at least 0.375 in of engaged length. The current cornering, parked and factored parked column torque calculations are 14.444, 23.698 and 35.547 N·m, respectively. The factored parked value already includes the workbook's 1.5 load factor.

Double-D fit and contact

The profile dimensions are shown in the earlier double-D geometry equations. For the male and female parts, the minimum and maximum across-flats clearances follow from the respective dimensional tolerances:

$$C_{\min} = C_0 - t_m - t_f, \qquad C_{\max} = C_0 + t_m + t_f$$



The following geometric relation estimates the angular take-up between perfectly concentric profiles as the male corners approach the female flats:

$$\theta_{\text{one}} = \sin^{-1}\left(\frac{a + C/2}{R}\right) - \sin^{-1}\left(\frac{a}{R}\right), \quad \Delta\theta_{\text{bi}} = 2\theta_{\text{one}}$$

The first angle is the take-up in one direction; twice that value is the total bidirectional lost motion. For 0.001 in of across-flats clearance this model gives approximately 0.324° of bidirectional play per joint. With an illustrative allowance of 0.5° per joint, the maximum actual clearance would be approximately 0.00154 in. Those values are fit-design sensitivities, not final drawing tolerances. The female socket may be wire EDM, but the male dimension also needs to be measured or controlled, since the team's ±0.005 in machining capability alone does not provide the required fit.

For two equally loaded opposing flats, the ideal minimum normal reaction per flank can be estimated from the maximum available half-chord lever arm:

$$N_{\text{min}} = \frac{T}{2b}, \qquad p_{\text{est}} = \frac{N}{L_e w_c}$$

The already-factored 35.547 N·m case gives a lower-bound reaction of approximately 3.95 kN per loaded flank. This does not determine the true bearing pressure at a clearance-dependent edge contact. The final mating geometry, corner radii, steel properties and contact distribution are still needed to evaluate stress and wear.

Axial pin and lug checks

The double-D transmits torque through the flats while the clevis pin retains the shaft in the axial direction. Assuming the minimum pin diameter is 0.121 in, the local support thickness is 0.094 in, the considered transverse lug width is 0.300 in, and the provisional material yield is 205 MPa with a factor of safety of 3, the nominal shear, bearing and net-section capacities are:

$$F_{\text{pin, shear}} = \frac{2(\pi d^2/4) S_y}{\sqrt{3}\, n_y} \simeq 585 \text{ N}$$

$$F_{\text{wall, bearing}} = \frac{tdS_y}{n_y} \simeq 501 \text{ N}$$

$$F_{\text{net}} = \frac{(w - d_h)tS_y}{n_y} \simeq 725 \text{ N}$$

These give approximately 585 N for double-shear pin capacity, 501 N bearing for one assumed loaded wall, and 725 N for one lug net-section check. They are separate load modes, not a verified axial service-load capacity. Pin bending also depends on the distance between the actual bearing reactions:

$$F_{\text{bend}} = \frac{\pi d^3 S_y}{8 L_s n_y}$$

For illustrative support-center spans of 0.10, 0.25 and 0.50 in, the bending screen gives about 307, 123 and 61 N. The corresponding lug shear-out relation depends on the center-to-free-edge distance along the applied axial withdrawal direction:

$$F_{\text{tear}} = \frac{2t(e - d_h/2)S_y}{\sqrt{3}\, n_y}$$

For a hypothetical 0.094 in steel wall, an actual edge distance of 0.200, 0.367 or 0.687 in would give approximately 658, 1,457 or 2,988 N, respectively. The earlier dimensions have not been associated with confirmed drawing datums. The separate rack-interface spring pins carry torque, so this axial retention calculation cannot be used to rate those joints.

Fatigue and shoulder sensitivity

The shaft experiences load reversals, but the final profile radii, steel condition, and torque-cycle spectrum are not yet defined. We can calculate the corrected endurance strength that would be required under an assumed fully reversed torque and selected fatigue notch factor:

$$S_{e,\,\tau,\,\text{req}} = n_f K_f \tau_{a,\,\text{nom}}$$



At an illustrative fatigue safety factor of 2 and the calculated cornering torque used hypothetically as an alternating amplitude, the provisional double-D peak shear is approximately 33.1 MPa. Corrected torsional endurance requirements would be about 99 MPa for a fatigue notch factor of 1.5 and 132 MPa for a factor of 2.0. These are required-property checks, not fatigue-life predictions.

The additional shoulder stress sensitivity may be written using an assumed transition multiplier:

$$\tau_{\text{local}} \approx K_t \tau_D, \qquad S_{y,\text{req}} \approx \sqrt{3}\,\tau_{\text{local}}$$

A multiplier of 1.0 to 2.0 on the provisional 81.4 MPa factored-torque double-D peak produces 81.4 to 162.8 MPa of local shear sensitivity. The real stress concentration must come from the final radius and geometry or a reviewed three-dimensional model. The weld toe and heat-affected zone require separate consideration. For the circumferential weld, the preceding weld-group equation and the current Design Review calculation use 74.21 N/mm of ideal shear flow at the already-factored 35.547 N·m torque; the actual effective throat has not yet been established.

Physical correlation quantities

The installed measurement chain can be summarized with local gains

$$K_{rx} = \frac{\mathrm{d}x_r}{\mathrm{d}\delta_{\text{SW}}}$$

$$K_{\delta x,L/R} = \frac{\mathrm{d}\delta_{L/R}}{\mathrm{d}x_r}$$

$$\frac{\mathrm{d}\delta_{L/R}}{\mathrm{d}\delta_{\text{SW}}} = K_{\delta x,L/R}\,K_{rx}$$

Forward and reverse sweeps should also report the path difference at matched input, for example $H_x(\delta_{SW}) = x_{r,\text{ forward}} - x_{r,\text{ reverse}}$, so backlash and hysteresis are not folded into an elastic stiffness estimate.

Code/MATLAB/Spreadsheets

FEA/CFD/Simulations

Pictures:	
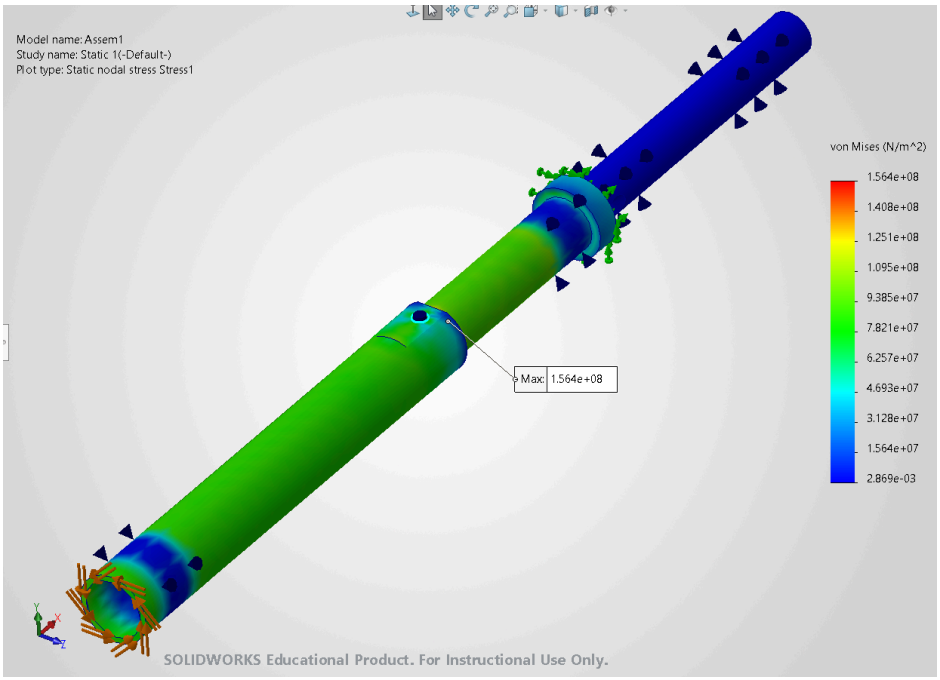Model name: Assem1 Study name: Static 1(-Default-) Plot type: Static nodal stress Stress1 von Mises (N/m^2) 1.564e+08 1.408e+08 1.251e+08 1.095e+08 9.385e+07 7.821e+07 6.257e+07 4.693e+07 3.128e+07 1.564e+07 2.869e-03 Max: 1.564e+08 SOLIDWORKS Educational Product. For Instructional Use Only. 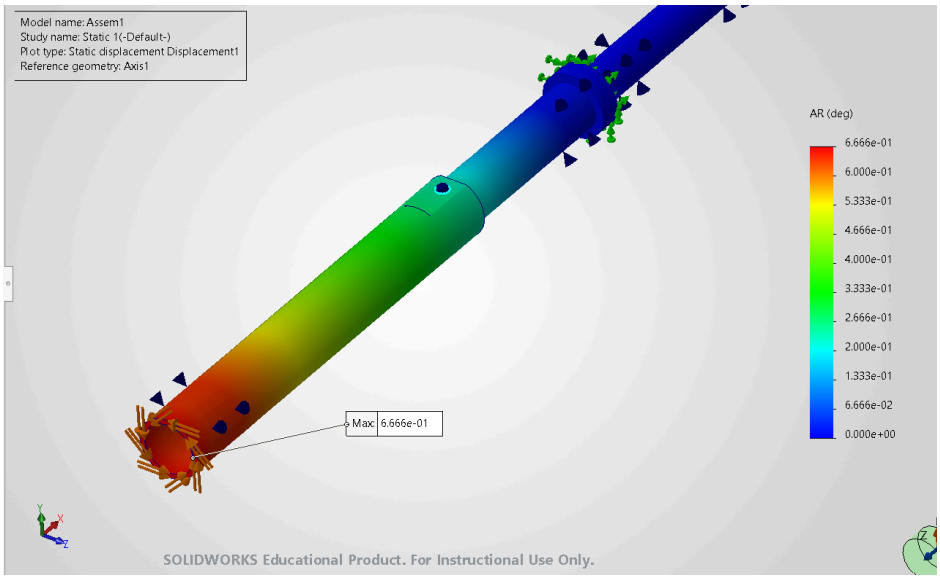Model name: Assem1 Study name: Static 1(-Default-) Plot type: Static displacement Displacement1 Reference geometry: Axis1 AR (deg) 6.666e-01 6.000e-01 5.333e-01 4.666e-01 4.000e-01 3.333e-01 2.666e-01 2.000e-01 1.333e-01 6.666e-02 0.000e+00 Max: 6.666e-01 SOLIDWORKS Educational Product. For Instructional Use Only.	

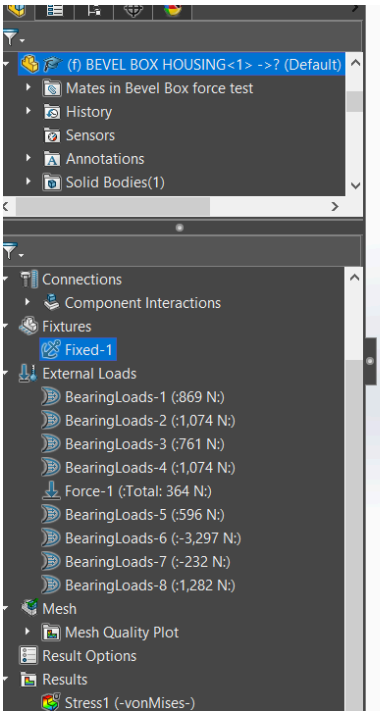

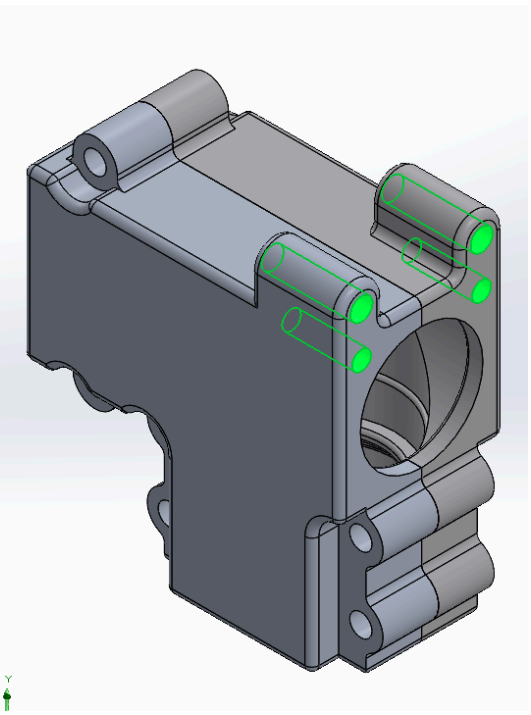

Fixtures

Fixed by the Truss Screws.

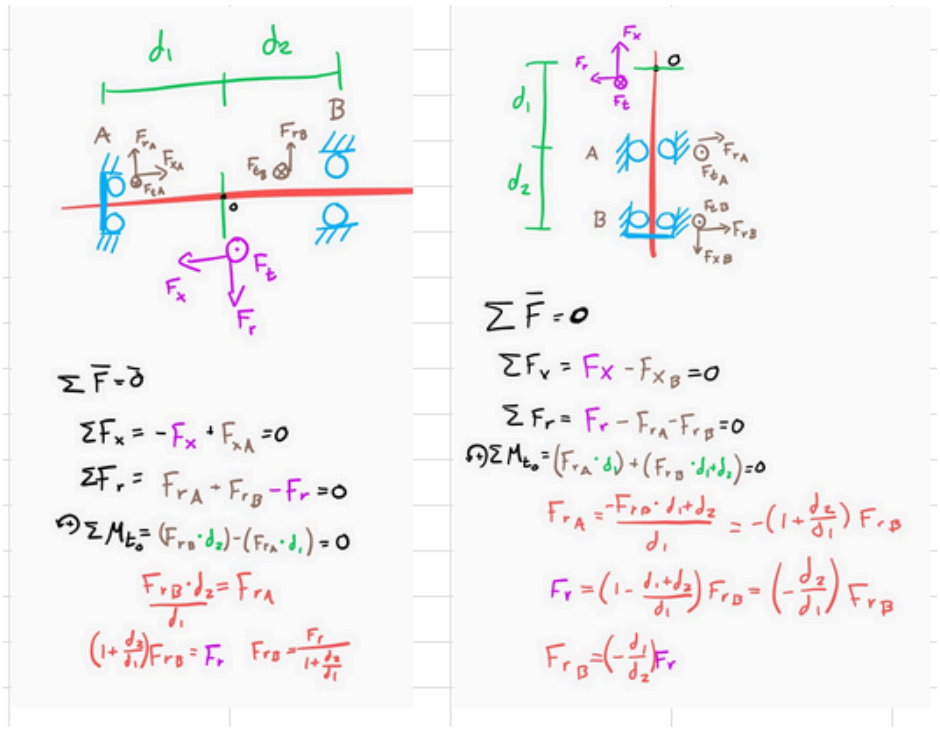

Forces

Bearing forces on all bearing locations. The regular forces come from the axial force retaining the tapered roller bearing.

Force calculations were obtained in the SUS Calculations Steering Column Forces Tab

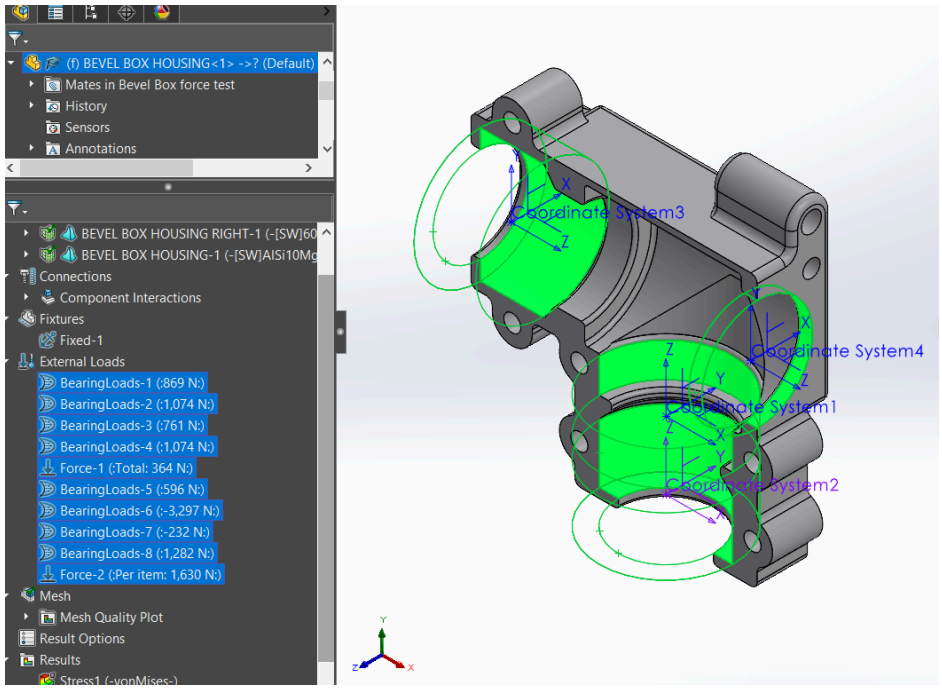

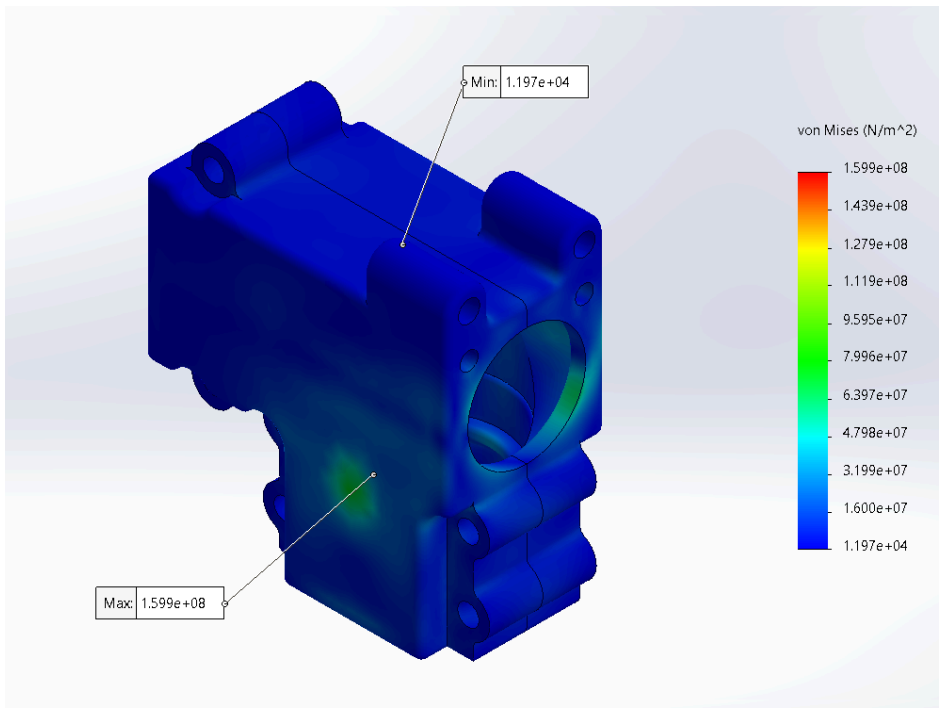

Von Mises stress [ksi]

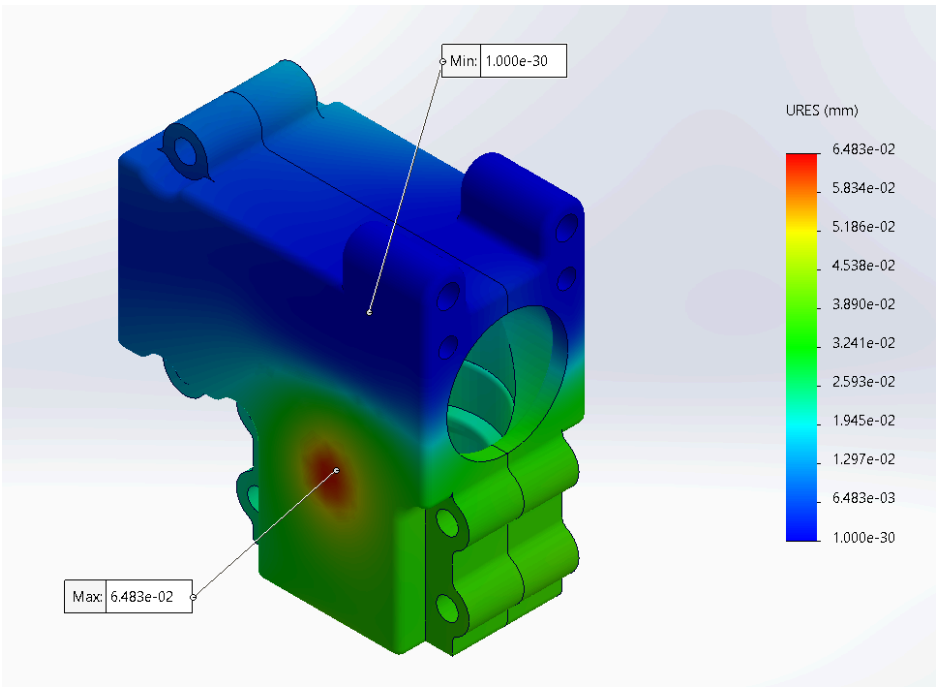

Displacement [in]

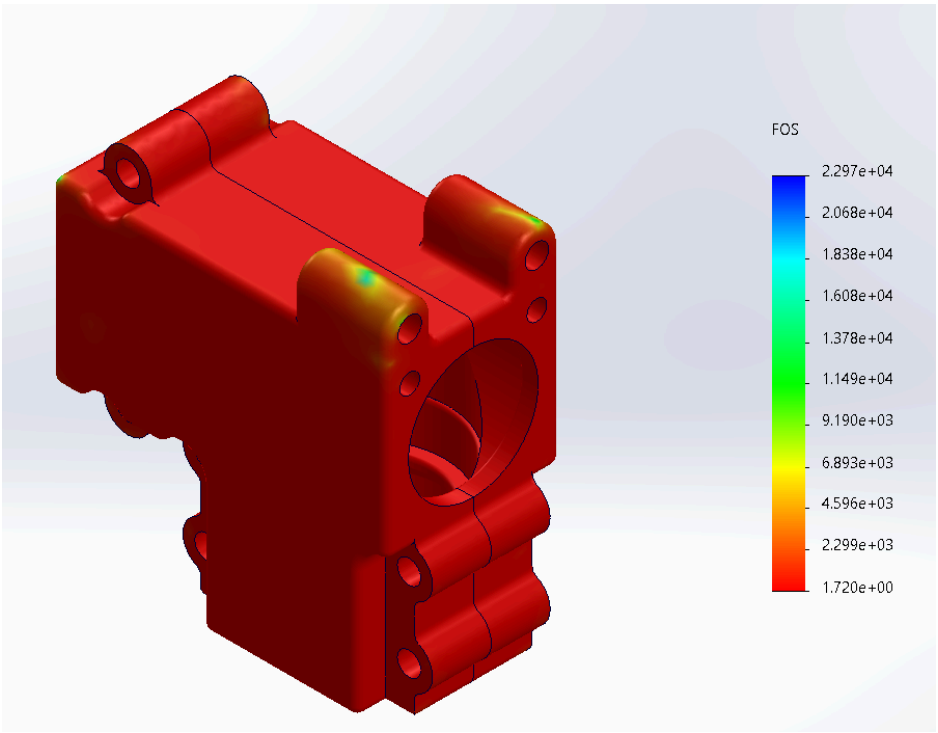

Factor of safety

Pictures:

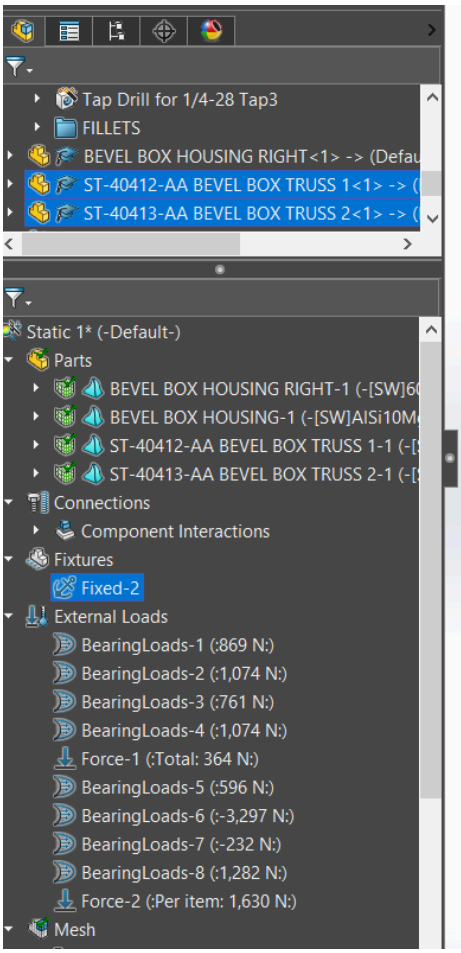

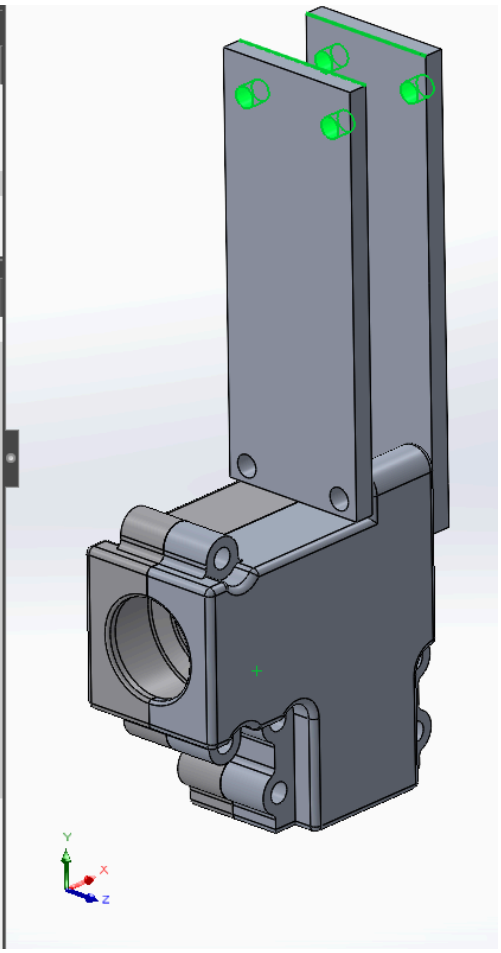

Fixtures

Fixed by the Truss Screws on the frame beam.

Forces

Bearing forces on all bearing locations. The regular forces come from the axial force retaining the tapered roller bearing.

Force calculations were obtained in the WAP SUS Calculations Steering Column Forces Tab

SUSPENSION CAL...

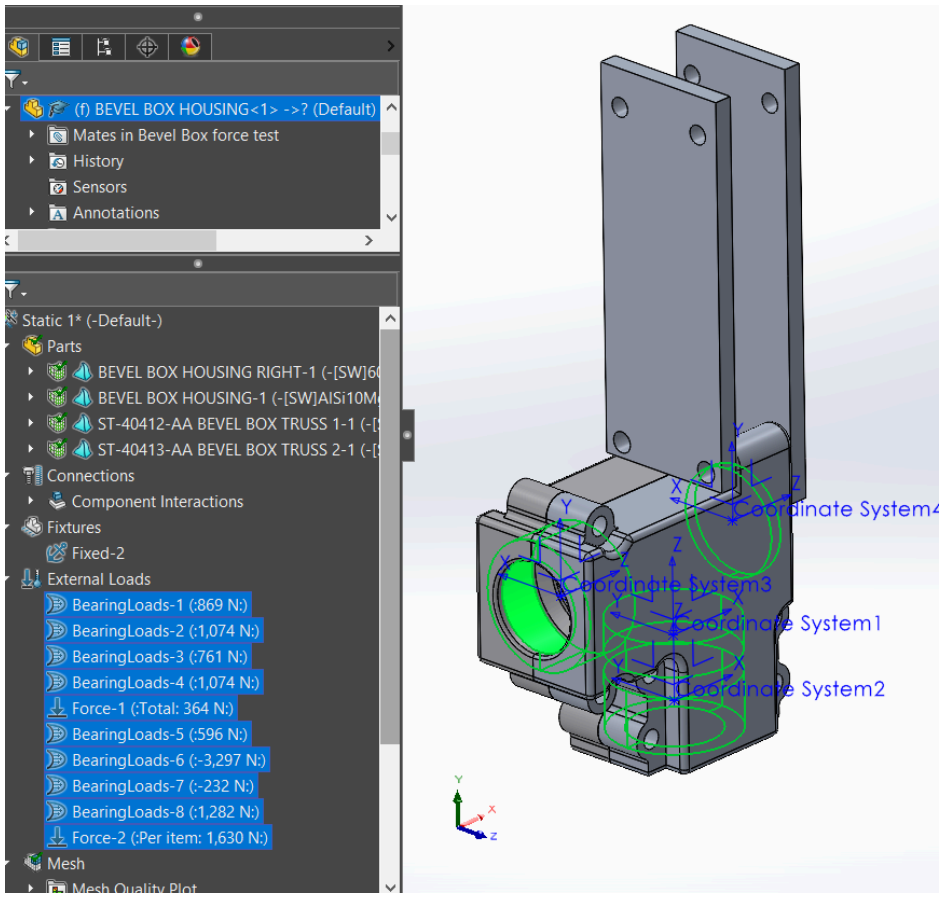

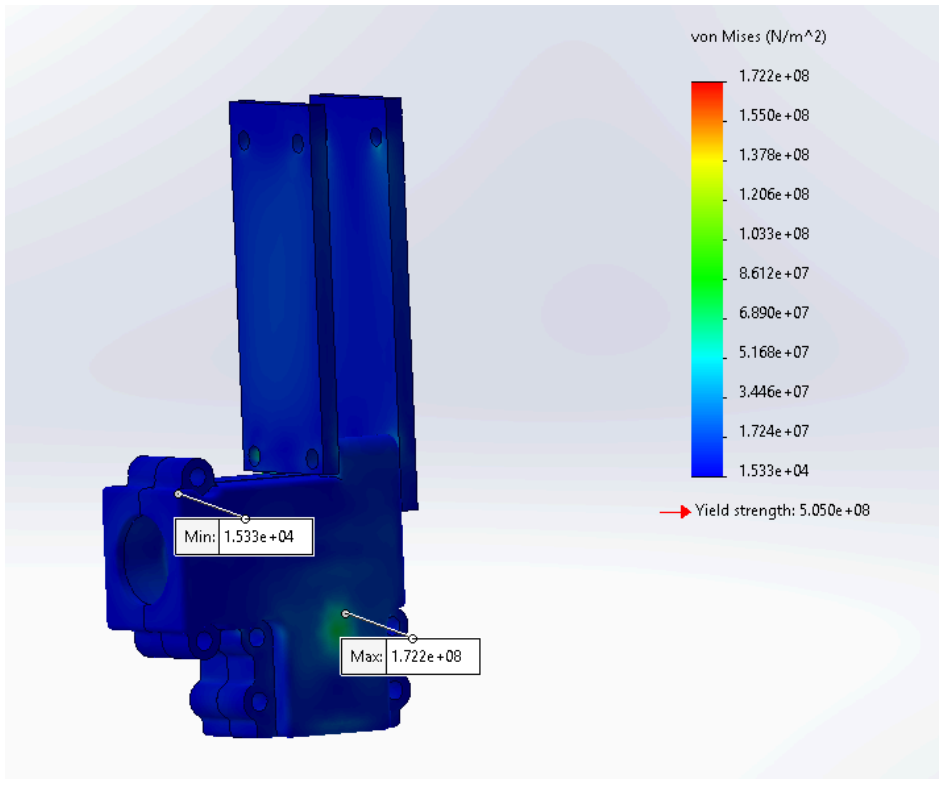

Von Mises stress [Kpi]

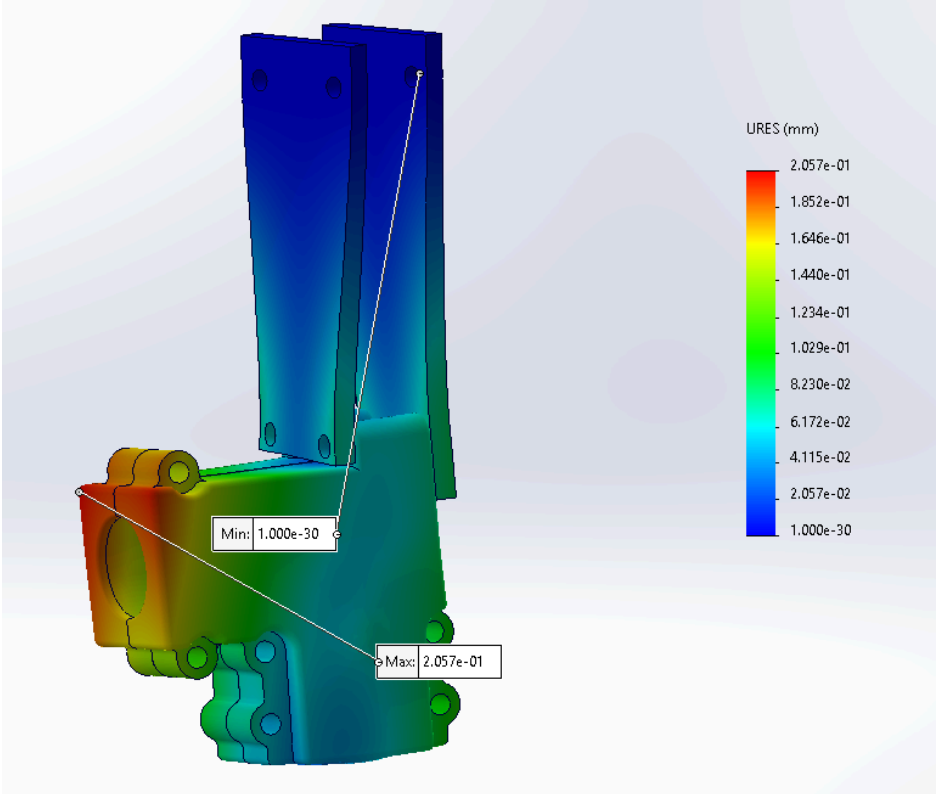

Displacement [in]

By small angle approximation the angle of the **deflection is on the order of 0.141 deg**

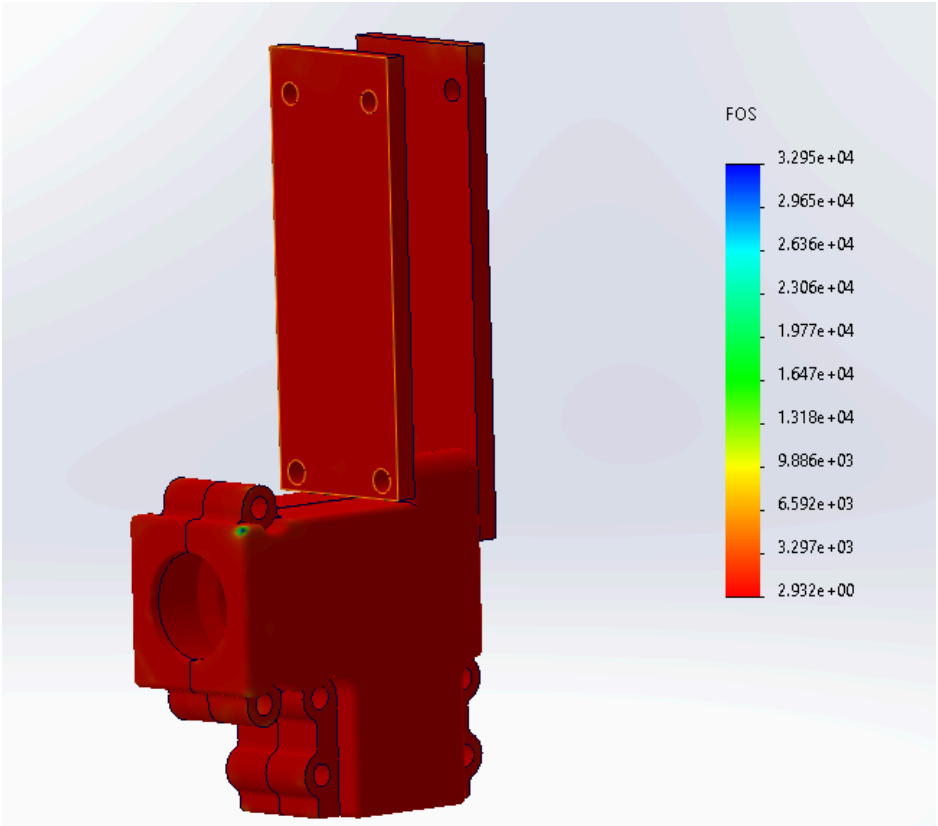

Factor of safety

One thing to add is that the forces added had a 1.5 FOS already included

So like, yeahhh it's excessive.

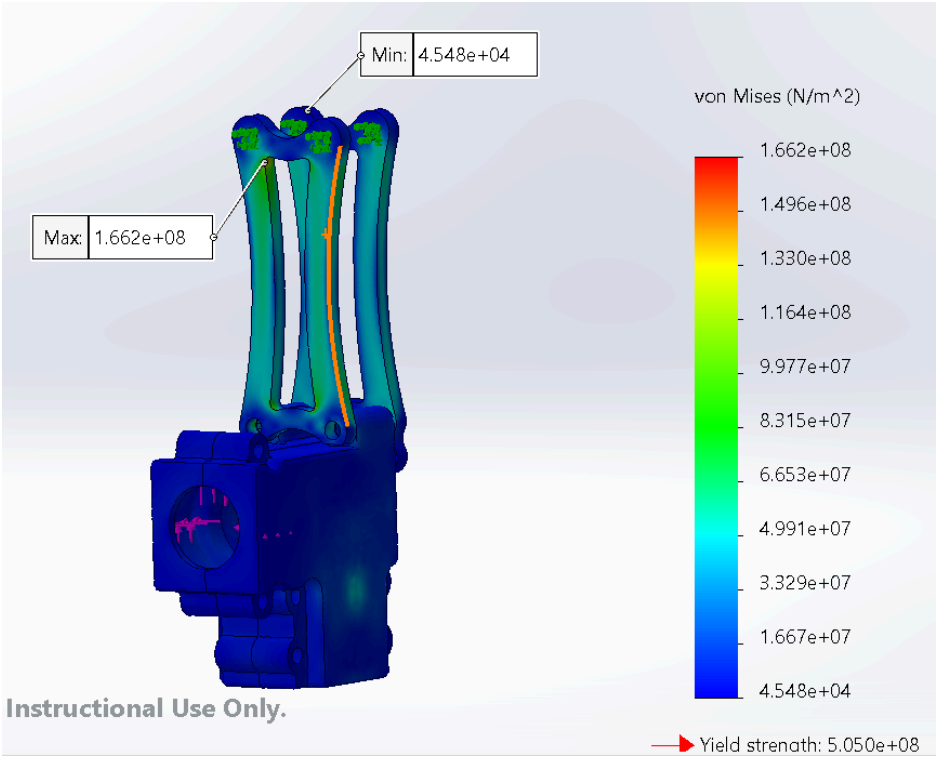

Weight Optimized Version.

Stress is def higher but it won't yield. Tried to do a fatigue analysis but solidworks said the stress isn't high enough to get an accurate result LMAO.

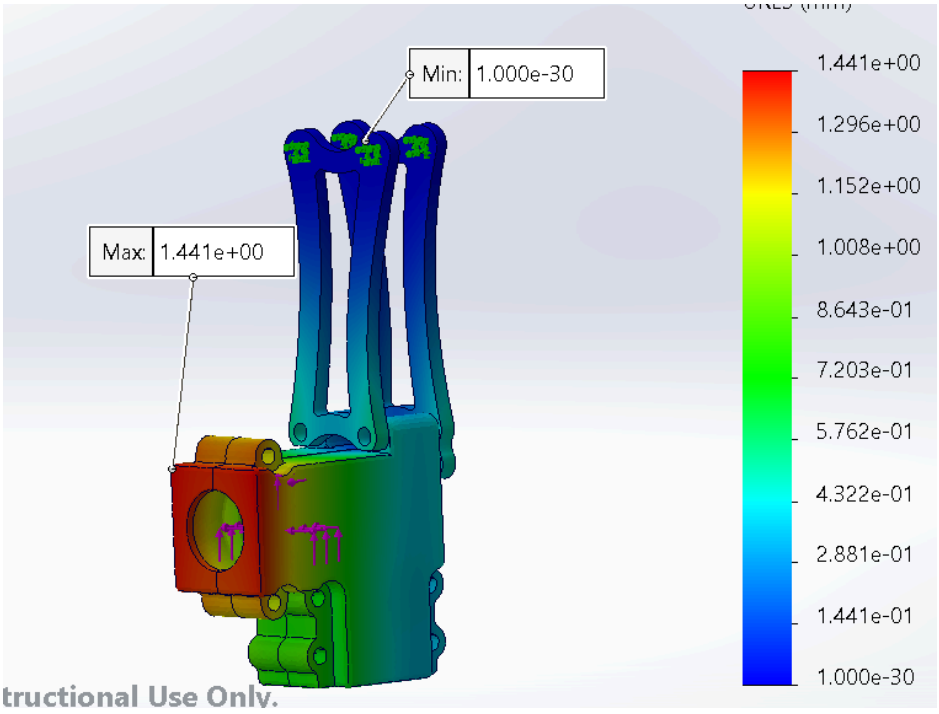

Displacement seems to be in the order of fuckall, so there shouldn't be any added backlash.

Bearing + Primary shaft shell

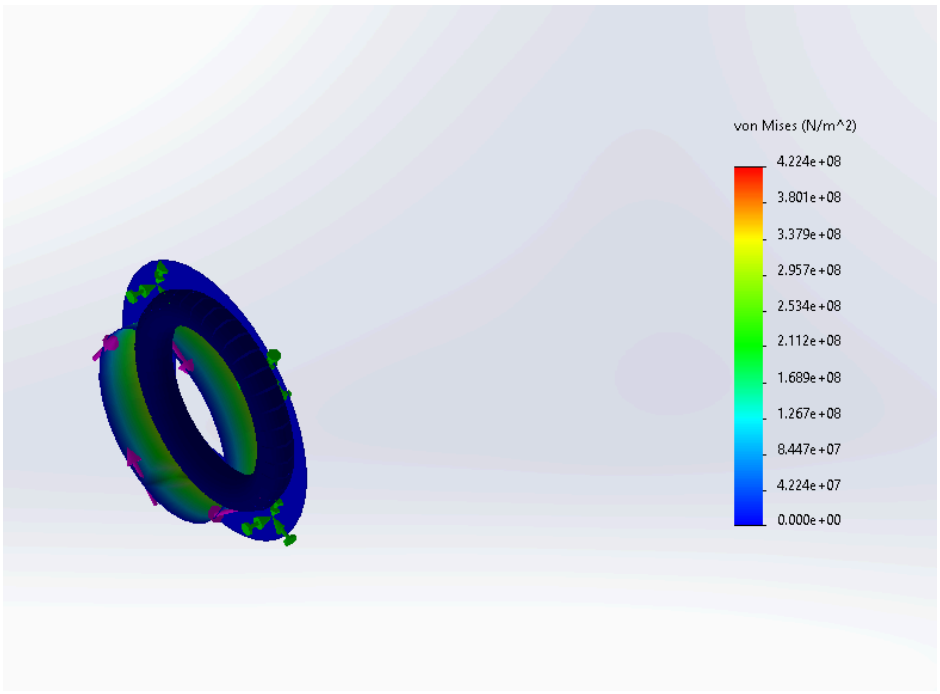

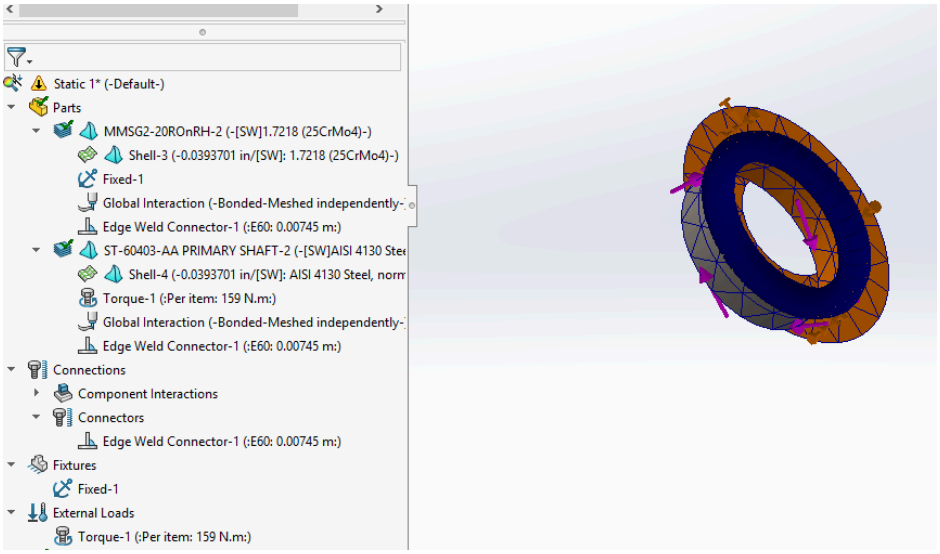

@ max parked scrub

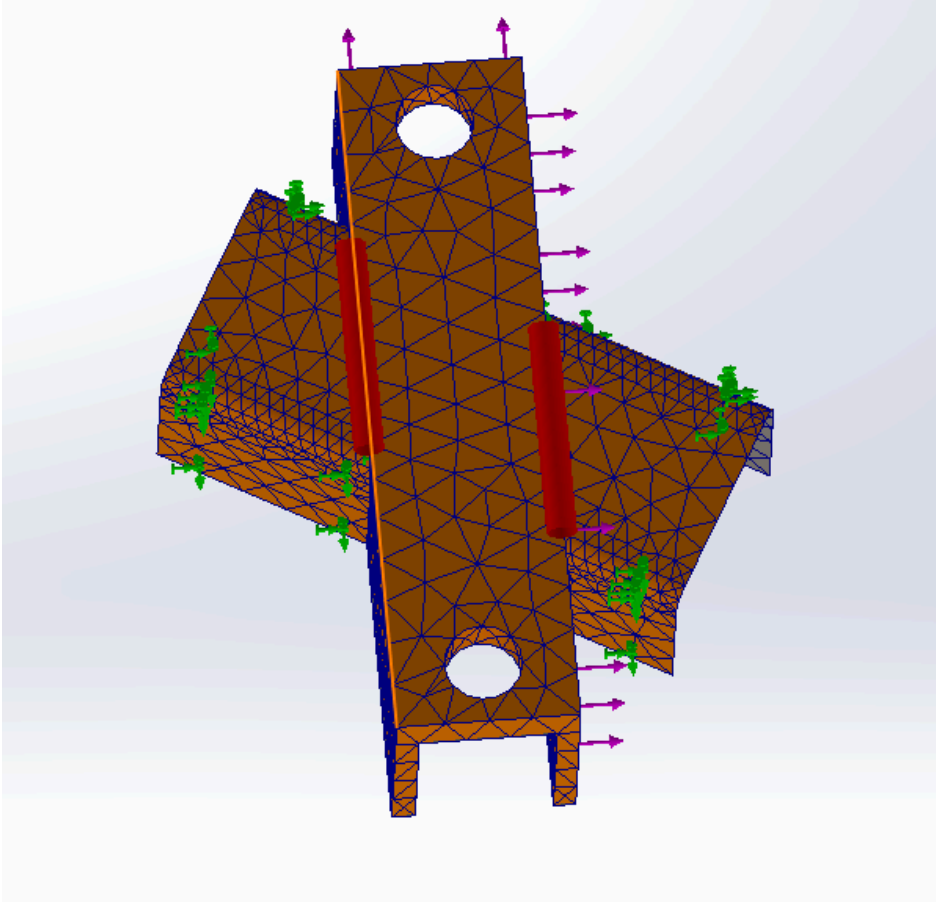

Solidworks doesn’t let you analyse welds that aren’t 90 degrees, so this is only the top weld contribution

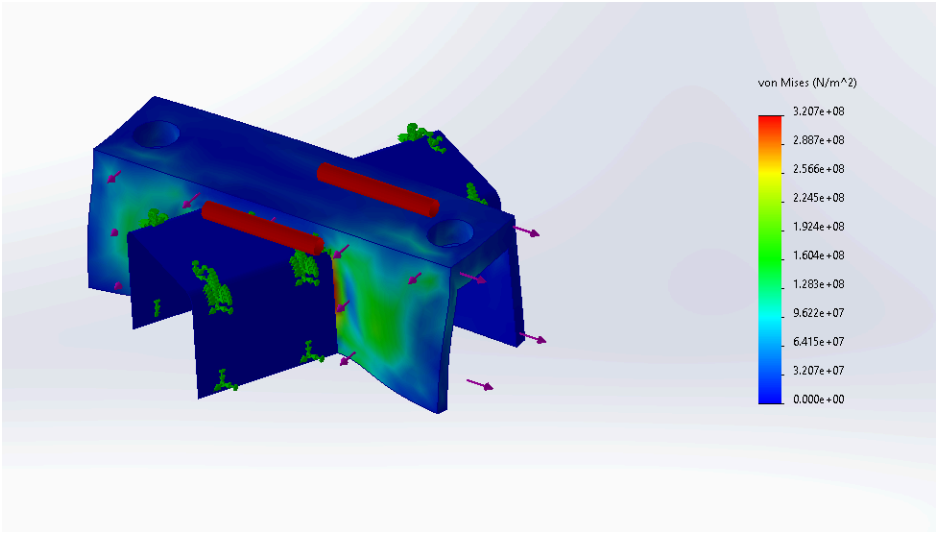

Expected there's a huge stress concentration where there isn’t a weld but still a mesh interaction there.

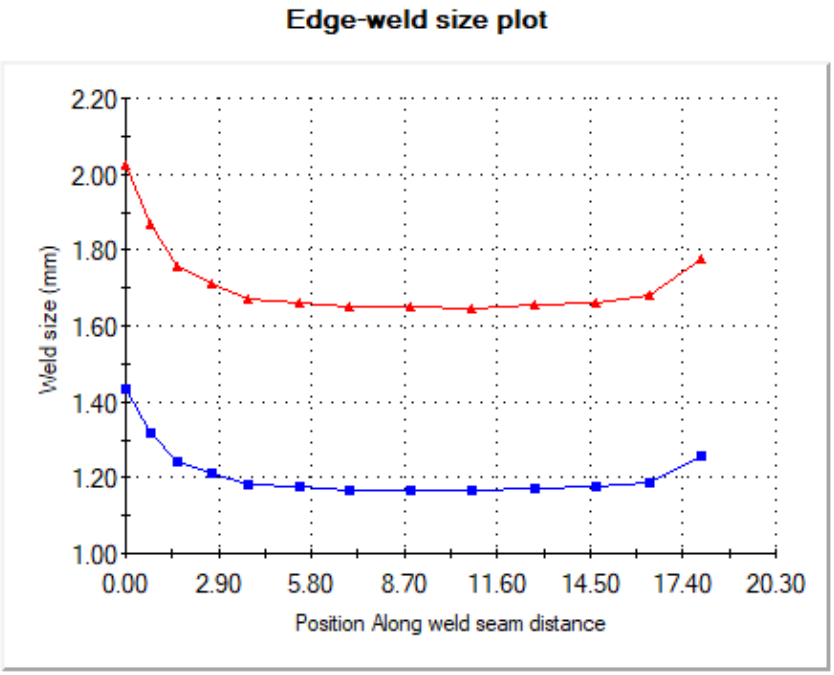

Type	Min	Max	Mean
Weld size (mm)	0.26807	2.0256	0.96008
Weld throat size (mm)	0.18955	1.4323	0.67888
Joint normal force (N/m)	-4,755.5	4,698	104.79
Shear-Weld axis force (N/m)	-16,086	16,550	71.72
Shear-Surface normal force (N/m)	0	0	0
Bending moment (N.m/m)	-24.47	29.858	0.66041

Contributes a pretty solid amount ig lol

I did hand calcs which are below to hopefully give a better rough estimate of what these welds can handle.

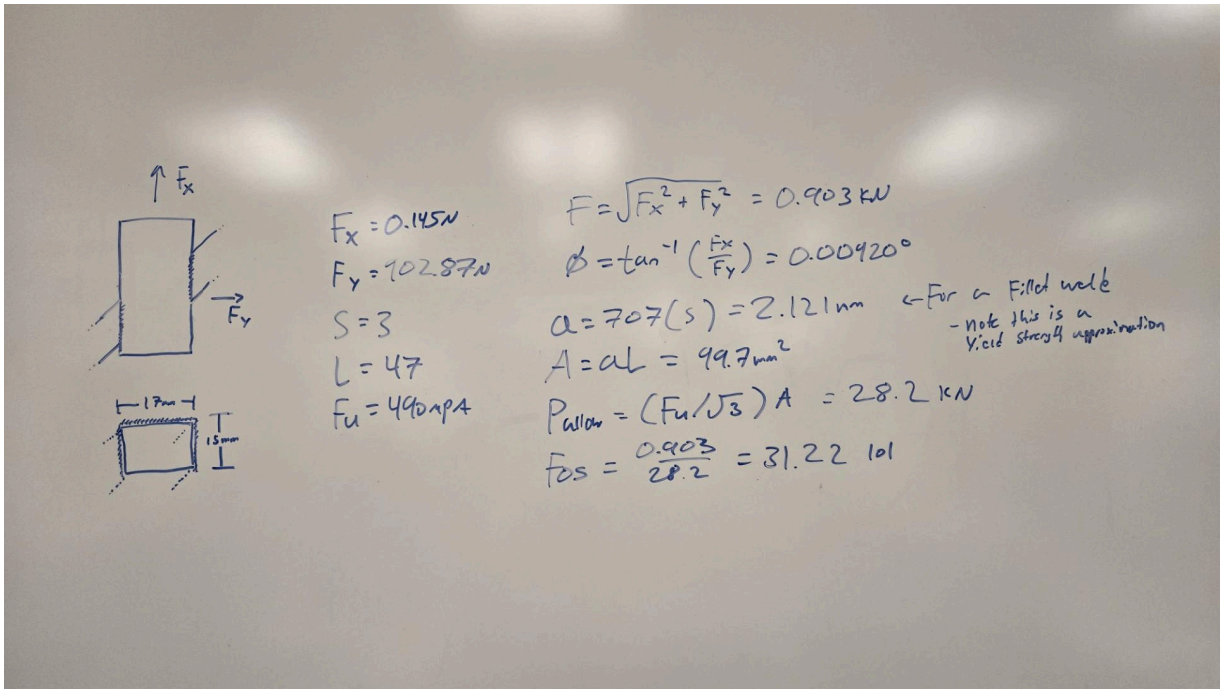

The calculation above is a Young's modulus approximation for the yield strength of the rack tab.

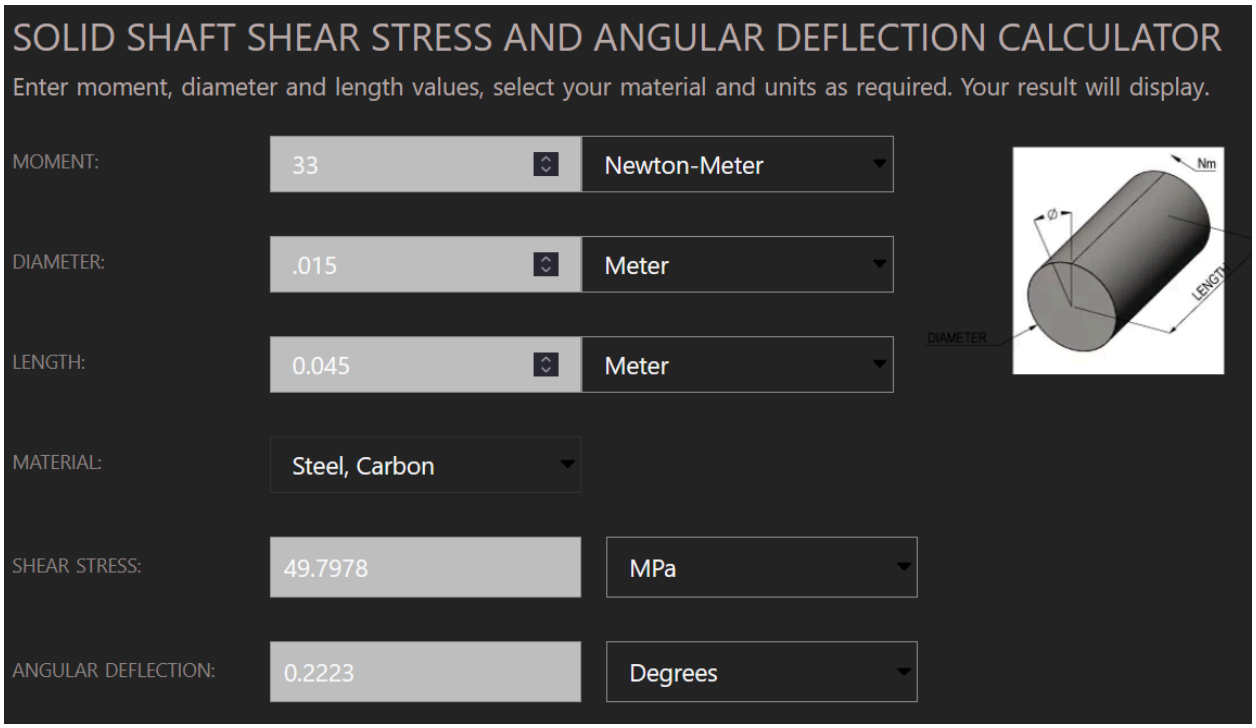

Compliance of the system, including the backlash from the Bevelbox and rack. [tube deflection, bevel box backlash, and rack backlash], it becomes stiffer as the backlash becomes a smaller and smaller part of the system as the aligning moment increases.

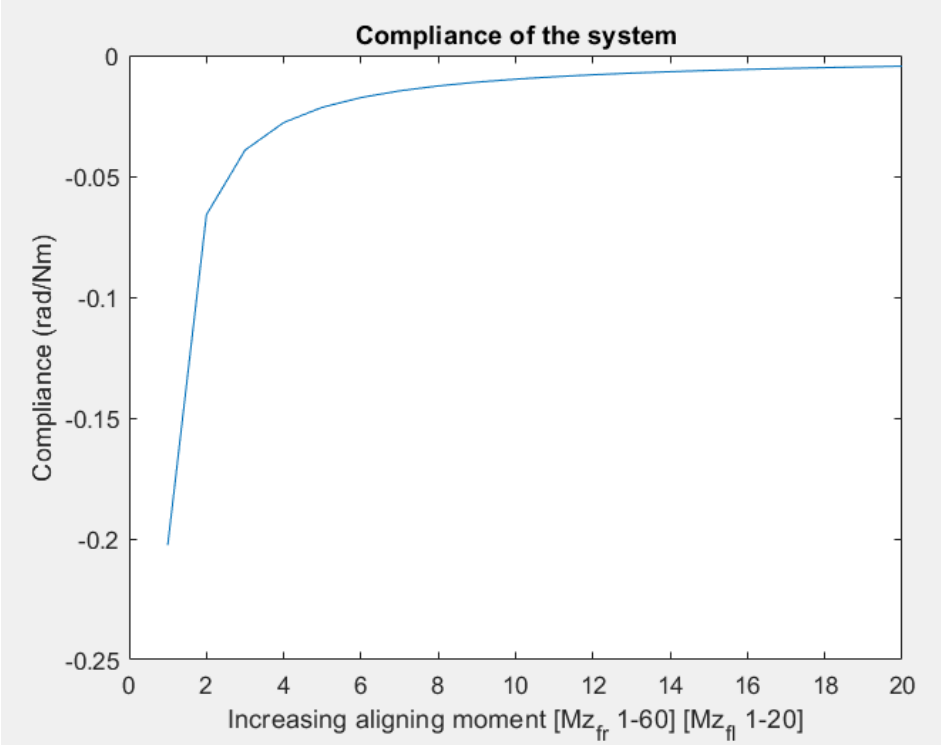

The software evidence below was regenerated from the merged steering/tire repository state used for this PDR. Canonical software figures retain figure manifests, configuration/source identity, authority notes, and hashes. The added branch-coverage, readiness, architecture, viewer, and load-path graphics summarize reviewed machine-readable results without inventing unavailable CAD or vehicle-state data.

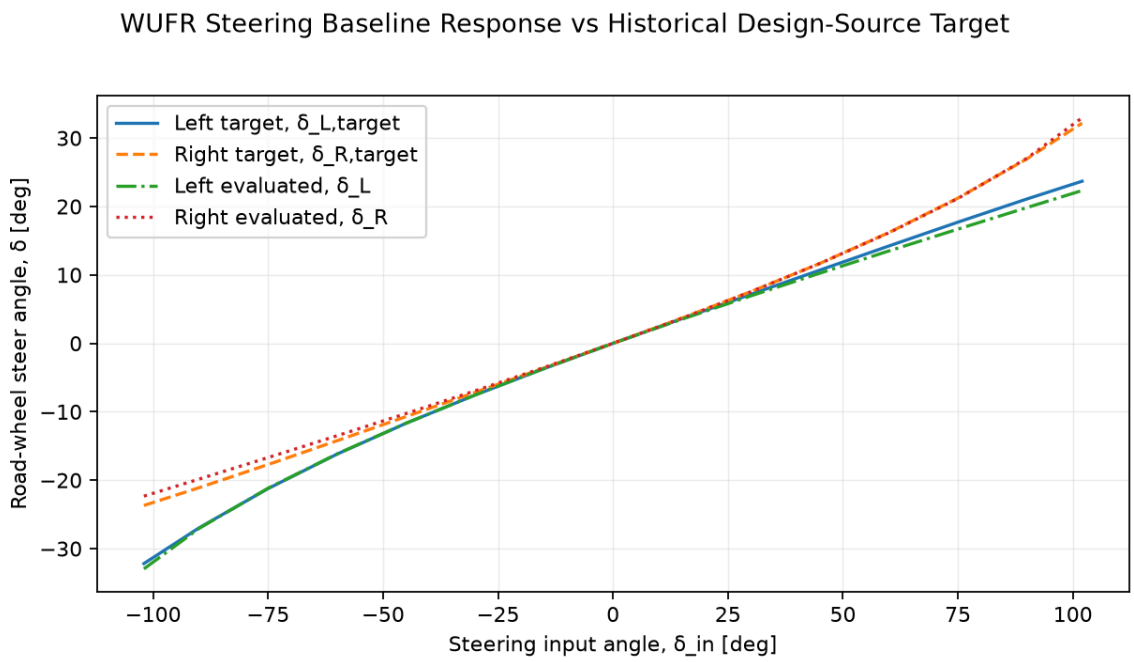

Notes: Target is the frozen WUFR-26/27 historical fit; evaluated curves come from MOD-STEER-0001. | This comparison does not include backlash, compliance, fabrication error, or physical stops.

FIG-STEER-RND-001 | model=MOD-STEER-0001 | config=WUFR27_STEERING_BASELINE_V0 | authority=historical design-source regression comparison; not installed-state validation
states=none | sources=benchmarks/steering/WUFR26_27_HISTORICAL_RESPONSE_REGRESSION_V0.toml, configurations/steering/WUFR27_STEERING_BASELINE_V0.toml

Figure A1. WUFR-27 nominal rigid steering response versus the frozen WUFR-26/27 historical design-source target. The evaluated response comes from MOD-STEER-0001. This is regression evidence only; it does not include installed backlash, compliance, fabrication error, or physical stops.

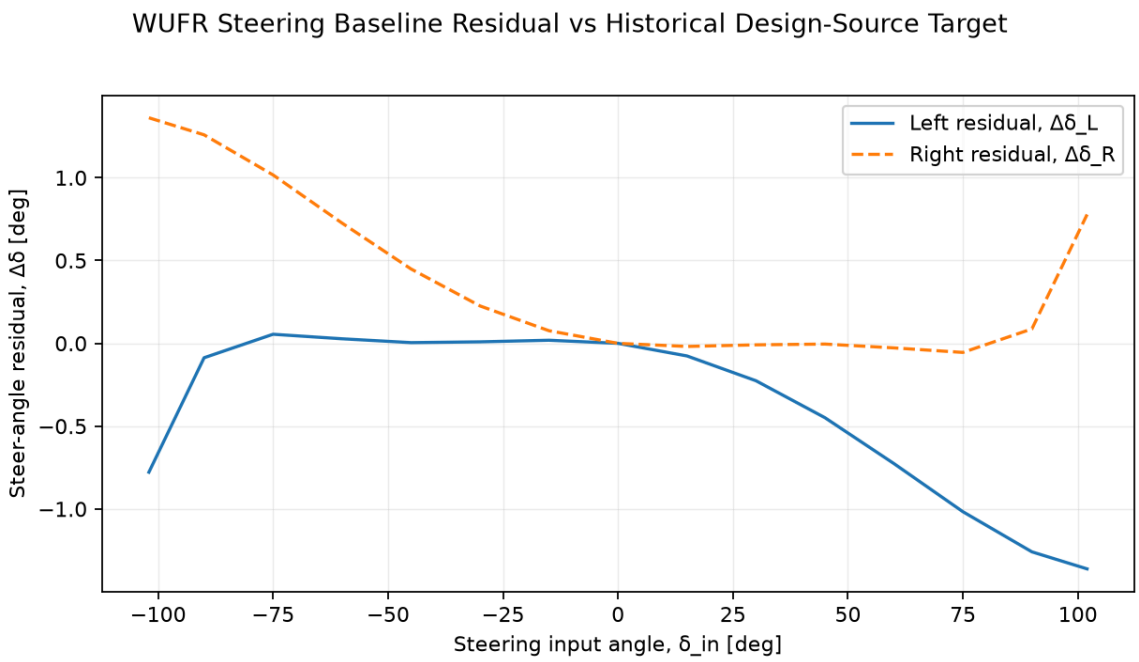

Notes: Residual = MOD-STEER-0001 evaluated heading minus historical target heading.

FIG-STEER-RND-002 | model=MOD-STEER-0001 | config=WUFR27_STEERING_BASELINE_V0 | authority=historical design-source regression residual; not installed-state validation
states=none | sources=benchmarks/steering/WUFR26_27_HISTORICAL_RESPONSE_REGRESSION_V0.toml, configurations/steering/WUFR27_STEERING_BASELINE_V0.toml

Figure A2. Evaluated-minus-target residual corresponding to Figure A1. The residual view exposes differences that are difficult to see where the absolute curves overlap.

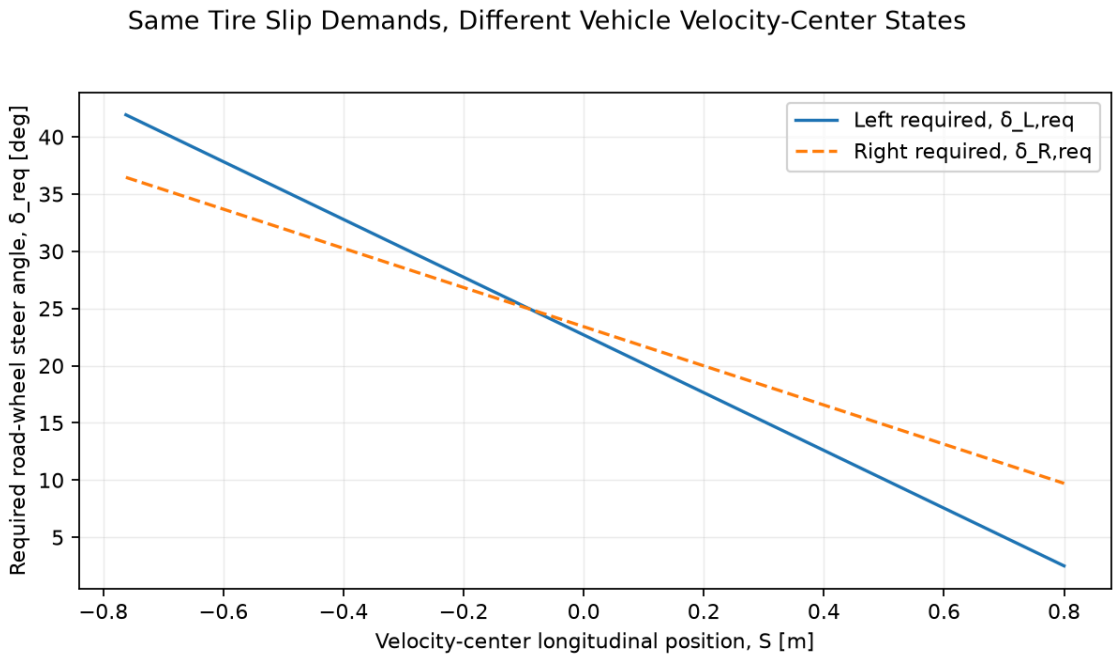

Notes: Required slips are held fixed at 2.5 deg inside and 9.71429 deg outside. | Rear-axle velocity-center result: pro_ackermann; front-state result: anti_ackermann. | Synthetic software evidence only; this demonstrates state dependence, not a WUFR handling prediction.

FIG-STEER-RND-004 | model=MOD-VEH-0002 | config=SYNTHETIC_MOTION_AWARE_FORCE_DEMAND_V0 | authority=synthetic motion/tire software evidence only
states=rear_axle_velocity_center, front_axle_velocity_center |
sources=benchmarks/tires/SYNTHETIC_FORCE_DEMAND_BRANCHES_V0.toml, scripts/run_motion_aware_force_demand_benchmarks.py

Figure A3. Synthetic motion-aware benchmark with identical tire slip demands and two supplied velocity-center states. The change from pro-Ackermann to anti-Ackermann verifies state dependence in the software architecture; it is not a WUFR handling prediction.

Exact R25B Steering Force-Demand Branch Handoff

Source branch identity is selected before projection to |Fy| and |α|. The graphic reports exact coverage without inventing a curve shape.

Reference state	Exact operating point	Samples	Slip-angle domain	Force domain	Source branch
Inside reference	Fz = 222 N γ = 0° p = 82.7 kPa gauge	64	0.07547° to 9.58491°	50.97 N to 694.04 N	negative_slip_pre_peak
Outside reference	Fz = 1112 N γ = 2° p = 82.7 kPa gauge	86	0.06349° to 10.85714°	275.84 N to 2737.89 N	negative_slip_pre_peak

Preserved boundaries

No zero-force anchor • no smoothing or refit • no sample deletion • no state interpolation • no force extrapolation • no track-surface scaling

Use boundary: these branches support bounded exact-state inversion and regression, not a WUFR steering target until synchronized vehicle demand is supplied.



Figure A4. Exact R25B pre-peak steering branch handoff coverage. The two source-backed reference states are reported with sample counts and explicit force/slip domains. No curve shape is inferred from endpoint metadata.

R25B Steering-Target Input Readiness Audit

Two existing 1.2 g development states were reviewed. A complete synchronized state is required; one usable field does not make a state ready.

State	Front inside Fz	Front outside Fz	Inclination	Pressure	Fy demand	Zero-steer pose	u-v-r	Weight	Ready?
1.2 g right turn	186.214 N BELOW 222 N min	1719.575 N ABOVE 1112 N max	Missing	Missing	Missing	Missing	Missing	0	NO
1.2 g left turn	516.848 N inside load interval; not exact knot	1388.941 N ABOVE 1112 N max	Missing	Missing	Missing	Missing	Missing	0	NO

Readiness counts: exact two-branch handoff = 0 • bounded complete-cell query = 0 • motion-aware target = 0

Blocked substitutions: no clipping, nearest-state selection, nominal camber/pressure insertion, inferred force allocation, Ackermann-derived motion, or hidden target weighting.

Program result: steering/tire target work pauses here until reviewed suspension pose and synchronized vehicle-state authority exist.

Figure A5. R25B steering-target input readiness audit for the two available 1.2 g vehicle states. Zero states are ready for exact handoff, complete-cell query, or motion-aware target construction.

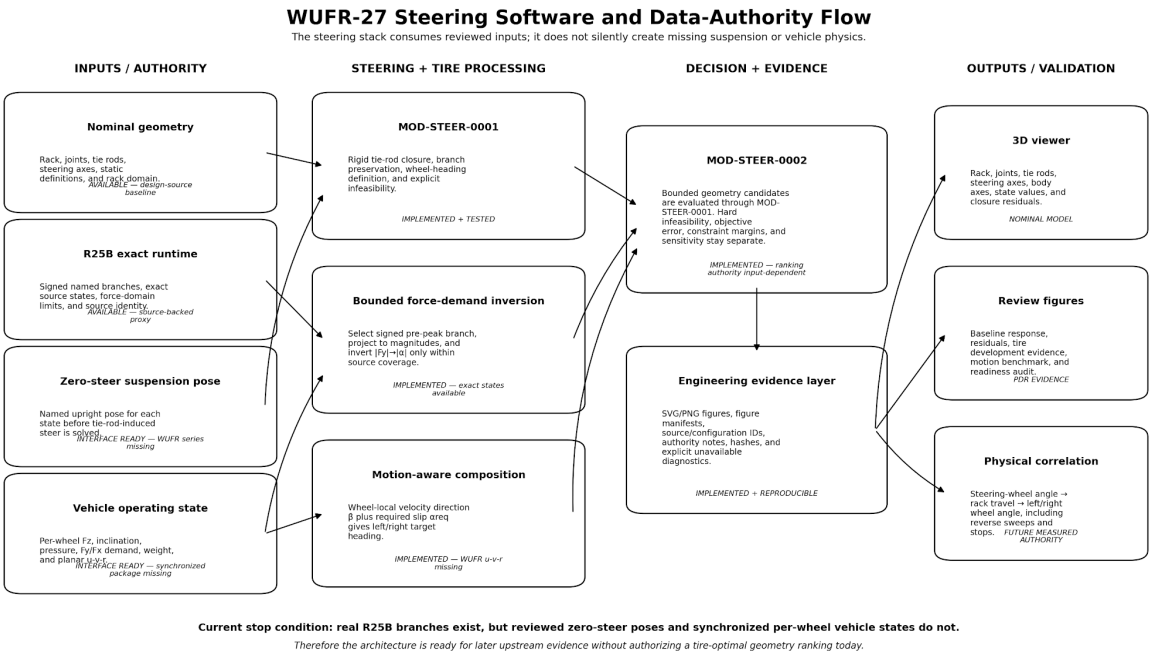

Figure A6. Steering software and data-authority architecture. Available source-backed inputs, implemented processing, missing upstream state authority, reproducible evidence outputs, and future physical correlation are kept as separate layers.

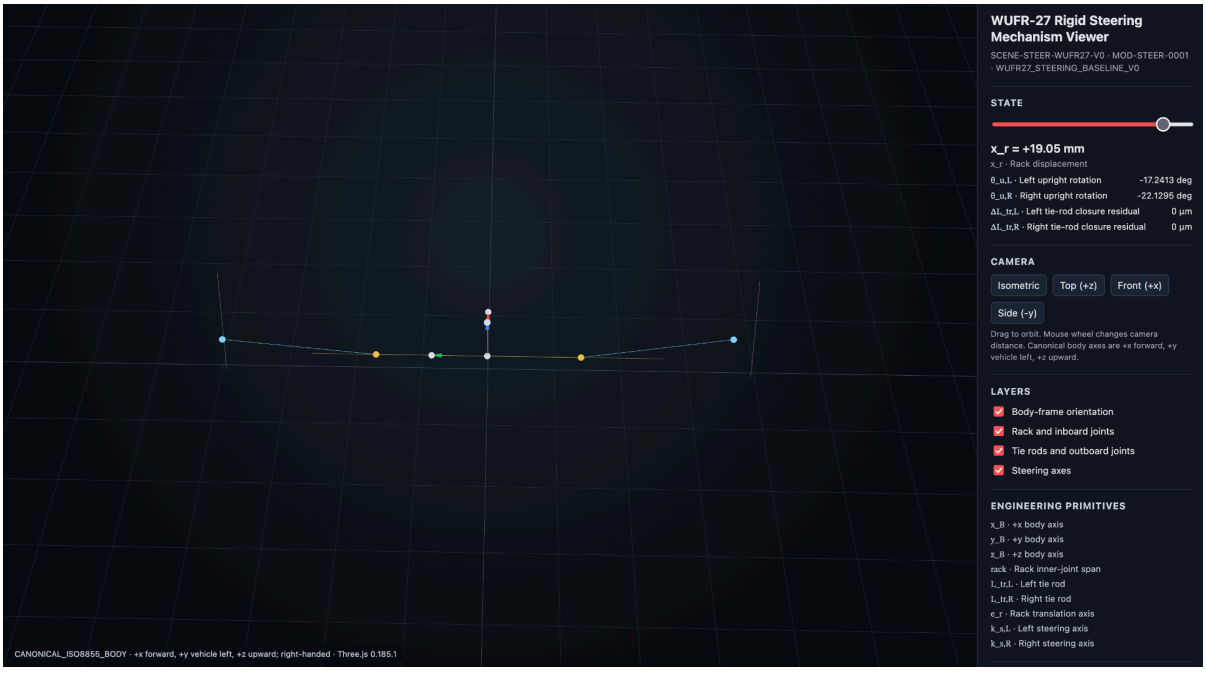

Figure A7. Static rendering of the provider-neutral steering viewer scene at x_r = +19.05 mm. The points and tie-rod states come from MOD-STEER-0001.

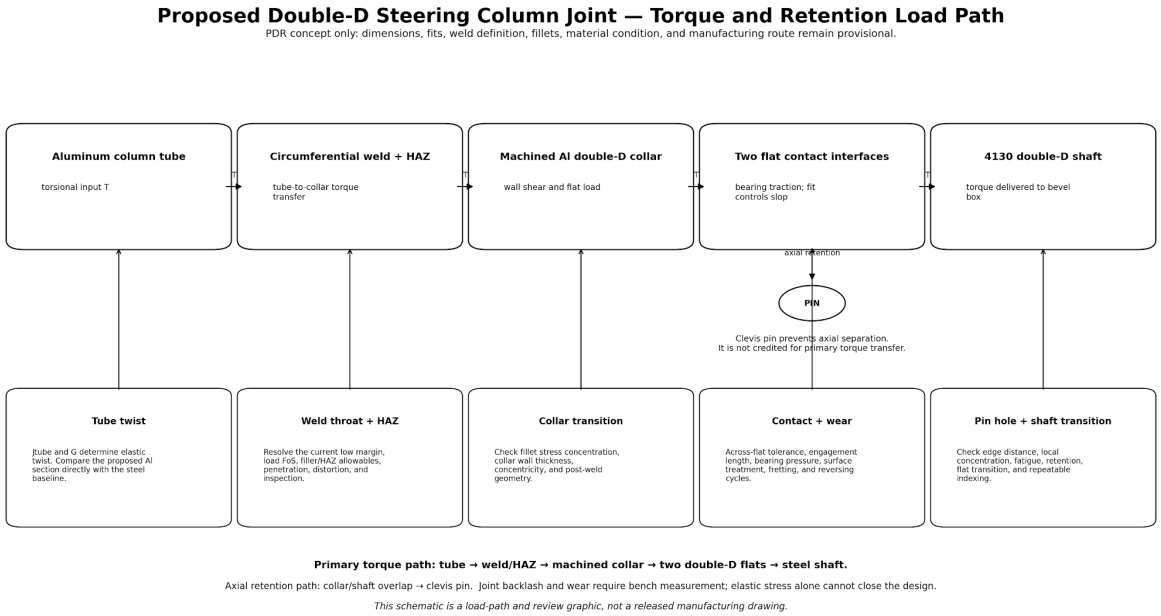

Figure A8. Proposed double-D column-joint torque and axial-retention load path. This is a PDR concept/review schematic, not a released drawing. It identifies the weld/HAZ, collar transition, contact interface, pin hole, wear, tolerance, and fatigue checks that remain open.

WUFR-27 Nominal Steering Performance Evidence

The following figures accompany the Steering Performance and Vehicle Dynamics discussion in Design Review. They are generated from the reviewed WUFR-27 nominal geometry, the design-source 3.5 in/rev input-to-rack mapping, and prescribed calculated torque cases. They are not installed steering measurements, a tire self-aligning-moment model or a physical validation of the complete column assembly.

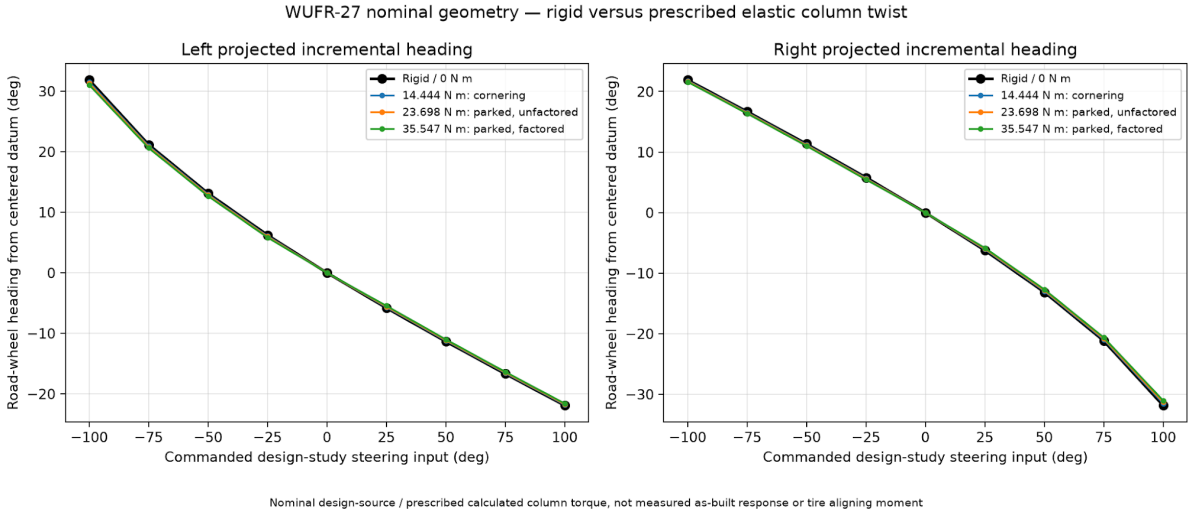

Figure A9. Rigid and elastically loaded left and right road-wheel heading versus nominal steering input for the prescribed cornering, unfactored parked and factored parked torque cases.

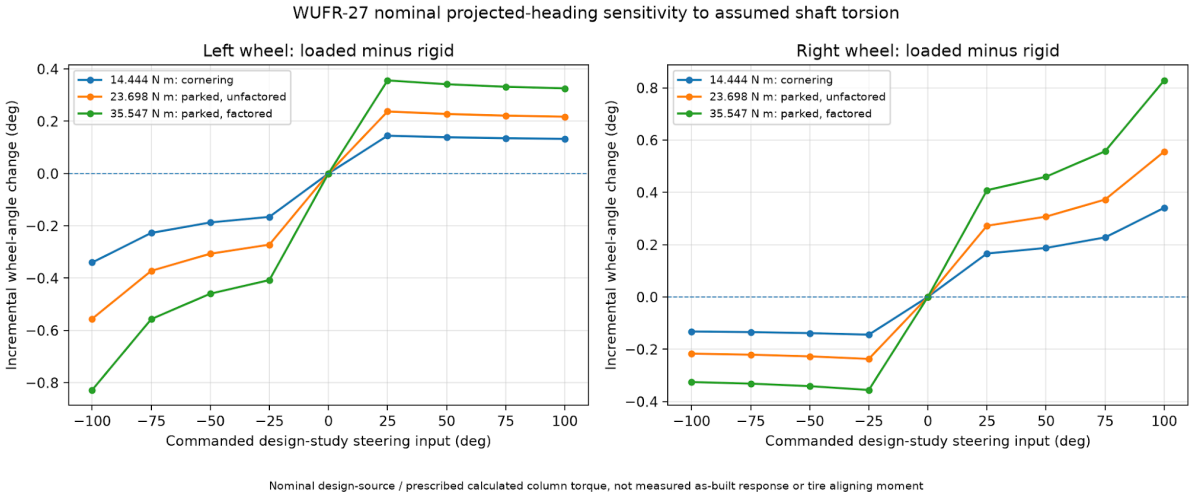

Figure A10. Loaded-minus-rigid projected road-wheel heading difference. The different left and right sensitivities are produced by the nominal steering linkage geometry.

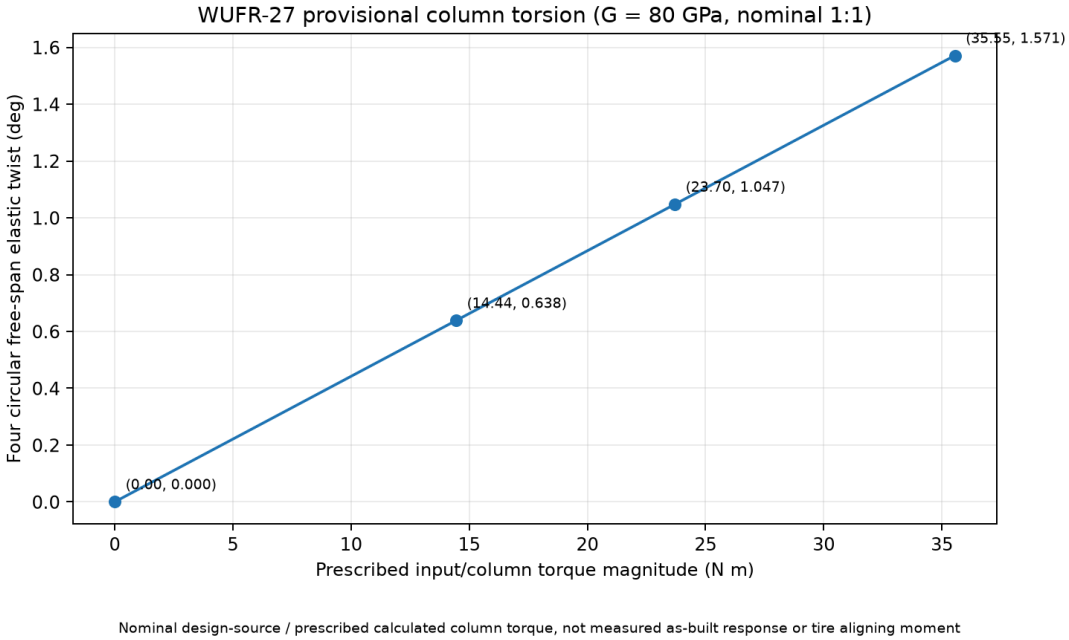

Figure A11. Provisional four-span circular steel-column and shaft twist versus prescribed input torque. Elastic deflection is distinct from mechanical free play and joint backlash.

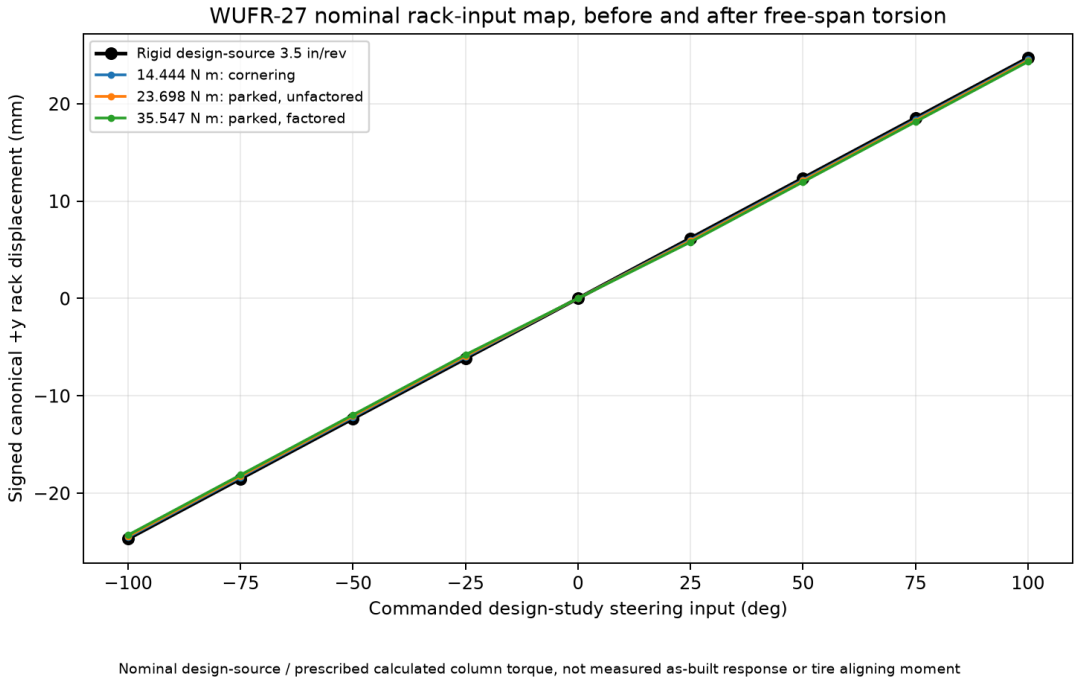

Figure A12. Nominal rack displacement and the reduction associated with modeled free-span torsion, using the design-source 3.5 in/rev steering transmission.

The figures use the source-controlled nominal report WUFR27_NOMINAL_DESIGN_SOURCE_COMPLIANCE_V1 and are reproduced by the WUFR-27 FDR evidence workflow. At +75° commanded input, the unloaded-to-loaded wheel-heading differences are approximately 0.135° (left) and 0.227° (right) at the cornering torque, rising to 0.332° and 0.557° at the factored parked torque. They describe the mechanical response of the steering system at prescribed loads and should not be interpreted as measured tire slip-angle differences.

FEA source interpretation

The existing FEA screenshots in this section belong to an earlier shaft and column analysis. The reported 146.7 MPa maximum is von Mises stress. This can be used to identify locations worth examining, but it cannot establish the final WUFR-27 factor of safety without the actual steel tensile yield strength and consistent geometry, loading, contacts and constraints. The reviewer-observed difference between the stress trend and the approximately sevenfold displacement change remains unexplained. No new FEA simulation is claimed here.

Prototypes/Experiments

- Different steel wheel angle / steering wheel force
- Seeing angles for skidpad
- Adjustable steer arm
- Adjustable ackermann / steering geometry
- Rack position
- Steer arm length
- Tie rod upright and rack

Resources (research papers/textbooks/websites/etc.)

NARRco Rack Documentation, including the best ways to mount it, useful rod angle, and load capacity.

https://cdn.shopify.com/s/files/1/0368/1989/files/NARRco_Rack_Mk_II_14.4_T13_181108.pdf?6

Bevel Gearbox Documentation, a published article discussing the challenges behind gear installation and the best methods. Here is where I took the idea of shims.

https://www.geartechnology.com/ext/resources/issues/0613x/bevel-gear-installation.pdf

Past published reasonings for our designs, largely outdated, but it does talk about the drawbacks of using a double u-joint design.

https://openscholarship.wustl.edu/cgi/viewcontent.cgi?article=1098&context=mems500

Past decisions for Rack and Column, this helped us determine the best rack manufacturer and column system; however, these were made before we had to deal with the bevel box.

Steering decision

SKETCHES/DRAWINGS/SCREENSHOTS

Figure 1. Arm, Hand, and Thumb/Finger Strength (5th Percentile Male Data)						
1	2		5		6	
Elbow Flexion	Pull		Down		In	
	L	R	L	R	L	R
⅝ π	187	**249**	80	89	67	89
⅔ π	151	137	93	**116**	89	**98**

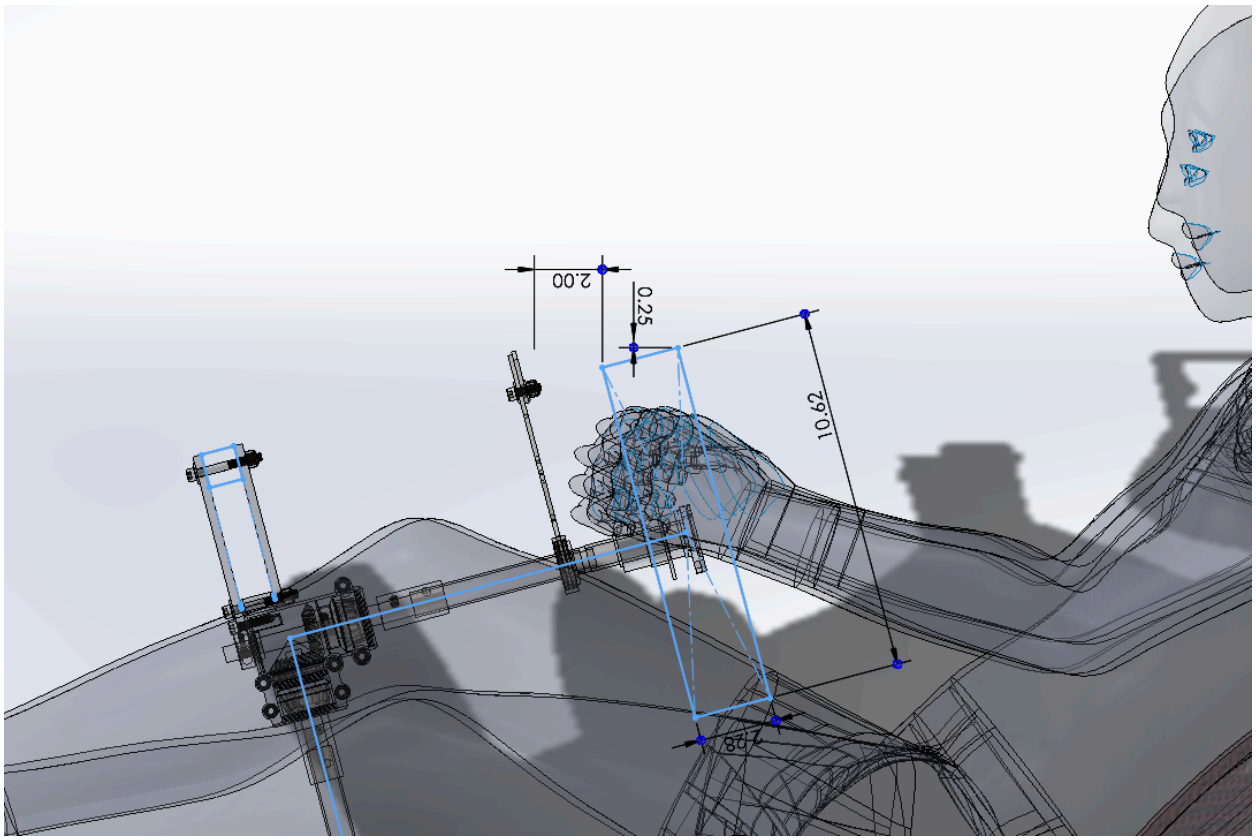

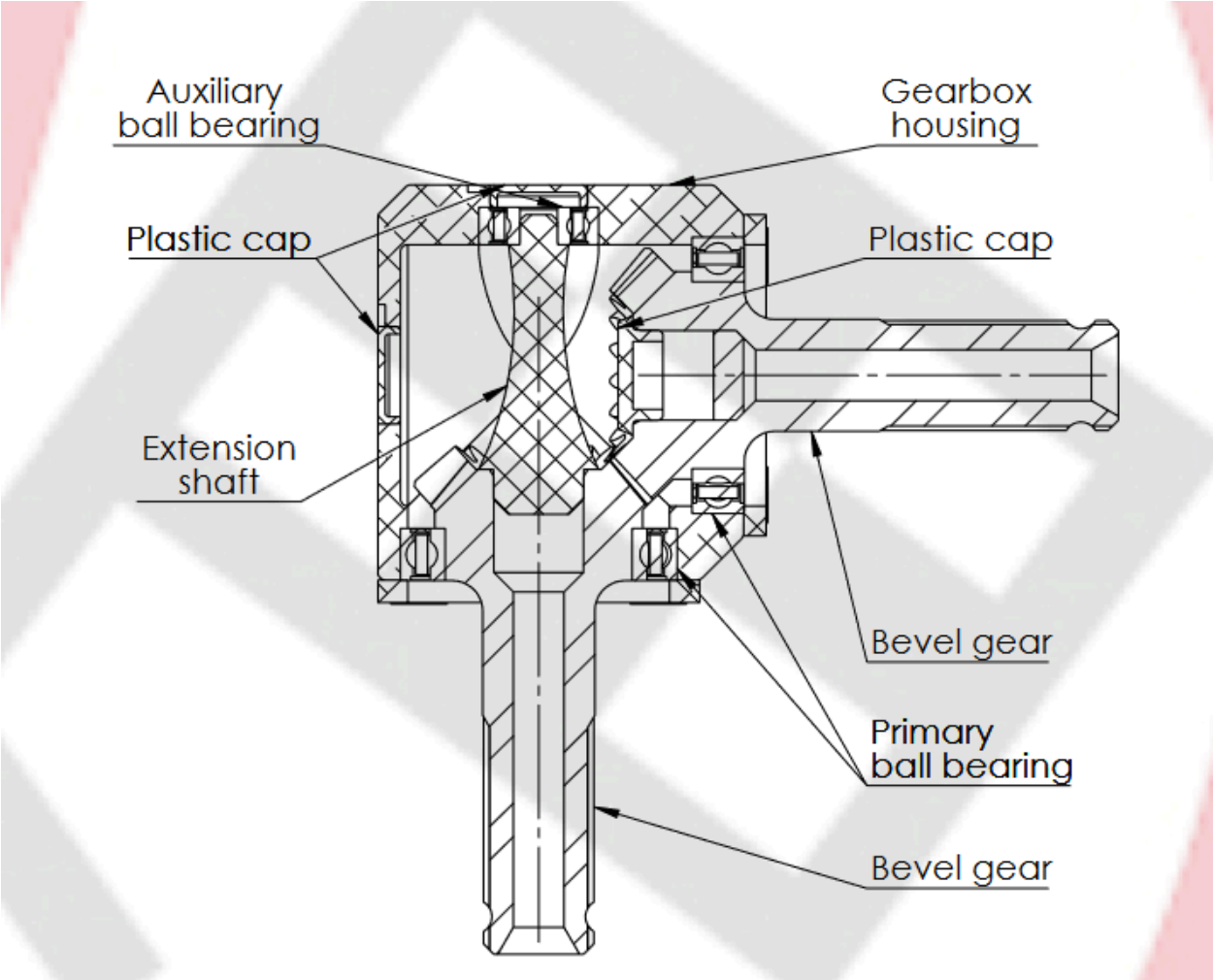
Auxiliary ball bearing
Gearbox housing
Plastic cap
Plastic cap
Extension shaft
Bevel gear
Primary ball bearing
Bevel gear



Spur Gears
Helical Gears
Internal Gears
Racks
P Racks & Pinions

MMSG Module 2~4
Ground Spiral Miter Gears

J



Specifications	
Precision grade	JIS B 1704: 1978 grade 1*
Gear teeth	Gleason
Pressure angle	20°
Helix angle	35°
Material	SCM415
Heat treatment	Tooth area carburized
Tooth hardness	55 to 60HRC

* The precision grade of J Series products is equivalent to the value shown in the table.

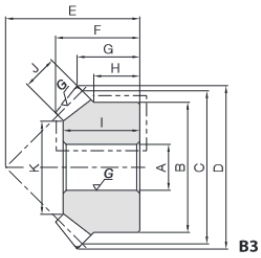

Catalog Number	Gear Ratio	No. of teeth	Shape	Direction of spiral	Bore	Hub dia.	Pitch dia.	Outside dia.	Mounting distance	Total length	Crown to back	Hub width	Hole length	Face width	Holding surface dia.	Allowable torque (N-m)		Allowable torque (kgf-m)		Backlash (mm)	Weight (kg)
					A_{H7}	B	C	D	E	F	G	H	I	J	K	Bending strength	Surface durability	Bending strength	Surface durability		
MMSG2-20R	1	20	B3	R	12	35	40	42.7	35	21.98	16.35	12.5	20	9	24.54	17.0	23.5	1.73	2.40	0.04~0.10	0.14
MMSG2-20L				L																	
MMSG2.5-20R				R	14	42	50	53.2	45	28.63	21.6	16	26	11	30.89	32.7	46.1	3.33	4.70	0.05~0.11	0.27
MMSG2.5-20L				L																	
MMSG3-20R				R	16	52	60	63.99	50	30.78	21.99	16	27	14	34.4	58.5	83.7	5.97	8.54	0.06~0.12	0.43
MMSG3-20L				L																	
MMSG3.5-20R			B4	R	20	50	70	74.53	55	32.45	22.26	14	29	16	42.75	91.8	133	9.36	13.6	0.07~0.13	0.51
MMSG3.5-20L				L																	
MMSG4-20R				R	20	55	80	84.99	65	39.13	27.5	17	35	18	49.08	136	199	13.8	20.3	0.09~0.15	0.80
MMSG4-20L				L																	

JIS grade (AISI/ SAE)*4	Chemical composition(%)					Tensile test		Brinell hardness	Heat treatment(°C)		Carbon*2 equivalent	Weldability*3
	C	Si	Mn	Cr	Mo	Tensile strength (MPa)	Elongation (%)		Quenching	Tempering		
SCM415 (-)	0.13 ~0.18	0.15 ~0.35	0.60 ~0.90	0.90 ~1.20	0.15 ~0.25	≧830	≧16	235 ~321	1st 850~900 Oil cooling 2nd 800~850 Oil cooling	150~200 Air cooling	0.56	△

Property	Value	Units
Elastic Modulus in X	6.900000067e+10	N/m^2
Elastic Modulus in Y	6.900000067e+10	N/m^2
Elastic Modulus in Z	6.900000067e+10	N/m^2
Poisson's Ratio in XY	0.33	N/A
Poisson's Ratio in YZ	0.33	N/A
Poisson's Ratio in XZ	0.33	N/A
Shear Modulus in XY	2.600000013e+10	N/m^2
Shear Modulus in YZ		N/m^2
Shear Modulus in XZ		N/m^2
Mass Density	2700	kg/m^3
Tensile Strength in X	450000000	N/m^2
Tensile Strength in Y	460000000	N/m^2
Compressive Strength in X		N/m^2
Compressive Strength in Y		N/m^2
Shear Strength in XY		N/m^2

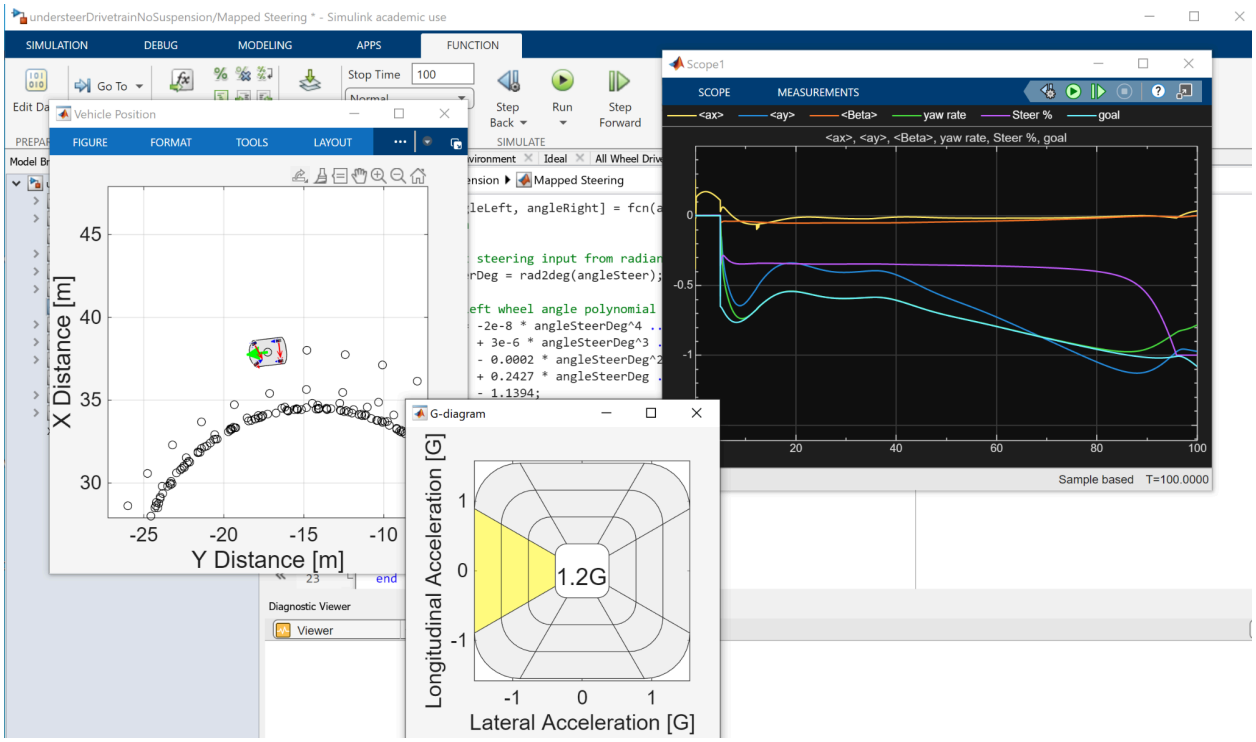



Increasing this ratio increases mechanical advantage of the driver. $\frac{Input\ angle}{Output\ angle}$

$$\frac{Steering\ Input\ angle}{Wheel\ angle} = \frac{Steering\ Input\ angle}{Bevel\ Gear\ angle} * \frac{Bevel\ Gear\ angle}{Rack\ movement} * \frac{Rack\ movement}{Wheel\ angle}$$

Bevel Gearbox Ratio

- [deg/deg]
- 1:1 basically

Rack Ratio

- [deg/mm]
- Inverse of what NaRRco gives which is 4 in/rev

Wheel Ratio

- [mm/deg]
- A smaller **total** steer-arm means more deg for the same rack distance
- Varies because of geometry